# Advances in Telematics

# Research in Computing Science

## Series Editorial Board




***Research in Computing Science*** es una publicación trimestral, de circulación internacional, editada por el Centro de Investigación en Computación del IPN, para dar a conocer los avances de investigación científica y desarrollo tecnológico de la comunidad científica internacional. **Volumen 75,** agosto 2014. Tiraje: 500 ejemplares. *Certificado de Reserva de Derechos al Uso Exclusivo del Título* No. : 04-2005-121611550100-102, expedido por el Instituto Nacional de Derecho de Autor. *Certificado de Licitud de Título* No. 12897, *Certificado de licitud de Contenido* No. 10470, expedidos por la Comisión Calificadora de Publicaciones y Revistas Ilustradas. El contenido de los artículos es responsabilidad exclusiva de sus respectivos autores. Queda prohibida la reproducción total o parcial, por cualquier medio, sin el permiso expreso del editor, excepto para uso personal o de estudio haciendo cita explícita en la primera página de cada documento. Impreso en la Ciudad de México, en los Talleres Gráficos del IPN – Dirección de Publicaciones, Tres Guerras 27, Centro Histórico, México, D.F. Distribuida por el Centro de Investigación en Computación, Av. Juan de Dios Bátiz S/N, Esq. Av. Miguel Othón de Mendizábal, Col. Nueva Industrial Vallejo, C.P. 07738, México, D.F. Tel. 57 29 60 00, ext. 56571.

**Editor responsable:** *Grigori Sidorov, RFC SIGR651028L69*

**Research in Computing Science** is published by the Center for Computing Research of IPN. **Volume 75**, August 2014. Printing 500. The authors are responsible for the contents of their articles.



Printed in Mexico City, at the IPN Graphic Workshop – Publication Office.

Volume 75

# Advances in Telematics

**Carlos Hernandez**
**Félix Mata**
**Miguel Martinez (Eds.)**


Instituto Politécnico Nacional, Centro de Investigación en Computación
México 2014

**ISSN: 1870-4069**



Instituto Politécnico Nacional (IPN)
Centro de Investigación en Computación (CIC)
Av. Juan de Dios Bátiz s/n esq. M. Othón de Mendizábal
Unidad Profesional "Adolfo López Mateos", Zacatenco
07738, México D.F., México

http://www.rcs.cic.ipn.mx
http://www.ipn.mx
http://www.cic.ipn.mx



Indexed in LATINDEX and Periódica / Indexada en LATINDEX y Periódica

Printing: 500 / Tiraje: 500

Printed in Mexico / Impreso en México

# Preface

With this volume, we show advances and new research directions in telematics, which is an interdisciplinary area where several fields converge, such as telecommunications, mobile computing, wireless sensor networks, data processing, electronics, and embedded systems. The combination and cooperation between these fields has been the key of the vertiginous advance of telematics and Information Technologies (IT), allowing the governments, industries, institutions, and individuals to be more open to communication than ever before.

The papers in this volume have been carefully chosen by the Editorial Board based on evaluation by at least three members of the reviewing committee. Acceptance rate for this volume was 30%. The main criteria for the selection were originality and technical quality of the papers.

This volume contains 13 papers related to various aspects of the development and applications of telematics, organized in the following sections:

– Telecommunications
– Communications
– Information processing
– Wireless sensor networks
– Mobile computing

This issue of *Research in Computer Science* will be interesting for researchers and students in telematics, telecommunications, mobile computing, and wireless sensor networks, as well as for general public interested in cutting-edge themes of telematics, communication, and information technologies.

This volume is the result of hard work and collaboration of many people. First of all, we thank the authors of the papers included in this volume for their technical excellence, which made possible the high quality of this volume. We also thank the members of the international Editorial Board of the volume and the reviewing committee for their hard work on selection of the best papers out of the many submissions we received. We would also like to express our gratitude to Prof. Arodí Carvallo, Director of UPIITA, Prof. Hector Mendoza, and the UPIITA staff and students for their true enthusiasm and help in preparation of this volume.

Submission, reviewing, and selection process was supported free of charge by the EasyChair system, www.EasyChair.org.

Carlos Hernández
Félix Mata
Miguel Martínez

August 2014

# Table of Contents

Page

# Effect of the error estimation of nodes in the cluster formation phase in wireless sensor networks with adaptive transmission probability

Edgar Romo[1], Mario Rivero[2], Iclia Villordo[3]

[1] UPIITA - IPN, Av. Instituto Politécnico Nacional 2580,
Barrio La Laguna Ticomán, Gustavo A. Madero, 07340, México .D.F.
eromom0900@alumno.ipn.mx
[2] CIC - IPN, Av. Juan de Dios Bátiz, Esq. Miguel Othón de Mendizábal,
Nueva Industrial Vallejo, Delegación Gustavo A. Madero, 07738, México D.F.
mriveroa@ipn.mx
[3] UPIITA - IPN, Av. Instituto Politécnico Nacional 2580,
Barrio La Laguna Ticomán, Gustavo A. Madero, 07340, México .D.F.
ivillordo@ipn.mx

**Abstract.** In this paper, the performance of a cluster-based wireless sensor network is studied when an adaptive transmission probability scheme is used to form the clusters. The cluster scheme is based on the well-known LEACH protocol, which organizes the nodes inside a wireless sensor network in clusters in order to distribute the energy load of each node. However, unlike LEACH, nodes are chosen to be cluster heads or cluster members only based on the order of arrival of nodes (called LEACH MOD), instead of whether or not a node has been a cluster head previously, in order to reduce the processing time and energy consumption added by the role selection scheme proposed by LEACH. The nodes transmit with a certain probability in order to create the cluster; as such, the adaptive transmission scheme, chooses the adequate value for the transmission probability based on the estimation of a number of nodes attempting a transmission in the following time slots. In this work, we study the impact of the error estimation on the energy consumption and the average formation cluster time when the network works with such scheme.

**Keywords**: Wireless Sensor Network, adaptive transmission probability, LEACH, energy consumption, clustering formation.

## 1 Introduction

The growing interest in control, knowledge and monitoring all sorts of physical variables around us causes the need to find new technologies that simplify such task. In order to perform such tasks, there are different techniques that allow doing that environmental sensing, from human supervision to technologies like closed circuit video surveillance, process automation or the use of sensor networks.

In this case, the use of a Wireless Sensor Network (WSN) gives the possibility to collect different information depending on the application, providing the possibility of

constant monitoring. Additionally, WSNs offer the advantage of the use of small nodes that can be installed inside different spaces, like a wall, a roof, under the pavement, etc. However, energy consumption becomes a focal parameter because the nodes, due to their small size, are provided with a battery of small size and capacity.

Efficient energy consumption inside the network allows extending the lifetime of the system. When a node drains all its battery, this node no longer operates in the network and all the nodes associated to it and the whole system suffers an operational degradation, due to information losses. Specifically, the effects in the system when a node consumes its battery energy are:

- Information loss.
- Reduction in the coverage area.
- Connection losses among nodes.

The energy consumption is even more critical in such scenarios where the coverage area is particularly high, such as monitoring in a desert, forest, or any other open place. In this case, the energy consumption increases due to the high-energy transmissions of nodes in order to reach the sink node. In this case the network have two options to cover the total coverage area:

- Increase the total number of nodes in the network
- Increase the distance between each node

This work focuses on such environments. Specifically, a clustering protocol is proposed, based on the well-known LEACH [1] protocol, in order to allow efficient network operation in large area. To this end we propose LEACH-MOD, which establishes a modification in the cluster formation phase as follows: unlike LEACH, nodes are chosen to be cluster head or cluster members only based on the order of arrival of the nodes in order to reduce the processing time and the energy consumption.

Furthermore, nodes do not transmit in the cluster formation phase with a constant transmission probability $\tau$, but rather this value varies according to the number of nodes remaining to transmit their control packet. As such, the transmission probability decreases in each successful transmission. According to the results presented in this work, this adaptive transmission probability reduces both energy consumption and cluster formation time.

## 2 System Model

In this section, the main system parameters and assumptions are presented. A square coverage area of 100 squared meters with a variable number of nodes is considered in order to analyze the performance of the cluster formation process under different scenarios.

The energy consumption model considered is now described in detail. We considered normalized energy units as values of energy required for the packet transmission and reception. This is basically in order to have a general energy consumption model that can be easily scaled to any commercial equipment. Building on this, we assume the following:

- The energy required to transmit a packet in the cluster formation phase (CF), is $E_{tx}^{CF}$ = 0.02 units.
- The energy required to receive a packet in the cluster formation phase is $E_{rx}^{CF}$ = 0.01 units.
- The energy required to transmit a packet from a cluster member to a cluster head in the steady state is $E_{tx}^{Steady}$ = 0.01 units.
- The energy consumed by the cluster head in order to receive a packet from a cluster member in the steady state is $E_{rx}^{Steady}$ = 0.01 units.
- The energy consumed by the cluster head to transmit a packet to the sink node (CH→Sink), is $E_{tx}^{CH->Sink}$ = 0.2 units.

Note that the energy required to transmit a packet is always higher than the energy required to receive such packet. Also the packet transmission from the cluster head to the sink node is the most energy consuming.

Finally we consider a percentage of nodes that act as cluster heads as follows: for LEACH, five percent of nodes in average act as cluster heads while in LEACH-MOD, $N_{CH}$ nodes always become cluster heads.

## 3 LEACH

LEACH is a protocol that organizes the nodes inside a wireless sensor network in clusters in order to distribute the energy load of each node. In this way, all nodes organize themselves to take part in a unique cluster as cluster head (CH) or as cluster member (CM). The cluster head of each cluster have the function of gather the sensed data of each node that belongs to the cluster. When the cluster head has gathered all the cluster information, it sends the data to the sink or base station.

We can easily see that CHs consume much more energy since they have to be constantly receiving data from the CMs, and perform high-energy transmissions to the sink node. Hence, CHs drain their energy faster. For that reason, LEACH rotates the function of cluster heads among all nodes in the network in order to balance the energy consumption equitably. This rotation occurs periodically. The LEACH protocol considers 20-second TDMA periods, after which clusters are broken and the cluster formation starts again selecting new CHs.

This protocol is composed by two phases: The cluster formation phase, where nodes are selected either as CHs or CMs and the steady state phase, where clusters are already established and data transmission is achieved. In the former phase, a random access protocol is used. Specifically, the slotted NP-CSMA scheme is applied, where nodes transmit in each time slot with probability τ. In the steady state phase, a TDMA based scheme is preferred since the CH already knows the number of nodes that will report data in the cluster. Hence, transmissions can be done in an orderly fashion.
Nodes will choose to become cluster heads according to the following equation [2]:

$$T(n) = \begin{cases} \dfrac{P}{1 - Px\left(r \bmod \dfrac{1}{P}\right)} & if\ n \in G \\ 0 & otherwise \end{cases} \quad (1)$$

Where $P$ is the percentage of cluster heads into the network, $r$ is the number of current cluster heads and $G$ is the group of nodes that have not been cluster head in a previous time. In this way the protocol allows the correct distribution of energy consumption in each node.

Fig. 1 shows how the network is organized in clusters, where nodes with a blue circle are the cluster heads.

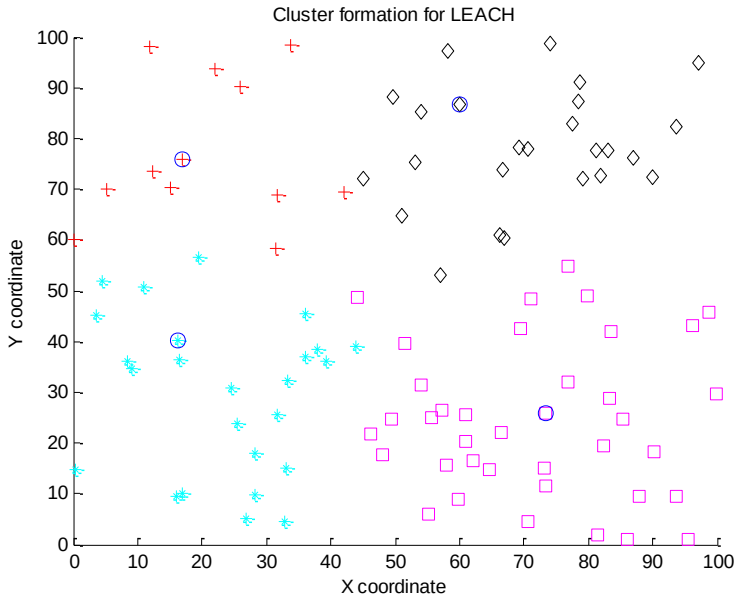


**Fig. 1.** Network organized in cluster for LEACH

## 4 Proposed Clustering Scheme

In this work, a new clustering protocol based on the well-known LEACH protocol is proposed and studied. This clustering protocol named LEACH-MOD, works as follows: nodes are chosen to be cluster heads or cluster members only based on the order of arrival of nodes. Specifically, in the cluster formation phase, nodes transmit in each time slot according to a geometric process with probability $\tau$. In any given time slot, if there are two or more transmissions, a collision occurs and non of the transmitted packets are received successfully and they have to be retransmitted. On the other hand, if only one packet is transmitted in a time slot, it is considered to be successful and all the nodes in the network recognize such transmission. Building on this, the LEACH-MOD scheme considers that the first $N_{CH}$ nodes that successfully transmit their packet become cluster heads while the rest become cluster members. The effect of the number of CHs on the performance of the system is investigated in a subsequent section.

Fig. 2 shows how the network is organized in clusters, where the nodes with a blue circle are the cluster heads. We can see that the position of each node and the number of nodes per cluster is different from Fig. 1 because both schemes have a random process with uniform distribution.

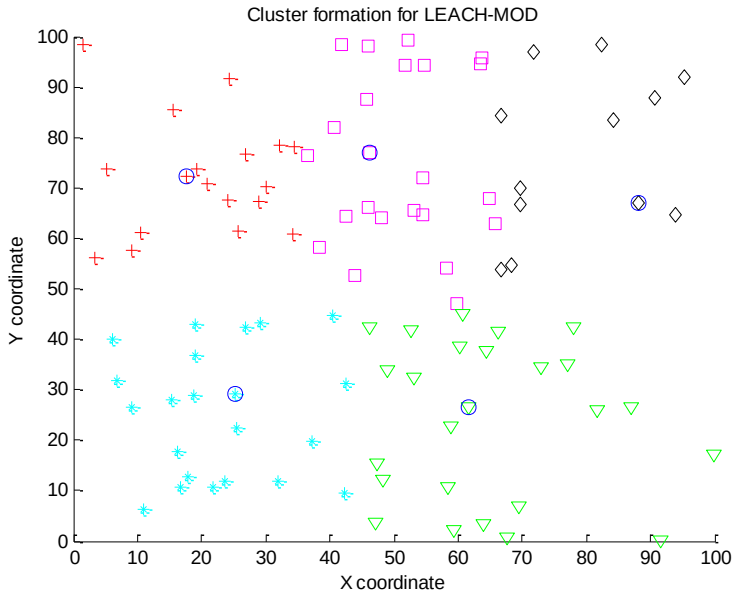


**Fig. 2.** Network organized in cluster for LEACH-MOD

The main reason to consider this modification to the LEACH protocols is as follows: As mentioned before, in the LEACH protocol, each node calculates its transmission probability according to the nodes that have been CHs before. As such, nodes need to calculate this transmission probability throughout the operation of the networks, which entails extra energy consumption and increases complexity. On the other hand, the LEACH-MOD strategy does not require this transmission probability computation. It is important to mention that the LEACH protocol ensures that no node can become CH in successive rounds. This cannot be guaranteed by our proposed protocol. However, since nodes transmit according to a geometric process with parameter $\tau$, the probability that a node is elected as a CH in consecutive rounds is very low. Also note that neither LEACH nor LEACH-MOD protocols ensure a uniform distribution of clusters in the system area.

On a more detailed study on the effect of the transmission probability in LEACH-MOD, note that when the number of nodes with a pending transmission is relatively high, the use of a high value of $\tau$ causes a high amount of collisions inside the cluster formation process, entailing a quick energy drain form all nodes in the system. On the other hand, the use of a low transmission probability in the same scenario entails a lower number of collisions. However, as nodes successfully transmit their control packet, the number of pending transmissions decreases accordingly. Hence, the low value of $\tau$ is no longer adequate when only a few nodes remain to transmit their packet since a high idle transmission period occurs. Building on this observation, it is clear that the value of the transmission probability has to vary according to the number of remaining nodes in the cluster formation procedure. As such, the adaptive transmission strategy is proposed.

### 4.1 Adaptive Transmission

As mentioned before, in the adaptive transmission probability strategy, the value of $\tau$ varies according to the number of nodes with a pending transmission. Hence, the transmission probability of each node depends on the inverse of the number of neighbor nodes. In this way, with a high number of contending nodes, the transmission probability is low, and viceversa. From this, each node computes the value of $\tau$ as follows:

$$\boldsymbol{\tau_A = \frac{1}{i}} \quad (2)$$

Where $\boldsymbol{i}$ is the number of remaining nodes in the cluster formation phase. As it can be seen, in order to calculate the value of $\tau$, it is required that each node estimates the number of nodes with a pending transmission. Also, the sink node, which does not have energy restriction issues, can perform this estimation and broadcast it to the rest of the nodes in the system. In this work, we consider the second approach.

This estimation can be done by detecting each successful transmission and assuming that the number of nodes in the system has not changed, i.e., that all initial nodes are still correctly functioning. However the successful transmission detection is not error-free in a wireless environment due mainly to fading, interference and noise. As such, we propose to study the effect of error estimation on the performance of the adaptive probability scheme. Specifically, we consider that two estimation errors can occur in such environment: false positive and false negative estimation. The latter corresponds to the case when the sink node does not detect a successful transmission while the former corresponds to the case when the sink node detects a successful transmission but in reality no such transmission occurred. As such, the estimation of $\tau$ can have a higher (in case of false negative estimation) or lower value (in case of false positive estimation) than the real value $i$. In this work, we assume that either false positive and false negative estimation errors are equally probable to happen. Hence, a uniform error distributed in the range of (-ε,ε) is considered. Consider that this assumption may not be accurate since the error can have different distribution or false negative and positive estimation may not be equally probable. However, the use of an accurate error model is outside the scope of this work and we leave it for future research.

From the previous discussion, we consider that the transmission probability in the cluster formation phase is now calculated as:

$$\boldsymbol{\tau_A} = \frac{\mathbf{1}}{\boldsymbol{i} + \boldsymbol{\varepsilon}} \tag{3}$$

Note that as in ( 2 ), the transmission probability varies in each time slot according to the estimated outcome of the previous time slot. As a particular case, when the estimation error is such that $i + \epsilon \leq 0$, the sink node broadcast the value of $\boldsymbol{\tau_A} = 0.9$ in order to avoid any operation malfunctions. Due to the fact that $\boldsymbol{\tau_A}$ and $\boldsymbol{\tau}$ are probabilities, they only can have values between 0 and 1, being 1 the maximum value where no more nodes are waiting to transmit and we can warrant a successful transmission to particular node; in the case when those probabilities have a minimum value represents that a big number of nodes are pending to transmit.

## 5 Numerical Results

In this section, we show some relevant numerical results. The main performance parameters considered in this section are the average cluster formation time and average energy consumption. Fig. 3 shows the average energy consumption in the system for different number of nodes in the network and different error estimation range ε. It can be seen that the use of the LEACH-MOD with the adaptive transmission scheme achieves lower energy consumption than the LEACH protocol. This is because in the LEACH-MOD the number of collisions and idle listening periods are reduced compared to the LEACH protocol. Similarly, the average cluster

formation time is lower in the LEACH-MOD compared to the LEACH protocol as shown in Fig. 4. As expected, the energy consumption and cluster formation time increase as the number of nodes increases.

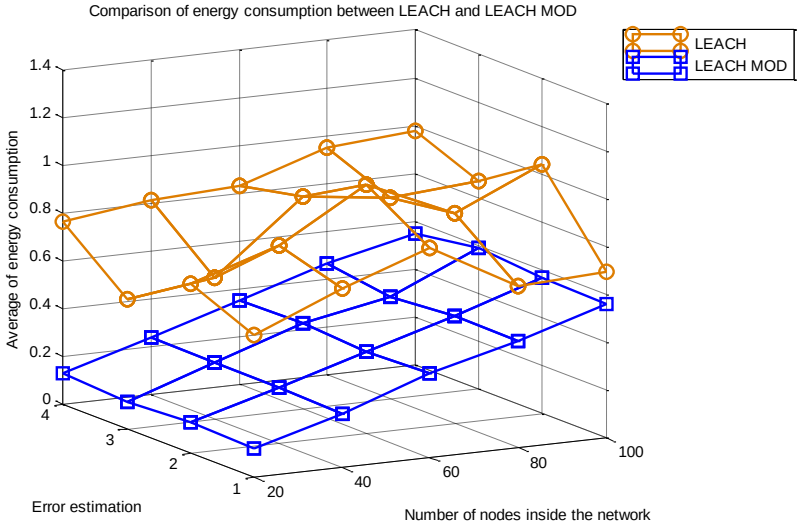


**Fig. 3.** Average cluster energy consumption under an adaptive probability of transmission

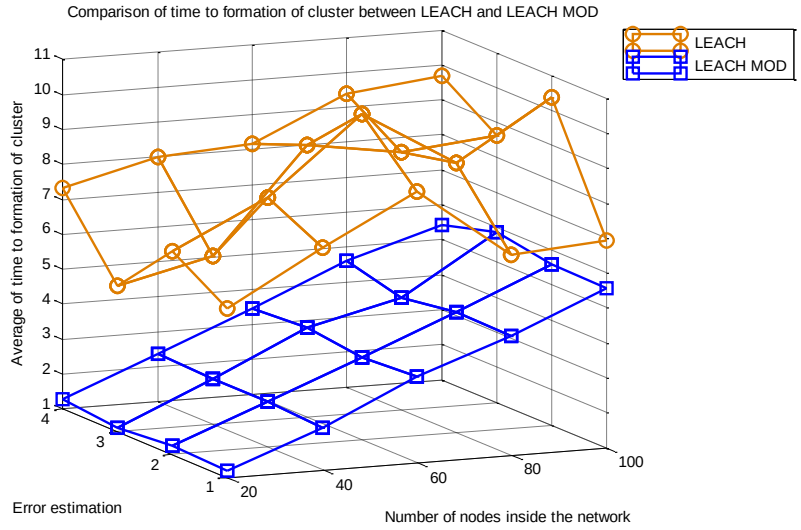


**Fig. 4.** Average cluster formation time under an adaptive probability to transmission

From these results, it can be seen that the effect of the error estimation is not high. The rationale behind this counterintuitive result is as follows: since a uniformly distributed estimation error is considered, in a given time slot a false positive error can occur while in the following slot a false negative error can happen with the same probability, cancelling out the effect of the error estimation. Hence, different estimation error distribution could be considered in a future work.

## 6 Conclusions

In this work, the LEACH-MOD protocol under an adaptive transmission probability is proposed and studied. From the results it is clear that a simple CH selection, like the LEACH-MOD protocol, can achieve a good system performance because the energy consumption and formation cluster time is lower than LEACH. Hence, energy consumption and complexity are reduced. Also, the use of the adaptive transmission strategy is of major importance to reduce energy consumption at the cluster formation phase. It is shown that a constant transmission probability entails a high amount of collisions and/or idle listening periods. However, the complexity of the adaptive scheme requires potential transmissions estimation. The design and proposal of an estimation algorithm is outside the scope of this paper due to its complexity.

However, we are interested on evaluating the system performance considering an estimation error. Furthermore, we proposed to study the effect of a uniformly distributed error in the range of $[-\varepsilon,\varepsilon]$ that models both the false positive and false negative estimation errors. From the presented results, it can be seen that the effect of such error is very low. Indeed, by considering a uniformly distributed error, the effect of a false negative error is cancelled out by the false positive errors. As such, following this line of research, different error distribution must be considered for a practical system implementation.

## 8 References

1. Handy, M. J., Haase, M., Timmermann, D.: Low Energy Adaptive Clustering Hierarchy with Deterministic Cluster-Head Selection. 4th International Workshop on Mobile and Wireless Communications Network, 2002.
2. Rabiner ,W., Chandrakasan A., Balakrishnam, H.: Energy-Efficient Comunication Protocol for Wireless Microsensor Networks. Massachusetts institute of Technology Cambridge, Massachusetts, USA, 2000.
3. Kredo, K.: Medium Access Control in Wireless Sensor Networks. University of California, California, USA.
4. Lee H.: Towards a General Wireless Sensor Network Platform. IEEE, Taiwan, ROC, 2012.
5. Johnson, D.B., Maltz, D.A.: Protocols for Adaptive Wireless and Mobile Networking. IEEE Personal Communications, vol. 3, no. 1, 1996.

6. Owojaiye G., Sun, Y.: Focal design issues affecting the deployment of wireless sensor networks for intelligent transport. IEEE, UK., 2012.
7. Ruizhong, L., Zhi, W., Youxian, S: Energy Efficient Medium Access Control Protocols for Wireless Sensor Networks and Its State-of-Art. National Laboratorv of Industrial Control Technology, Institute of Modem Control Engineering, Hangzhou, China, 2004.
8. Spyropoulos, T., Psounis, K., Raghavendra, C.: Performance Analysis of Mobility-assisted Routing. Department of Electrical Engineering, USC, Florence, Italia, 2006.

# Performance Evaluation of Energy-Efficient Game-Theoretic Resource Allocation Schemes in OFDMA Cellular Networks

Emmanuel Duarte-Reynoso, Domingo Lara-Rodríguez

Electrical Engineering Department, CIVESTAV-IPN, México
{eduarte,dlara}@cinvestav.mx

**Abstract.** In this paper, we study the performance of energy-efficient resource allocation schemes for multi-cell OFDMA networks based on Game Theory. These schemes have been evaluated in the literature; however, the evaluations have been done under different system models and simulation environments, making a fair comparison unfeasible. Hence, we first develop an appropriate system model for comparison. Then, we analyze the implementation of the selected schemes under constraints introduced by the proposed system model. Finally, throughout extensive numerical simulations on a realistic environment, we evaluate the performance and tradeoffs between energy efficiency, throughput, outage probability and fairness, highlighting the need for some scheme that improves the outage probability and the throughput maintaining high energy efficiency.

**Keywords:** resource allocation, OFDMA, energy efficiency, game theory.

## 1 Introduction

The growing demands of higher speed and reliable communications in next-generation wireless networks have motivated to adopt OFDMA in the current proposals for this kind of networks (3GPP LTE and IEEE 802.16m for instance) due to its robustness and flexibility. Dynamic resource allocation allows OFDMA systems to exploit multi-user diversity leading to a significant performance improve in terms of throughput, fairness and efficiency. Due to this feature, the problem of resource allocation in OFDMA has caught researchers' attention in the last years (e.g. [1-3]).

Resource allocation schemes are designed with a specific objective, typically capacity maximization [4]. However, the need to transmit user generated content and the limited power available at user devices has motivated researchers to address the resource allocation problem in OFDMA through an energy-efficient approach. Nevertheless, the subcarrier assignment problem as demonstrated in [5] is a non-convex optimization problem thus, the global optimization of this problem is unfeasible and some alternative methods should be studied to address it.

Besides, game theory [6] that focuses in distributed solutions to agent interaction problems is presented as a valuable tool that enables the abstraction of resource allo-

cation problem through a different approach and the application of its fundamental results to simplify the analysis of this problem. Numerous energy-efficient game-theoretic allocation schemes have been proposed in the open literature (e.g. [8-14]). Our aim in this paper is to establish a common system model to perform a comparison between some selected of these schemes.

This paper is structured as follows. Next section describes the system model used in the comparison. Section 3 gives an overview of the compared schemes. Section 4 presents the simulation environment as well as the corresponding numerical results. Last, conclusions are presented in Section 5.

## 2 System Model

The system model presented is based on the 3GPP LTE physical layer specifications [15]. We consider the uplink channel of a multi-cell OFDMA network with universal frequency reuse. Let $M = \{m,\ m = 1,2,...|M|\}$ denote the set of cells in the network, and $K = \{k,\ k = 1,2,...,|K_m| \cdot |M|\}$ , the set of active users (mobile stations) with $K_m = \{k | m_k = m\}$ the set of active users in cell $m$, where $m_k$ is the base station to which user $k$ is assigned.

The available spectrum is divided into physical resource blocks (PRBs); each PRB is formed by $N_b$ subcarriers with frequency spacing $BW$, so we let $N$ be the set of PRBs in the system. Each cell $m$ allocates the complete set of PRBs among its active users through the allocation matrix $A = \{a_{m,n}\}$, where element $a_{m,n}$ indicates the user to which PRB $n$ has been allocated. PRB allocation is repeated each transmission interval which consists of $D_s$ signaling symbols and $D_d$ user information symbols.

It is assumed that the receiver and the transmitters have perfect channel state information (CSI) and that it is possible to use a single coefficient $h_{m,k}^2(n)$ to represent the channel power gain between user $k$ and base $m$ in PRB $n$. The transmit power vector of user $k$ is denoted by $p_k = \{p_{k,n} | p_{k,n} \geq 0\}$, where element $p_{k,n}$ indicates the transmit power of the user for every subcarrier in PRB $n$. This vector has the following restrictions:

$$p_{k,n} = 0,\ a_{m_k,n} \neq k \tag{1}$$

$$\sum_{n \in N} p_{k,n} \leq \frac{P_{\max}}{N_b} \tag{2}$$

where (1) prevents the existence of intra-cell interference and (2) stands for the limited power source at mobile station.

We consider the effect of additive white Gaussian noise (AWGN) with power $\sigma^2$ at the receiver; thus, the signal to noise plus interference ratio (SINR) of user $k$ at base $m$ such that $a_{m,n} = k$ over PRB $n$ is computed as:

$$\gamma_{m,n} = \frac{p_{k,n} h_{m,k}^2 (n)}{\sigma^2 + I_{m,n}} \tag{3}$$

where $I_{m,n}$ is the power of the interference received at base $m$ over PRB $n$:

$$I_{m,n} = \sum_{j \in K | j \neq k} p_{j,n} \cdot h_{m,j}^2 (n) \ . \tag{4}$$

Given the SINR $\gamma_{m,n}$ the goodput at base $m$ over PRB $n$ is obtained as:

$$r_{m,n} = \frac{D_s}{D_s + D_d} N_b \cdot BW \cdot e\left(\gamma_{m,n}\right) \ , \tag{5}$$

where $e\left(\gamma_{m,n}\right)$ is an efficiency function dependent of the modulation used by the mobile station, that gives the effective data rate in bps/Hz. Energy efficiency is computed for user $k$ transmitting to base $m$ over PRB $n$ as

$$u_{k,n} = \frac{r_{m,n}}{p_{k,n}} \ , \ a_{m,n} = k \tag{6}$$

Finally, we define the no-transmission probability as the probability that in a given transmission interval, the total transmitted power of a user is equal to zero, i.e. $\sum_{n \in N} p_{k,n} = 0$.

## 3 Energy-Efficient Resource allocation schemes

Since the seminal works presented by Goodman et al [16] many game theoretic energy-efficient power control and subcarrier allocation schemes have been reported in the literature (e.g. [8-14]). As stated before, we aim to compare the performance of these schemes; however, it is worthless to make a comparison between all of them because some schemes are not feasible or simply it has been demonstrated that they are outperformed by others. Hence, we have selected three schemes for comparison, taking into account that their system models are close to the one presented in section 2 and that they consider both, subcarrier and power allocation. In the following, we give a brief description of these schemes.

### 3.1 Scheme 1

The first scheme is the one presented in [13]. In this scheme the problem is decoupled into subcarrier assignment and a subsequent power allocation. Subcarrier assignment is done in a centralized manner, i.e. it is performed by the base stations. To address this problem, the authors propose a heuristic algorithm to be executed by each base station in the network.

This algorithm divides the set of subcarriers $N$ into $C$ clusters denoted as $N^{(1)},...,N^{(C)}$, where each cluster has a number of subcarriers equal to the number of active users in the cell. In order to provide farther users with a significant performance and, in this way improve the fairness of the allocation, the algorithm tries to allocate one subcarrier per user in each cluster. This is done by allocating each user with its best available subcarrier starting by the users with the lowest channel gains. Nevertheless, this could induce negative effects to the global performance if users are experiencing deep fading conditions. To limit such negative effects, no subcarriers are allocated to users with too weak channel conditions. To place and adaptive threshold, it is prevented a user from receiving any subcarrier if its channel gain in its best subcarrier is $\lambda$ times lower than the highest one in that subcarrier. The value of the threshold is set in the interval $0<\lambda<1$ which allows to trade off performance and fairness in the network.

When subcarrier assignment has been done by the base stations, the power control is addressed as a non cooperative game between the users in the system considering QPSK fixed modulation. Particularly, based on the results on [16], a best-response dynamic is proposed in which user $k$ adopts a transmit power

$$p_{k,n}^{*}=\min\left(p_{\max},\frac{\gamma_k^{*}\left(\sigma^2+I_{m,n}\right)}{h_{m,k}^{2}\left(n\right)}\right) \tag{7}$$

where $\gamma_k^{*}$ is the SINR such that

$$\frac{f\left(\gamma_{i_k}^{*}\right)}{\gamma_{i_k}^{*}}=f'\left(\gamma_{i_k}\right)\Big|_{\gamma_{i_k}=\gamma_{i_k}^{*}} \tag{8}$$

where $f\left(\gamma\right)$ is the efficiency function for the used modulation, defined in (5) as $e\left(\gamma\right)$. The model considered in scheme 1 is very close to that proposed in section 2. We only introduce the constraint of a minimum SINR threshold that has to be achieved and we consider the allocation of PRBs instead of subcarriers.

### 3.2 Scheme 2

Scheme 2, was first presented in [12]. Here, the authors claim that due to the difficulty of optimizing the non-convex function of the sum of energy efficiency, it is

more feasible to maximize it in a time-averaged manner instead taking an averaging window of size $w$.

This scheme proposes a framework where the base stations are the players that form $|N|$ independent non-cooperative games, one game per subcarrier. In each game, at transmission time interval $t$, the base stations will attempt to maximize the average efficiency in the corresponding subcarrier, allocating it to the user with the greatest ratio between optimal achievable rate $r_{m,n}^{k^*}$ and its average transmit power at $t-1$ $P_{k,n}(t-1)$. It is considered that users are capable of select its modulation scheme adaptively from a set $Q$ so that the optimal achievable rate could be not feasible; thus, it is necessary to define an efficiency gap:

$$\Delta g_{m,n}^{k}(t) = \min_{q \in Q} \left| \tilde{r}_q - r_{m,n}^{k^*}(t) \right| \tag{9}$$

where $\tilde{r}_q$ is the rate corresponding to modulation scheme $q \in Q$. Hence, each subcarrier is assigned to the user that maximize

$$\eta_{m,n}^{k}(t) = \frac{\hat{r}_{m,n}^{k^*}(t) - \beta \Delta g_{m,n}^{k}(t)}{P_{k,n}(t-1)} \tag{10}$$

where $\beta$ is a design parameter that takes values between 0 and 1. After this, each user adopts the modulation scheme that minimizes its efficiency gap and the transmit power need to achieve the SINR threshold corresponding to this modulation scheme.

It is worth noting that in the proposed game, a change in the strategy of a base station might change the assigned user which usually results in different interfering power to other cells, so other cells will continue the best response dynamic until an equilibrium point is reached. However, the game doesn't guarantee to converge to an equilibrium so it is necessary to limit the maximum iteration time to prevent infinite loop.

Some refinements are needed to implement this scheme considering the model proposed in section 2. First, we consider the modulation schemes and its BLER curves reported in [17]; those curves give us the information needed to compute the efficiency function $e(\gamma_{m,n})$ and the goodput in (5). Second, this scheme does not consider the case where a user is not capable to achieve the minimum SINR threshold, so we established that in this case, the user set its transmit power to cero. Finally, as we stated for scheme 1, we consider PRBs instead of subcarriers.

### 3.3 Scheme 3

This last scheme proposed by Buzzi et al [10], resorts to potential game theory as a potential game is guaranteed to converge to the Nash equilibrium point through the best (or better) response dynamic. It is considered a strategy space in which each user

choose an equal number of subcarriers $L$ as well as its transmit power aiming to maximize the system energy efficiency.

Taking into account these considerations, a non-cooperative potential game is proposed. The potential function is defined as the natural logarithm of the efficiencies of each user over each subcarrier:

$$V = \ln\left(\prod_{k=1}^{K}\prod_{\substack{n\in N,\\ a_{m,n}=k}}\frac{e\left(\gamma_{m,n}\right)}{p_{k,n}}\right) \tag{11}$$

where $e\left(\gamma_{m,n}\right)$, the efficiency function of the fixed QPSK modulation is defined as:

$$e\left(\gamma_{m,n}\right) = \left(e^{-\beta/\gamma_{m,n}}\right)^{D_d} \tag{12}$$

where $\beta = \gamma^* / M$, and $\gamma^*$ is the optimum SINR defined by (8).

In [10] it is shown that $V$ is the potential function when the user's utility is given by

$$\begin{aligned} u_k\left(a_{m_k,n}, p_{k,n}\right) = &-\beta D_d \sum_{\substack{n\in N\\ a_{m,n}=k}} \frac{\sigma^2 + \sum_{j=1,\, j\neq k}^{K} p_{j,n} h^2_{m_k,j}(n)}{p_{k,n} h^2_{m_k,k}(n)} \\ &-\beta D_d \sum_{i=1, i\neq k}^{K} \sum_{\substack{n\in N\\ a_{m_i,n}=i}} \left(\frac{p_{k,n} h^2_{m_i,k}(n)}{p_{i,n} h^2_{m_i,i}(n)}\right) - \sum_{\substack{n\in N\\ a_{m,n}=k}} \ln\left(p_{k,n}\right) \end{aligned} . \tag{13}$$

This indicates that the best response dynamic, in which every user updates its subcarriers and transmit power to maximize (13) (in a combinatorial fashion) will converge to a Nash equilibrium point. Once that we have presented this scheme some aspects have to be pointed out with respect to the model presented in section 2.

As it was established, all the PRBs have to be allocated; thus, the value of $L$ becomes a function of the number of active users in each cell. The authors don't impose any constraint to prevent the frequency reuse within the cell, so the best dynamic response could lead to this situation. If so, we set the next rule: if more than one user is allocated a given subcarrier the base station takes a decision, allocating the subcarrier to the user which achieves the higher efficiency. Due to the need of the base station intervention and the form of the potential function, which require CSI from all users this scheme is considered as a centralized scheme. In order to reduce the computational complexity of this scheme, which comes from the combinatorial search performed for each user, we adopt the sub-optimal implementation proposed in [10]. As in the previous cases, we consider the allocation of PRBs instead of subcarriers and a minimum SINR threshold $S_{\min}$.

# 4 Numerical results

## 4.1 Simulation setup

In order to compare the presented schemes under realistic conditions, we set our simulation environment according to [15]. We considered a 19 cell grid, i.e. a center cell and the first two tiers of surrounding cells. To mitigate the border effect we make use of the wrap-around technique [18]. Cell radius is $R = 1000$ m.

The number of PRBs available in the system is $|N| = 50$, these PRBs consist of $N_b = 12$ subcarriers and the space between subcarrier frequencies is $BW = 15$ kHz. Location of active users follows a uniform distribution restricted to distances larger than 35 m from the base station. Maximum transmission power per user $P_{\max}$ is set to 21 dBm and noise power spectral density at base stations is $N_0 = $ -170 dBm/Hz. Channel coefficients are computed as:

$$h^2_{m,k}(n) = \mu_{m,k} \hat{h}^2_{m,k}(n) \tag{14}$$

where $\hat{h}^2_{m,k}(n)$ models fast fading and is computed from ITU pedestrian-A channel profile [19]; while $\mu_{m,k}$ is a frequency-independent factor which includes shadowing and path-loss effects:

$$\mu_{m,k} = 10^{\frac{-L_{m,k} + X_\sigma}{10}} \tag{15}$$

where $X_\sigma$ is a gaussian random variable with standard deviation of 10 dB and $L$ represents path-loss which is computed as:

$$L_{m,k} = 128.1 + 37.6 \log_{10}\left(\frac{d_{m,k}}{d_0}\right) \tag{16}$$

where $d_{m,k}$ is the distance between user $k$ and base $m$; and $d_0$ is the reference distance equal to 1 km. We consider a transmission time interval of 1 ms, having $D_s = 4$ signaling symbols and $D_d = 10$ information symbols.

The parameters concerning each compared scheme are detailed in the following. According with the results reported in [13], we set the value of threshold $\lambda$ to -20 dB for scheme 1. The averaging window size of scheme 2 is $w = 10$ and parameter $\beta$ was set to 0.7. We consider a minimum SINR threshold for all schemes equal to -1.43 dB.

### 4.2 Simulation results

Having established a common simulation environment we are able to compare the performance of the resource allocation schemes. This subsection presents the results for different performance metrics as a function of the distance between the user and its base station considering a fixed number of users per cell $|K_m| = 20$.

Fig. 1 shows the average efficiency performance. As can be seen scheme 1 achieves the largest efficiency for distances shorter than 250 m while scheme 2 outperforms it for larger distances. Efficiency decays with the distance as farther users require more power to achieve the same SINR that center users. Nevertheless it is worth noting that all three schemes decay with a different rate, in particular we observe that this rate is higher for scheme 1, followed by scheme 2 and by scheme 3.

To have a better understanding of what happens with efficiency, we can resort to the results of Fig. 2 and Fig. 3 which present the average goodput and average transmit power respectively. Scheme 1's goodput is the greater for distances less than 750 m. However its transmit power is not the lowest, hence it is outperformed in terms of efficiency by scheme 2 which achieves an intermediate goodput and maintains the lowest transmit power. This is done by means of the modulation adaptation considered in scheme 2. On the other hand, scheme 3 has the lowest goodput and the highest transmit power which results in a low efficiency, which is due to the PRB assignment rule in scheme 3 that tries to introduce some fairness by allocating the same number of PRBs per user. By doing so, the performance gap between cell-center users and edge users is reduced but the goodput for all users is reduced as well.

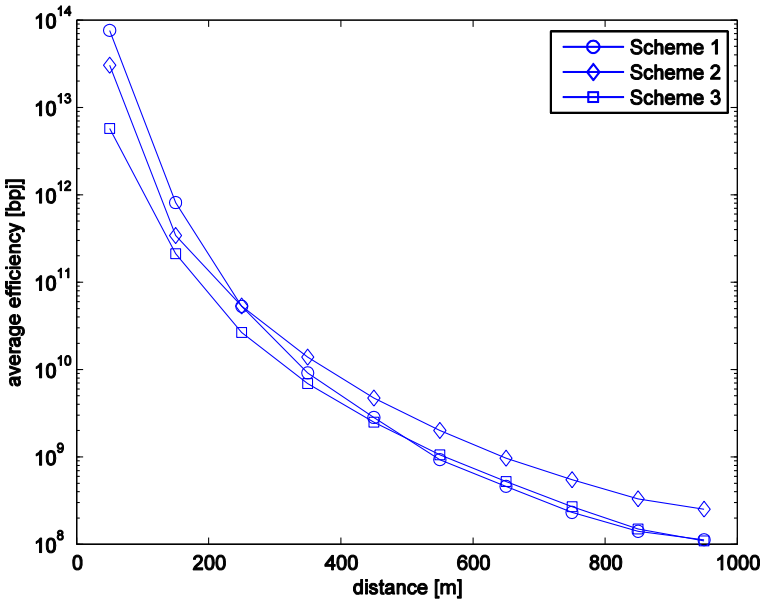


**Fig. 1.** Average energy efficiency as a function of the user distance

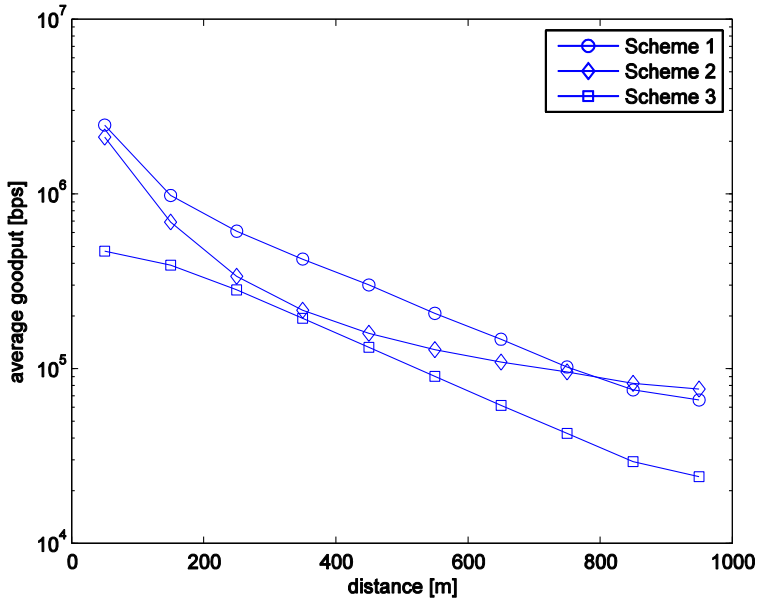


**Fig. 2.** Average goodput as a function of the user distance

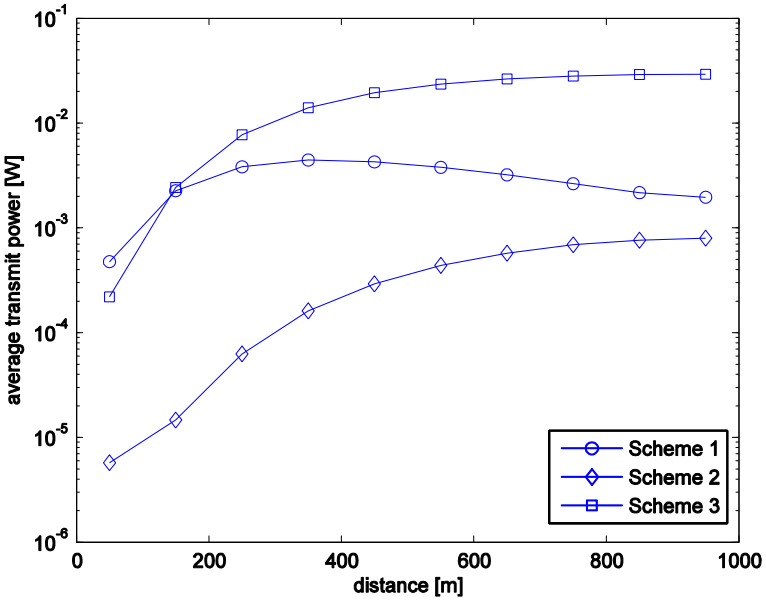


**Fig. 3.** Average transmit power as a function of the user distance

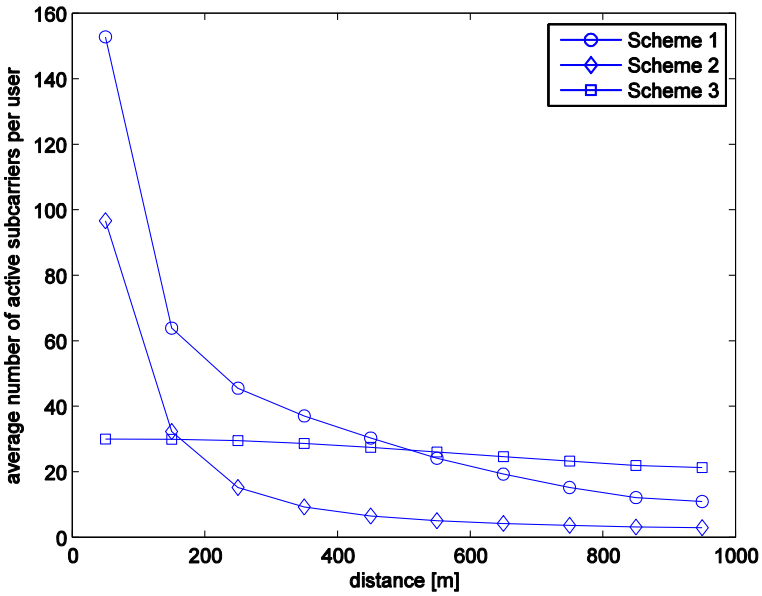


**Fig. 4.** Average number of active subcarriers as a function of the user distance

Another interesting result comes from the shape of the transmit power curve for scheme 1. Unlike schemes 2 and 3, the transmit power of scheme 1 decreases for distances greater than 350 m, which means that the number of subcarriers allocated to users at those distances by scheme 1 decreases significantly.

The number of active subcarriers per user, depicted in Fig. 4, gives us information about the PRB allocation method of each scheme. As can be seen, scheme 1 and scheme 2 tend to allocate a greater number of subcarriers to users near the base having a drastic drop down in this number for the farther users. However, users in scheme 1 have always more active subcarriers than users in scheme 2 which indicates that the introduction of the threshold $\lambda$ for allocation in scheme 1 helps edge users to improve its performance. In contrast, scheme 2 doesn't have any notion of justice as it tries to maximize the overall energy efficiency sum. Besides, scheme 2's centralized allocation guarantee that all users receive the same number of PRBs and the slight decrease for farther users only indicates that their channel conditions are too bad to transmit in some of the allocated PRBs.

Finally, Fig. 5 presents the average no-transmission probability, which has not been reported for any of the compared schemes. It is noted that schemes 1 and 2 have no-transmission probabilities that are above 90% while scheme 3 maintains it below 20%. These results are directly related to the way in which PRBs are allocated and the way in which the interference is managed. In the first two schemes most PRBs are allocated to users with the best channel conditions which turn out to be the users near the base, while the farther users receive less PRBs as discussed above. Furthermore, these two schemes try to mitigate interference only through power control. On the

other hand, scheme 3 performs an equal number allocation in a centralized manner; in this way, it can control the interference by means of both PRB allocation and power control. Analyzing these results we note that each scheme implies a different trade-off between energy efficiency, fairness and no-transmission probability. However, the need of a novel scheme that reduces the no-transmission probability while maintaining the energy efficiency and throughput is evidenced.

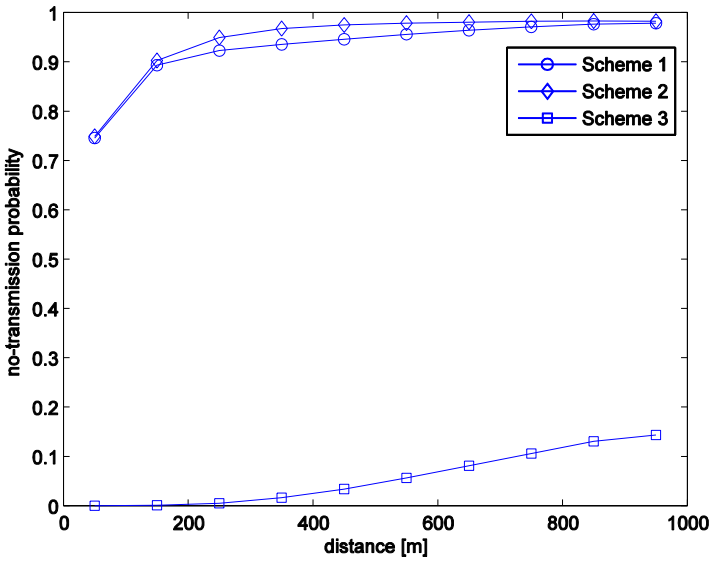


**Fig. 5.** No-transmission probability as a function of the user distance

## 5 Conclusions

A comparison considering a common system model and a realistic simulation environment between three different energy efficient game-theoretic resource allocation schemes is presented in this paper. The results show the tradeoffs in the different schemes, evidencing the need of a novel scheme which improves the fairness of the system by reducing the no-transmission probability while maintaining the energy efficiency per user.

## References

1. Wong, C.Y., Cheng, R.S., Letaief, K.B., Murch, R.D.: Multiuser subcarrier allocation for OFDM transmission using adaptive modulation. In: IEEE Vehicular Technology Conference, pp. 479-483. IEEE Press, Texas (1999)

2. Tham, M. L., Chow, C.O., Utsu, K., Ishii, H.: BER-driven resource allocation in OFDMA systems. In: IEEE 24th International Symposium on Personal Indoor and Mobile Radio Communications (PIMRC), pp.1513-1517, IEEE Press, San Francisco (2013)
3. Hanly, S.V., Andrew, L.L.H., Thanabalasingham, T.: Dynamic Allocation of Subcarriers and Transmit Powers in an OFDMA Cellular Network. IEEE Transactions on Information Theory, vol. 55, no. 12, 5445-5462 (2009)
4. Yiwei, Y., Dutkiewicz, E.; Xiaojing H., Mueck, M.: Downlink Resource Allocation for Next Generation Wireless Networks with Inter-Cell Interference. IEEE Transactions on Wireless Communications, vol. 12, no. 4, 1783-1793 (2013)
5. Wei, Y. Wonjong, R., Boyd, S., Cioffi, J.M.: Iterative water-filling for Gaussian vector multiple-access channels. IEEE Transactions on Information Theory, vol. 50, no. 1, 145-152 (2004)
6. Ya-Feng L., Yu-Hong D.: On the Complexity of Joint Subcarrier and Power Allocation for Multi-User OFDMA Systems. IEEE Transactions on Signal Processing, vol. 62, no. 3, 583-596 (2014)
7. Fudenberg, D., Tirole, J.: Game Theory. MIT Press, Cambridge, MA (1991)
8. Hui, L., Wei, Z., Haijun, Z., Zhicai, Z., Xiangming, W.: An iterative two-step algorithm for energy efficient resource allocation in multi-cell OFDMA networks. In: Wireless Communications and Networking Conference (WCNC), pp. 608-613, IEEE Press, Shangai (2013)
9. Alavi, S.M., Chi, Z., Wan, W. G.: Efficient and Fair Resource Allocation Scheme for OFDMA Networks Based on Auction Game. In IEEE Vehicular Technology Conference, pp.1-5, IEEE Press Quebec (2012)
10. Buzzi, S., Colavolpe, G., Saturnino, D., Zappone, A.: Potential Games for Energy-Efficient Power Control and Subcarrier Allocation in Uplink Multicell OFDMA Systems. IEEE Journal of Selected Topics in Signal Processing, vol. 6, no. 2, 89-103 (2012)
11. Dan W., Liang Z., Yueming C., Rodrigues, J.: Energy-efficient resource allocation for uplink OFDMA systems using correlated equilibrium. In: Global Communications Conference (GLOBECOM), pp.4589-4593, Anaheim (2012)
12. Chieh Y. H., Ching-Yao H.: Non-Cooperative Multi-Cell Resource Allocation and Modulation Adaptation for Maximizing Energy Efficiency in Uplink OFDMA Cellular Networks. Wireless Communications Letters, vol.1, no.5, 420-423 (2012)
13. Bacci, G., Bulzomato, A., Luise, M.: Uplink power control and subcarrier assignment for an OFDMA multicellular network based on game theory. In: Int. Conf. Perf. Eval. Methodol. Tools (ValueTools), Paris (2011)
14. Jing, Q., Zheng, S.: Distributed Resource Allocation Based on Game Theory in Multi-cell OFDMA Systems. International Journal of Wireless Information Networks. Vol. 16 . No. 1-2, 44-50 (2009)
15. 3GPP TR 25.814.: Physical layer aspects for evolved UTRA (release 7), 3GPP (2006)
16. Goodman, D., Mandayam, N.: Power control for wireless data. IEEE Personal Communications, vol. 7, no. 2, 48–54 (2000)
17. 3GPP TR 25.892.: Feasibility study for OFDM for UTRAN enhancement (release 6), 3GPP (2004)
18. Lin, Y.B., Mak, V. W.: Eliminating the boundary effect of a large-scale personal communication service network simulation. ACM Transactions on Modeling and Computer Simulation, vol. 4, no. 2, (1994)
19. ITU-R. M.1225.: Guidelines for Evaluation of Radio Transmission Technologies for IMT-2000: ITU-R (1997)

# Implementation of the communication protocols SPI and I2C using a FPGA by the HDL-Verilog language

Tatiana Leal-del Río[1], Gustavo Juarez-Gracia[1], L. Noé Oliva-Moreno[2]

[1] CICATA, Legaria, México
[2] ESCOM, México
mileydy.1125@gmail.coma, agjuarez@ipn.mxb,loliva@ipn.mx

**Abstract.** Currently, the most used serial communication protocols to exchange information between different electronic embedded devices are the SPI and I2C. This paper describes the development and implementation of these protocols using a FPGA card. For the implementation of each protocol, it was taken into account different modes of operation, such as master/slave mode sending or pending data mode. For the implementation of the I2C protocol was necessary to perform a tri-state buffer, which makes a bidirectional data line for a successful communication between devices, allowing to take advantage of these sources provided by the FPGA. Verilog is a hardware description language better known as HDL and it was used in the work to implement and simulate these communication protocols with the software version 14.7 of Xilinx ISE Design Suite.

## 1 Intorduction

Nowaday the integration of different embedded electronic modules include at least some of these functions: intelligent control, general purpose circuits, analog and digital I/O data ports, volatile memories (RAM), non-volatile memories (EEPROM, FLASH), real time clocks, ADC, among others. The integration is possible because of the development of different kind of wired and wireless communications.

The integrated circuit peripherals allow for the interaction among electronic devices for exchanging data, either the integrated circuit performs the default connection tasks or has to be implemented by software.

The wired communication protocols SPI e I2C are important for this work, so this paper summarizes their main features.

I2C (Inter-Interface Circuit). The I2C bus uses a bit in the device address to indicate read or write operations. The Master transmits the Slave's Address and a Read or Write bit to indicate the direction of the transfer. The I2C bus can be either a single-master or multi-master. Each electronic embedded device has a unique 7-bit or 10-bit address and it is limited to 8 bit's transfers. The I2C supports three basic modes of operation providing different levels of performance and device's address mapping: standard mode (up to 100 Kbits/sec, 7 bit addressing); fast mode (up to 400 Kbits/sec, addressing between 7 to 10 bits); high-speed mode (up to 3.4 Mbits/sec, addressing between 7 to 10 bits) [1] [2].

SPI (Serial Protocol Interface). The SPI bus is a 4-wire full-duplex interface synchronous serial data link [3]. Indeed, it is a (3+N)-wire interface where N is the number of devices connected to a single master device on the bus. Only one master can be active on the bus. Unlike I2C, SPI supports a transfer size of integer multiples of 8 bits. Technically the SPI bus shift register's length limits the size of the data transfers. The SPI bus can support a variety of transfer speeds but the bus is limited by the system´s clock. The SPI interface is generally is able data rates of several Mbits/sec.

This paper describes the procedure used to implement the synchronous serial communication protocols SPI and I2C by means of the hardware programming language Verilog HDL (Hardware Description Language).

The outline of this paper is divided in four sections. Section 2 discusses the research course; section 3 illustrates the methods used in the development of this work. Section 4 reports the obtained results and conclusions.

## 2 Justification

There are many software applications developed in the implementation of the communication protocols SPI and I2C [4] [5] [6] [7]. In general, these researches are focused on the comparisons and implementations of different architectures in order to meet characteristics required by current technologies.

In 2006, Oudjida et al., developed a code to implement to medium/low speed a transmitter slave I2C in a VLSI-architecture that allowed meeting some requirements that were not implemented in other systems such as drive noise filtering, a data unit, a unit equipment side interface, a control unit, among others [4].

More recently, in 2009 Oudjida et al., present an implementation of the SPI and I2C protocols in different FPGA devices, to help designers choose the right architecture for their system. To do this, they designed the code in Verilog (according to each protocol) for the slave SPI and I2C to the different FPGA devices, comparing their functionality in response times and clock settings, concluding that logic can predict certain behaviors for master devices from the results of the slaves [5].

Then in 2011 Lazaro et al., presented a new design in Verilog I2C protocol, focusing on the security of the electronic communications devices, integrating AES-GCM authentication and encryption algorithms [6]; To do this, they adapted the features of the I2C protocol with authentication techniques and encryption of data, comparing the final design with the original protocol, and they concluded that their work reduces the overhead of data flow and it is easily implemented in FPGA.

Zhou et al., developed a verification environment of complex electronic systems from the master SPI interface, and integrate Verilog with object-oriented programming (OOP). To achieve this, they started with the functional description of the requirements for the master SPI and environment design, and they implemented the APB controller in OOP classes [7]. The SPI Master interface was developed and implemented in FPGA Verilog.

Finally, it is important to note that in the above-mentioned works, the designers have used the method of hardware description (Verilog HDL), which helps to imple-

ment and to model the concurrent behavior of the electronic embedded devices, especially when it is a new architecture design [8].

## 3 Methods

For the realization of this article, it was taken into account certain key features of the standard communication protocols SPI and I2C [1] [2] [3] for implementing them in a FPGA, by using Verilog programming language. The methodology developed for each protocol is presented below.

### 3.1 SPI protocol

The following features were taken into account for implementing in a FPGA:

- The clock signal (CLK_3) that works at the speed of 3.6Mhz, generated by the master module (which may vary according to the criterion of designer).
- The data signal (SDA), which can be read and / or written by the master or the slave.
- The control signal (CS) enables in the low state and disables in the high state the slave communication.
- MOSI calls the master by sending data and the slave by receiving data.
- MISO calls the master by receiving data and the slave by sending data.
- The MOSI / MISO communication ends with the positive transition of CS.
- The master clock signal sets polarity (CPOL) and phase (CPHA) to "1".
- The master transmits data with positive edge, and receives with negative edge of CLK_3.
- The slave receives with the negative edge, and transmits with positive edge of CLK_3.

### 3.2 I2C protocol

The following features were taken into account for implementation in FPGA:

- The clock signal (SCL) is set at the frequency of 396Khz. (the frequency can be modified according to the standard: 100Khz/400Khz and 3.4Mhz).
- The data signal (SDA) is a bidirectional line, which can be read and written, by the master and the slave.
- The communication between a master and a slave begins with a START condition followed by the slave address to be reached, one read/write bit, a bit of recognition that can be ACK (if the communication was successful) or NACK (if the communication was unsuccessful or the end of the message is set by the master), the 8 bits of data to send or to receive, the ACK or NACK bit, and finishes with a STOP condition or a condition Repeated START.

- If there is no communication between a master and a slave, the data and clock signals remain in the high impedance state.
- The protocol neither implements the designed multi-master function, nor the extension function clock, nor the sending and receiving of more than one datum.
- Each master and slave manages two operating modes: receive and send data.
- The slave address is 7-bits length.
- If the master receives a non-recognized signal by the slave, a STOP condition is generated.
- When the master or the slave does not acknowledge the received data, both the clock and the data signals change to the high impedance state and thus releasing the bus.

Below shows part of the code developed for the I2C master and slave. The master code is showing a read operation of 8-bit data, the generation of the SDA and SCL (bidirectional) signals using a tri-state buffer.
The slave code shows an example of the writing operation ACK bit in the SCL line using a tri-state buffer. To synchronize data from the slave, reading has handled SDA data on the rising edge of SCL, and for writing the data on SDA, has handled the falling edge of SCL.

```
//**********************************//
//MASTER I2C CODE VERILOG
//**********************************//

`timescale 1ns / 1ps

module maestro(SDA,SCL,clk_50,Dir_esclavo,
Data_out,RW,ACK,NACK,contador_32,clk_3,scl_out_1,scl_out);

inout SDA;         // bidirectional SDA line
inout SCL;         // bidirectional SCL line
parameter sda_in = 0;
parameter sda_in_1 = 0;
input clk_50;      //frequency 50Mhz FPGA
reg [0:6]Dir_modulo = 7'b0011011;
reg [0:7]Data_in = 8'b01011010;
input RW;          //read/write line
reg [0:7]prueba = 8'b11011110;
output reg [0:7]Data_out = 0;
output reg ACK = 0;
output reg NACK = 0;
reg sda_out = 0;
reg sda_z = 0;
output reg scl_out_1 = 0;
output reg scl_out = 0;
reg scl_z = 0;
reg control_scl = 0;
reg control_sda = 0;
output reg clk_3 = 0;
//frequency divider counter FPGA
reg [7:0]contador_div = 0;
//read/write data counter
```

```
output reg [4:0]contador_32 = 0;
reg [0:7]Dato_Esperado = 8'b00000000;
reg [0:6]direccion_modulo = 0;   //control flags
reg ACK_MTx= 0;
reg ACK_MRx= 0;
reg NACK_MTx= 0;
reg NACK_MRx= 0;
reg bd_ACK = 0;
reg bd_NACK = 0;
reg bd_ACK_MRx = 0;
reg bd_NACK_MRx = 0;

                  //*********THIRD STATE LINE********//

assign SCL = control_scl ? 1'bz : scl_out;
assign SDA = control_sda ? 1'bz : sda_out;
//************************************//

always@(posedge clk_50) begin
//operating frequency 396KHz
contador_div = contador_div +1;
if(contador_div == 67) clk_3 =~ clk_3;
if(contador_div == 68) contador_div = 0;
end

always@(negedge clk_3) begin
contador_32 = contador_32 + 1;
end

always @(contador_32) begin
//START
if(contador_32<2 ) begin
control_sda = 1;
bd_ACK = 0; bd_NACK = 0;
bd_ACK_MRx = 0;
bd_NACK_MRx = 0;
direccion_modulo = Dir_modulo;
ACK = 0; NACK = 0;
ACK_MRx = 0;
ACK_MTx = 0;
end
if(contador_32 == 2) begin
control_sda = 0;
sda_out = 1'b0;
end
if(contador_32>2 && contador_32<10) begin
sda_out = Dir_esclavo[contador_32-3];
end
if(contador_32 == 10)
sda_out = RW;
if(ACK_MRx == 1 && contador_32 == 12 && RW == 0)
 begin
       sda_out = 1'b0; control_sda = 0;
 end
 if(ACK_MRx == 1 && contador_32 == 13 && RW == 0)
  bd_ACK_MRx = 1;
if(ACK_MRx == 1 && contador_32 > 13 && RW == 0)
   control_sda = 1;
```

```
if(contador_32 > 11 && contador_32 < 20 && ACK_MRx == 0 && RW == 0)
begin
Data_out[contador_32-12] = prueba[contador_32-12];
control_sda = 0;
sda_out = prueba[contador_32-12];
end
if(contador_32 == 20 && RW == 0 && ACK_MRx == 0 && Data_out ==
Dato_Esperado) begin
control_sda = 0;
NACK = 1;
NACK_MRx = 1;
sda_out = 0;
end
if(contador_32 == 20 && RW == 0 && ACK_MRx == 0 && Data_out !=
Dato_Esperado) begin
control_sda = 0;
NACK = 0;
NACK_MRx = 0;
sda_out = 0;
end
if(ACK_MRx == 0 && NACK_MRx == 1 && contador_32 == 21 && RW == 0)begin
sda_out = 1'b0;
control_sda = 0;
bd_NACK_MRx = 0;
end
if(ACK_MRx == 0 && NACK_MRx == 0 && contador_32 == 21 && RW == 0) begin
sda_out = 0'b0;
bd_NACK_MRx = 1;
end
if(contador_32 > 2 && contador_32 < 22 && (RW == 1 && bd_ACK == 0 &&
bd_NACK == 0))begin
control_scl = 0; end
else begin
control_scl = 1;
scl_out_1 = 0;
end
if(contador_32 >= 22)
control_sda = 1;
end

always @(clk_3) begin
       scl_out = (scl_out_1 & clk_3);
end;

endmodule

//**********************************//
//SLAVE I2C CODE VERILOG
//**********************************//

`timescale 1ns / 1ps

module esclavo (SDA,SCL,Direccion_Eslave,Direccion_Master,b_D);

inout SDA;   // bidirectional SDA line
input SCL;   // bidirectional SCL line
input[0:6]Direccion_Eslave;
reg [0:6]Direccion_Eslave_1 = 0;
reg control_sda = 1;
reg control_sda_p = 1;
```

```
reg control_sda_n = 0;
output reg [0:6]Direccion_Master = 0;
output reg b_D = 0;
reg [0:7]Data_in_Eslave = 0;
reg [0:6]prueba = 7'b0101011;
//synchronization counters
reg [4:0]contador_32=0;
reg [4:0]contador=0;
reg RW = 0;     //read/write register
//control flags
reg ACK = 0;
reg NACK = 0;
reg b_ACK_Rx = 0;
reg b_NACK = 0;
reg b_ACK_Rx_1 = 0;
reg b_NACK_1 = 0;

//*********THIRD STATE LINE********//
assign SDA = control_sda ? 1'bz : 1'b0;
//**********************************//

always @(posedge SCL) begin  //read data SDA
contador_32 = contador_32 + 1;
if(contador_32 == 1) begin
b_D = 0;
b_NACK = 0;
b_ACK_Rx = 0;
control_sda_p = 1;
end
  if(contador_32 >= 1 && contador_32 < 8 ) begin
Direccion_Master[contador_32-1] = SDA;     end
 if(contador_32 == 8 ) begin
RW = SDA;
 if(contador_32 == 8 && Direccion_Master == Direccion_Eslave_1 ) begin
  b_D = 0;
  b_ACK_Rx = ACK;
 end
 if(contador_32 == 8 && Direccion_Master != Direccion_Eslave_1 ) begin
  b_D = 1;
  b_ACK_Rx =~ ACK;
 end
 if((contador_32 == 10 ) || (contador_32 == 19 && b_ACK_Rx == 0 &&
b_NACK == 1))begin
  contador_32 = 0;
  control_sda_p = 1;
 end
 if(contador_32 == 0 && SCL == 0) Direccion_Eslave_1 <=
Direccion_Eslave;
end

always @(*) begin
 control_sda = ~(control_sda_n^control_sda_p);
end

always @(negedge SCL) begin //write data SDA
contador = contador + 1;
 if(contador == 9 && SCL == 1 )
    control_sda_n = 0;
 if(contador == 10) contador = 0;
 if(contador != 9) control_sda_n = 1;
```

```
end

endmodule
```

The communication protocols master/slave SPI and I2C were implemented in two Spartan 3-E FPGA's of 500 and 1200 system gates of the Xilinx [9]. This work was to implemented with the software version 14.7 of Xilinx ISE Design Suite.

## 4 Results

The following figures were obtained from the Verilog code and the physical implementation into a FPGA.

Fig. 1 shows the CLK_3, SDA and CS signals generated by the master using the SPI module. The data writing process occurs when the CS signal from slave is in the low state.

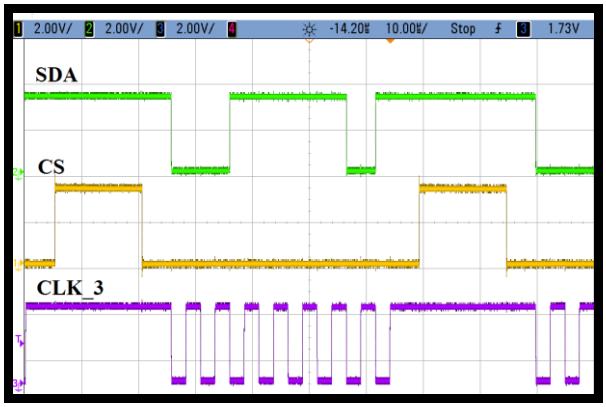


**Fig. 1.** SPI master write

In Fig. 2, the SDA and SCL signals from the I2C protocol are shown. Here we observe the non-recognition of the address (ACK) from the slave (counter 9). The completion of the communication happens when a STOP condition is performed by the master (counter 10).

The case in which the master writes data to the slave is shown in Fig. 3. The communication ends when the master receives the NACK bit written by the slave SDA, which generates the STOP condition.

In Fig. 4 we observe a similar case as that shown in Fig. 3 but with the difference that the slave does not acknowledge the data sent by the master. The communication ends with the setting the SDA and SCL signals to the high impedance state by the master after the bit NACK.

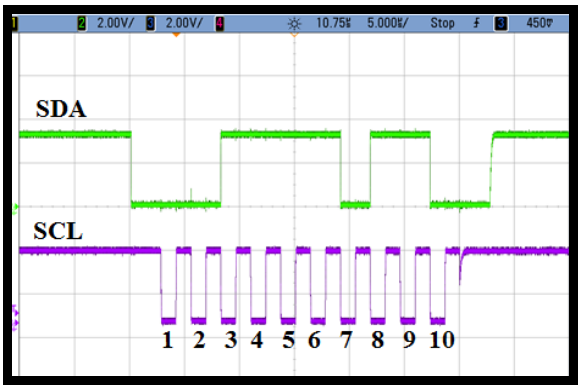


**Fig. 2.** The I2C signal from slave does not respond to the address sent by the master

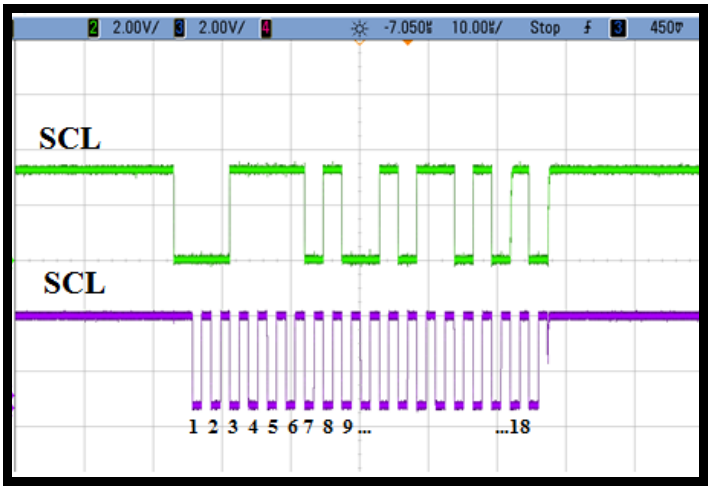


**Fig. 3.** Correct I2C communication between a master and a slave

## 5 Conclusions

In the development and implementation of the SPI and I2C protocols into a FPGA, the following conclusions were obtained:

- Verilog is a high level programming language that runs concurrently, to the difference with other programming languages that work sequentially as those used by microcontrollers, so it performs a faster and more efficient communication when implementing the SPI and I2C communication protocols.
- The developed code for the implementation of the I2C protocol is more robust and complex compared to the developed for the SPI protocol, due to the

number of events to take under consideration in communicating devices such as the start and the stop conditions, bit recognition, and read/write data on bidirectional lines.

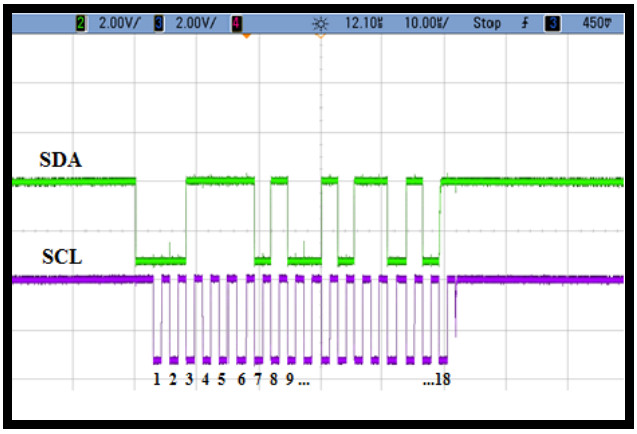


**Fig. 4.** The slave does not recognize the data sent by the master

- It is needed to set at least two operating conditions for input and output data in, each device acting as master or slave for a correct reading and / or writing process between them, because it is not possible to ensure an ideal behavior in the rising and falling edges of the signals, which are necessary for the execution of the code.
- A tri-stated buffer is implemented in the I2C slave for reading and writing data to the bidirectional SDA line, besides the high impedance statehood protects the FPGA peripherals against the phase shift operation signals.
- In the I2C slave, it is necessary to consider the lag introduced in the SDA and SCL signals at the time of writing the data, because the reading process occurs in the rising edge and the writing process occurs in the falling edge of the clock signal, so that these match the structure of the data line SDA.

## References

1. J. Irazabel y S. Blozis, Philips Semiconductors, "I2C-Manual," Application Note, ref, *AN10216-0, March,* vol. 24, 2003. F. S. Motorola y S. B. Guide, V03. 06, February 2003, *Freescale Semiconductor Inc.*
2. I2C-bus specification and user manual, Rev, vol. 3, p. 19, National Semiconductors, 2007.
3. Freescale Motorola Semiconductors Guide, V03. 06, February 2003, Freescale Semiconductor Inc.
4. A. K. Oudjida, A. Liacha, D. Benamrouche, M. Goudjil, R. Tiar y A. 5. Ouchabane, Universal low/medium speed $I^2C$-slave transceiver: a detailed VLSI implementation, International Conference on Design and Test of Integrated Systems in Nanoscale Technology, 2006. DTIS 2006, 2006.

5. A. K. Oudjida, M. L. Berrandjia, R. Tiar, A. Liacha y K. Tahraoui, FPGA implementation of I2C & SPI protocols: A comparative study, Electronics, Circuits, and Systems, 2009. ICECS 2009. 16th IEEE International Conference on, 2009.
6. J. Lazaro, A. Astarloa, A. Zuloaga, U. Bidarte y J. Jimenez, I2CSec: A secure serial Chip-to-Chip communication protocol, Journal of Systems Architecture, vol. 57, n. 2, pp. 206-213, 2011.
7. Z. Zhou, Z. Xie, X. Wang y T. Wang, Development of verification envioronment for SPI master interface using SystemVerilog, 2012 IEEE 11th International Conference on Signal Processing (ICSP), 2012.
8. R. Dubey, Introduction to embedded system design using field programmable gate arrays, Springer, 2009.
9. Xilinx Inc., Spartan-3E FPGA Family Data Sheet, DS312 Product specification, 2013, http://www.xilinx.com/support/documentation/data_sheets/ds312.pdf

# Design of hybrid wireless sensor network to monitor bioelectric signals focused on the study of epilepsy

Sergio Martínez[1], Mario Rivero[2], and Laura Garay[3]

[1] SEPI-ESCOM IPN, Av. Juan de Dios Bátiz Col. Lindavista. Del. Gustavo A. Madero, C.P. 07738 México
smartinez@ipn.mx

[2] Communication Networks Laboratory, CIC-IPN, Av. Juan de Dios Bátiz, Esq. Miguel Othón de Mendizábal S/N, Nueva Industrial Vallejo, C.P. 07738 México
mriveroa@ipn.mx

[3] SEPI-UPIITA IPN, Av. Instituto Politécnico Nacional 2580, Barrio La Laguna Ticomán, Gustavo A. Madero, C.P. 07738 México
lgaray@ipn.mx

**Abstract.** Epilepsy is considered a disorder in which a person has certain episodes of disturbed brain activity. There are different studies that allow monitoring physiological signals associated with a possible epileptic episode. However, these require wired connections and therefore monitoring is restricted to factors such as limited physical movements and loss of information by disconnecting sensors. Hence, there is not a system to monitor patients in a mobile (ambulatory) and wireless fashion. This paper describe a design of a wireless sensor network for a body area network (*BAN*) for continuous monitoring (electroencephalogram [*EEG*], electrocardiogram [*ECG*]) and events monitoring (electrogastrogram [*EGG]*) defined by the expert. The system is based on a *TDMA* protocol that allows sensor nodes to continuously transmit their information as well as the event nodes access to the network when needed. The system is mathematically studied and numerical results are verified through discrete event simulations.

**Keywords:** Wireless Sensor Network (*WSN*), Time Division Multiple Access (*TDMA*), Body Area Network (*BAN*), Electroencephalography (*EEG*), Electrocardiography (*ECG*), Electrogastrography (*EGG*) and Epilepsy

## 1 Introduction

Epilepsy is one of the most common serious brain diseases. It is a chronic disease with complex side effects on professional, occupational, psychological, social and economical implications [1]. However, in a large number of conditions is not possible to make a diagnosis of epilepsy syndrome. In general, there are symptoms of epilepsy crisis in different body parts; studies carried out today require the

patient to attend a hospital or medical cabin in order to be monitored using a wired system. As such, patients are greaty restricted during medical analyses.

Addressing the above problematic, an alternative solution is proposed for the evaluation of different studies, including but not restricted to, epilepsy . Medical examinations like electroencephalogram ($EEG$), electrocardiogram ($ECG$) and electrogastrogram ($EGG$) can be monitored using a wireless system, eliminating any restrictions on medical instrumentation wiring. Specifically, a Body Area Network ($BAN$) through the use of a wireless sensor network ( $WSN$) is proposed for such task. Furthermore, this article develops the design of a hybrid wireless sensor network for continuous monitoring signals of $EEG$ and $ECG$, and event detection driven for $EGG$ signals is evaluated. By this hybrid approach, the system ensures the operation efficiency in terms of channel occupancy and packet loss. A mathematical model and discrete event simulations are performed in order to calculate the system occupancy.

In the literature, there are different $WSN$s deployed for $BAN$s. However, most studies are focused on other types of measurements, for example, in [4–6] or [7] where the monitoring of bioelectrical signals are mainly for e-health applications. Nowadays on the market there are non-invasive sensors, conduct to monitoring bioelectric signal and recording anomalies indicating bearer studies and monitoring. Both works, the developed on this article and the market, are made in order to indicate a simple and *transparent* system to the user, monitoring their respective body functions in different parts and can take the necessary measures to stabilize homeostasis. Brand new sensors like *Medtronic* or *IntraMed* have this kind of functionality.

The $WSN$ is based on a $TDMA$ scheme where the first time slots are assigned to the continuous monitoring data transmission while leaving the rest of time slots available for the event-driven detections. By doing this, a collision-free system is design in such a way as eliminating any information loss.

## 2 System Model

In this section, the main assumptions and the protocol operation are explained in detailed. wireless wensor network are composed of a set of autonomous devices (sensor nodes) that are capable of sensing, communicate and operate in a distributed fashion. Nodes are typically randomly scattered in a specified area [2]. In contrast, $WSN$s applied at $BAN$s are placed in a relatively small area. Hence, nodes are rather close to each other. In fact, transmission radius coverage is confined to no more than 2 or 3 meter distances. Also, the energy emissions of such technologies are very low, which contributes to the long life of the system [3]. Transmissions are made within, around or on the human body.

In the particular case of medical measurements for $EEG$, $EGG$ and $ECG$ analyzes, i.e., for $BAN$s that can be constantly checked by the medical staff, it is also possible to know the exact number of nodes that compose the network (nodes in operating conditions). As such, it is available to replace damaged nodes or even to charge all the node's batteries before operation. Hence, a $TDMA$

protocol is proposed because it is a collision-free protocol. As such, there is no energy wastage due to idle listening, collisions or overhearing as in the case of random access protocols, typical in *WSN*s. Indeed, in the specific types of *BAN*s considered in this work, it is possible to pre-assign a time slot for each specific node.

In the Fig. 1, it is illustrated the basic operation of the system. It can be seen that in a system with 26 nodes, the *TDMA* system consists of 26 time slots. Note that in the first part of the *TDMA* frame, nodes with continuous monitoring tasks are assigned to a particular time slot, which is always occupied with such transmissions. However, the second part of the frame is composed of the event driven transmissions. In this case, we assume a system where $N_c$ nodes are deployed for continuous monitoring tasks while $N_e$ nodes are focused on event driven reporting. As such, the frame is composed by $N_c + N_e$ time slots.

It is important to notice that nodes monitoring the *EGG* signals, are not required to constantly transmit all the sensed information. In particular, the medical staff is only interested on receiving information when a certain predefined event occurs. For instance, when signals measured from the patient are outside the *normal* operation range. As such, nodes do not constantly transmit in tis part of the frame. However, the system guarantees the successful transmission of these events. In the first part of the frame, the channel occupation is always 100%. In the second part of the frame, the occupancy greatly depends on the rate at which events occur, i.e., how often a patient experiences out of range activity in the heart.

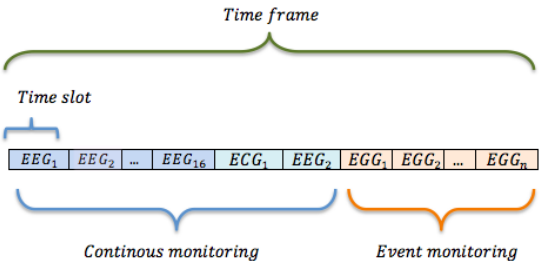


**Fig. 1.** *TDMA*-based system

## 3 Mathematical Model

The mathematical model presented in this section is mainly focused on the channel occupation in the event reporting phase. To this end, an event arrival rate of $\lambda_e$ events per second is assumed. Events in this context refers to the

readings of the *EGG* signals that falls outside the *normal* range for the particular patient. Note that the system can be further developed in order to consider multiple events. Indeed, the proposed *BAN* can easily adapt to multiple types of biological sensors with very different event characteristics. It is also assumed that events arrive according to a Poisson process, (the time between events are a random variable with negative exponential distribution with mean $1/\lambda_e$ seconds). Again, the event distribution can change for different patients and biological signals. However that does not impact the system operation since the network has always available resurfaces for the nodes in order to transmit their information. The occupancy calculated in this work can be quiet different in case that events follow a different distribution.

In the proposed model, it is consider the case where sensor nodes do not detect the event, (it does not consider a perfect sensing system). The rationale behind this is that, nodes are placed in the clothes or an elastic band around the interest area. Hence, in an ambulatory device, it is possible for nodes to move due to the patients position or movement. So, whenever the event occurs, the sensor nodes will not detect the appropriate signal. We model this by introducing the probability, $\rho$ that, given that an event occur, a particular sensor node detect it and transmit the associated information. On the other hand, a node does not detect the event with probability $1-\rho$ and hence, it does not transmit packets in the appropriate time slot. From the previous description, the channel occupancy in the event report in phase can be calculated as follows:

$$O_e = \frac{\lambda_e \sum_{i=0}^{n} i\binom{N_e}{i}\rho^i(1-\rho)^{(N_e-1)}}{N_e} \tag{1}$$

Occuppancy refers to the number of $N_e$ slots per frame being used to transmit information.

### 3.1 Discrete event simulation

Discrete events simulations are implemented in order to verify the mathematical analysis. It is considered that 18 nodes are deployed for continuous monitoring ($N_c = 18$) where 16 channels are on the *EEG* and the remaining 2 are for *ECG*. Also, the event transmission nodes ($N_e$) are subject to variation starting with at least 2 sensors for electrogastrography up to 10. It is also considered that the probability of detecting the event whenever it occurs, $\rho$, can vary in the range of 0.2 to 0.7.

## 4 Numerical Results

It is consider three different values of the event arrival rate, $\lambda_e$ and the performance evaluation of the system. we present numerical results for different values of $\rho$ and $N_e$. In all cases, $N_c = 18$. Fig. 2 presents results for a value of $\lambda_e = 0.3$.

On each occasion that the ocuppancy term is used, it is referring to the portion of time slots that are being used. It can be seen that the values obtained in

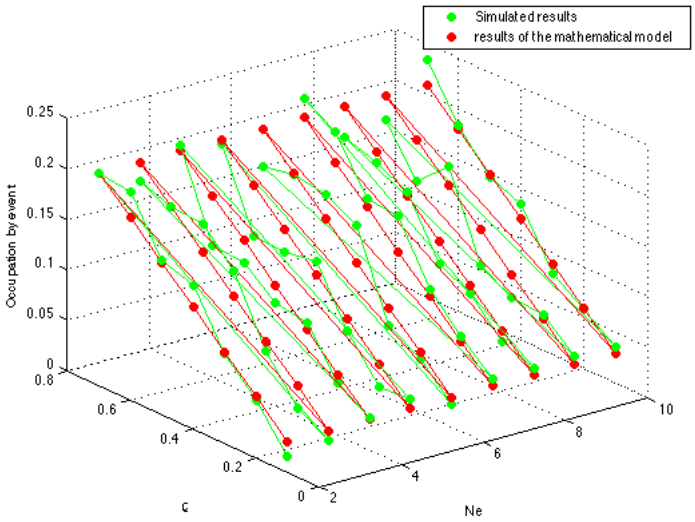


**Fig. 2.** Occupation per event $\lambda_e = 0.3$ and $N_c = 18$

the simulation are very similar to the mathematical model. Occupancy decreases as the value of $\rho$ decreases. Indeed, as the probability that nodes detect the event is low, there are just a few transmissions, leaving many time slots empty. This can correspond to the case of the patient in movement, walking or jogging for instance. In this sense, it is advisable to use many redundant nodes in order to capture readings in case of an event occurrence.

Fig. 3 and 4 present results for $\lambda_e = 0.5$ and $\lambda_e = 0.7$ respectively. This case corresponds to a system with more heart activity. Note that occupancy increases compared to the previous figure.

## 5 Conclusion

Considering the *EEG*, *ECG* and *EGG* studies by a separate set of interconnected nodes, a design was developed for a hybrid *WSN* using a *TDMA*-based protocol. A mathematical model and the respective discrete event simulations for comparison of results was performed. Performance evaluation is made in terms of the channel occupancy validating the mathematical model. It is considered that based on the results, the maximum efficiency is obtained for a high rate of arrivals and to a high probability of transmission nodes per event. However, channel occupancy is never higher that 50% in the considered environments.

It is important to notice that even for high arrival rates and considering that nodes detect most events, for instance $\rho$ =0.7, the channel occupancy is

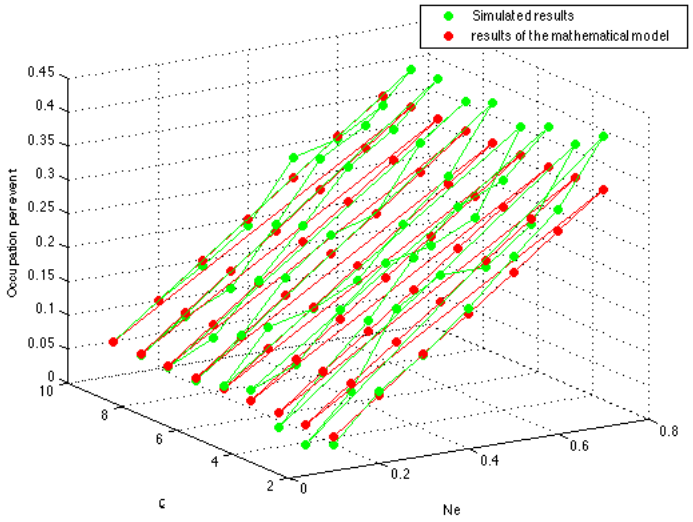


**Fig. 3.** Occupation per event $\lambda_e = 0.5$ and $N_c = 18$

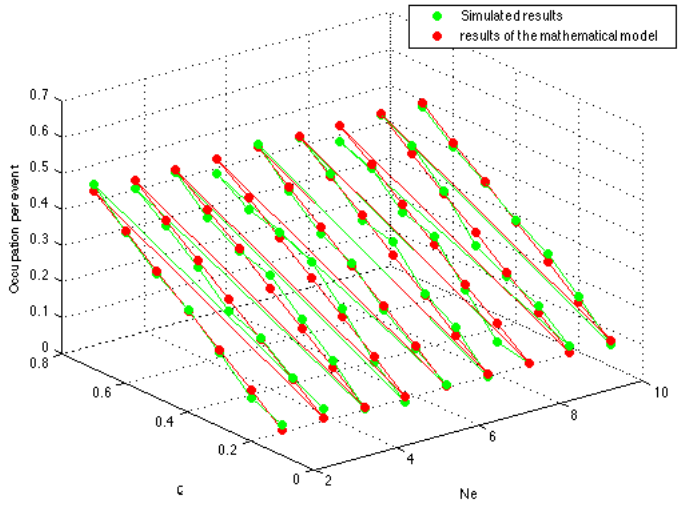


**Fig. 4.** Occupation per event $\lambda_e = 0.7$ and $N_c = 18$

rather low. This is because when no event occurs, all the times slots dedicated to event reporting are empty. This suggests that a more efficient system can be implemented that takes advantage of this fact.

## References

1. Hernndez, A.; vila, L.; Arch, E.; Bueno, A.; Espinoza, G.; Alfaro, A.: La epilepsia como un problema de discapacidad. Disability Research, 2, 122-130 (2013)
2. Dargie, W.; Poellabauer, C.: Fundamentals of Wireless Sensor Network. John Wiley & sons Ltd (2010)
3. Enderle, J.; Blanchard, S.; Bronzino, J.: Introduction to biomedical engineering. Elsevier academic press (2004)
4. Chung, W. Y.; Lee, Y. D.; Jung, S. J.: A Wireless Sensor Network Compatible Wearable U-healthcare Monitoring System Using Integrated ECG, Accelerometer and SpO2. Institute of Electrical and Electronics Engineers, 8, 1529-1532 (2008).
5. Castillejo, P.; Martnez, J. F.; Rodrguez, J. M.: Integration of wearable Devices in a wireless sensor network for an e-health application, Institute of Electrical and Electronics Engineers, 13, 38-49 (2013)
6. Phunchongharn, P.; Hossain, E.; Camorlinga, S.: A cognitive radio system for E-healt applications in a hospital environment, Institute of Electrical and Electronics Engineers, 10, 20-28 (2010)
7. Sivaraman, V.; Grover, S.; Kurusingal, A.; Dhamdhere, A.; Burdett, A.: Experimental study of mobility in the soccer field with application to real-time athlete monitoring, Institute of Electrical and Electronics Engineers, 6, 337-345 (2010)

# Designing a virtual domotic system applied in educational environments

Chadwick Carreto[1], Elena F.Ruiz[1], Marina Vicario[2]

[1] Escuela Superior de Cómputo - Instituto Politécnico Nacional.
Av. Juan de Dios Bátiz s/n Unidad Profesional “Adolfo López Mateos”
C.P. 07738, México D.F.Tel. (5255)5729-6000 Ext. 52051
[2]Unidad Politécnica Interdisciplinaria de Ciencias Sociales y Administrativas
Av. Instituto Politécnico Nacional s/n, Unidad Profesional "Adolfo López Mateos",
Edif. 1, 2, 3, 4 y 5, Col. Lindavista, México, D.F. C.P. 07738
[1]ccarretoa@ipn.mx, [2]elen_fruiz@yahoo.com.mx,
[3]marina.vicario@gmail.com

**Abstract.** In this paper the design of a Domotic Model applied on an educational setting, according to the proposed model, users can access environment seamlessly, anytime, anywhere shown by different mobile devices to information and services available within the different domains of work (administrative areas, classrooms, libraries, etc.). available to this environment. The proposed model seeks to be independent of the technology that is implemented (Wi-Fi, Bluetooth, etc..) And any network topology (wired, wireless, P2P, etc.) the proposed model fits the concept of Internet of Things and define a concept of "Virtual Domotic" beacuse extending the concept to larger workspaces and mobile.

## 1 Introduction

In the last years, the technological advance on domotic systems, mobile computing systems and wireless networks has been too relevant. These technologies make out an important basis in the current development schemes, so the provision of services for each technology represents a challenge for technological development, scientific and research communities.

*Domotic* means *automation* (provision of services for the management of resources, security, communications, comfort and leisure) within a limited and closed space. This concept has been classified according to the extension of the space that it can cover. There are three main elements into this classification: Domotic, which acts on the extension of small buildings as homes. Inmotic, that operates on the extension of buildings such as hospitals or offices, and Urbotic which unfolds on cities covering tertiary buildings and outdoor urbanization [1,2]. Mobile computation involves a simple concept: information process without wires, whereas the mobile device is not visibly connected to any computer.

This concept includes two fundamental technological advances: wireless networks for data transmission (implemented on various wireless technologies such as Wi-Fi, Wimax, Bluetooth, etc.), and the miniaturization of computer device components that allows the development of more robust mobile devices, with a bigger capacity for processing (PDA's, Laptops, NoteBooks, SmartPhones, etc.). Their own portability has become them in a clothing accessory; an indispensable tool for every day.

Ubiquitous computing is based on the device perception capacity; it aims to build devices and highly sensitive systems that detect user's actions and environmental changes, in the same way as another person could do it. Once the user comes into the domain field, the devices may act according user's demand in order to provide him services for his requirements, in a totally transparent way [3]. Because of different aspects about the Administration and the security of the information, it becomes necessary to integrate and to divide networks into different topologies and administration logical distributions which aim a restructure in the global access and in the available services. By a Division of a network into domains (limited spaces, inside of which, there is some connection between devices) [4] [7], we'll have access to information that will be useful, because it will be focused on the staff and on the executed activity in such domains. This scheme of work claims to provide automatically several available services that are trying to deal with this administration at the level of communication protocols to improve the security of the system [5] [8].

Taking into account all these aspects, domotic, mobile computing and ubiquitous computing can provide several solutions to problems of diverse nature, which can range from simple consultation and/or information exchange to systems that allow users to collaborate from anywhere and at any time, so the main objective of this work is to develop a model, which will have as goal to offer to the educational environment user an access to the information and/or to the services of each work domain, in a transparent way from anywhere, at any time, providing him in this way, comfort within the educational environment. In the model proposed in this document, we take advantage of Virtual Domotic concept which let us out extend the original concept of *Domotic*, about automate certain limited space, taking the automation towards more spaces as it is the educational environment (all the buildings and physical facilities inside an educational campus) covering it completely.

Below, section 2 describes the model to develop. Section 3 explains model design and its development. Finally, in section 4, we give you a conclusion of the whole work and after that, we comment about future work.

## 2 Virtual Domotic System Model

The Virtual Domotic System Model (VDSM) (Fig. 1) is made up by modules of discovery, identification, services reporting, collection services and interaction network. The VDSM modules are described below:


**Fig. 1.** Virtual Domotic System Model

**Network discovery module.-** In this module, the user's mobile device detects the network or domain from the educational environment using access points, in order to start the communication between the device and the domain, where the access point perceives through the MAC address of the mobile device, if you are a user already registered in the database of the server.
**Identification module.-** This module performs validation on the server, by an identifier (password) that the user employs to register himself into the domain and in order to get access to the services. If the user's identification is positive, it proceeds to give him access to the domain and provide him the legal services.
**Services Presentation module.-** This module performs the services administration which each user accounts. It undertakes to present the services to the user in an organized and available way, when they are required. This module depends on the identification module, because in order to establish the services administration, the user needs previously require authentication.
**Services Obtaining module.-** This module implements the connection and the disconnection between the server and services domains. Also, the module presents depends on the identification module in order to establish the connection previously required for authentication by the user.
**User interaction module.-** It is the last of the modules and it is responsible for initializing the application by the user and display the response to that request, i.e. the denial or the delivery of information and/or services required according to the user's profile. This interaction should be simple, transparent and ubiquitous.

## 3 VDSM Architecture

For VDSM Architecture, we use the Unified Modelling Language (UML). Afterwards, based on the general model use case, we're going to establish the different states in which the VDSM will go through.

A) VDSM Design.

In order to satisfy with the expectative of the VDSM, we will divide the whole system in five use cases based on the VDSM modules (Figure 2). The user will interact directly with each one of use cases.

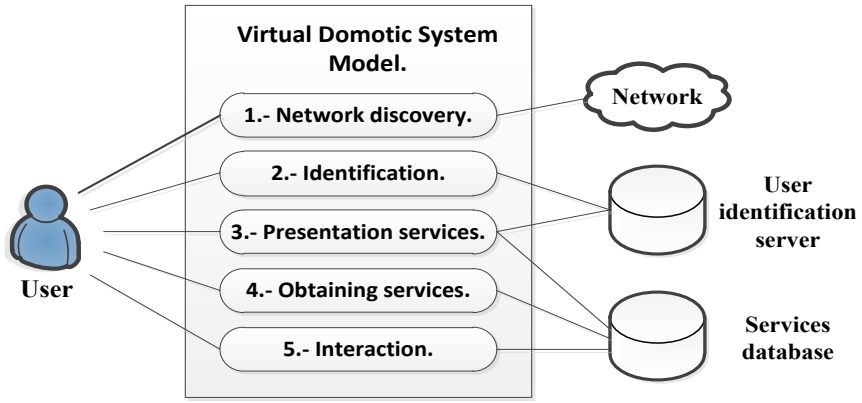


**Fig. 2.** Cases of use of the virtual domotic system model.

In the first case, user's computer identifies a network and it attempts to get access in order to receive the services that exist within it. The network assigns a valid address and links it with the next module.

The second case identifies the user. It refers to the ID module which identifies and authenticates the user. The authentication server will send the user an identification request. Then, the user will reply to the server and if it determines that the user answered correctly, the request will give him access to services according his preset profile. If the user does not fulfill the request, any access to the local network will be denied, so he'll get limited access.

The third case involves the service presentation module which is responsible for organizing the available services. In this way, the user can easily decide which service he'll use.

In the fourth case, the user requests a service according his profile which is previously identified. In this way, we set out and close the connection between the user and the services.

The final case is the interaction that the user has with the services. This one should be transparent and simple as possible each time the user requests information.

## 4 VDSM Implementation testing

VDSM architecture will be implemented within an educational environment, in order to ensure a functional model. Currently, we are pre-testing before take it to an educational environment. The network for this pre-testing is formed by:

- S.O.Ubuntu (VMWare) server.
- Access point Linksys WRT54G Wi-Fi 802. 11b/g (OS OpenWRT).
- S.O. Windows XP (user) Laptop Compaq
- An educational services server (AAVAE).

These are modular tests, so we have carried out as follows:

A) Network discovery module.

First of all, we have configured a Linksys AP (model WRT54GS), where successfully, we have uploaded a Linux distribution called OpenWRT, which is able to program a Shell in charge to update each certain time, users connected list to the AP.

After that, we have developed in a Java language (within the server), a program that will be retrieving the users connected list to the AP. Also, it will be verifying in a database (within the server), the MAC address of the users connected to the AP. In this way, once a new user connected to the AP has already registered in the database, this module will pass control to the next one, in order to identify the user and give him access to the services according his profile.

B) Identification module.

According to the concept described in the 802.1X standard, we will implement an authentication server that will verify the authenticity of the user using the data that are sent because of the connection with the AP.

The new user is redirected to an HTML page where we inform him that it is necessary to carry out a prior authentication before access to the network services. To request data from the user, it establishes a secure communication, which presents to the user a template where should type the data required for authentication.

In this Authentication Server Module, we'll use RADIUS server to provide an authentication decision-making centralized mechanism.

C) Services Presentation Module.

In this module we are reusing the AAVAE system and its services (located on a services server) that are submitted to the user according to his profile, so he won't need to identify himself once again.

AAVAE (Fig. 3) is an architecture that will provide virtual educational services to IPN teachers and students, in order to interact in a synchronous and asynchronous mode, using tools such as streaming video, archives management, forums and chat.

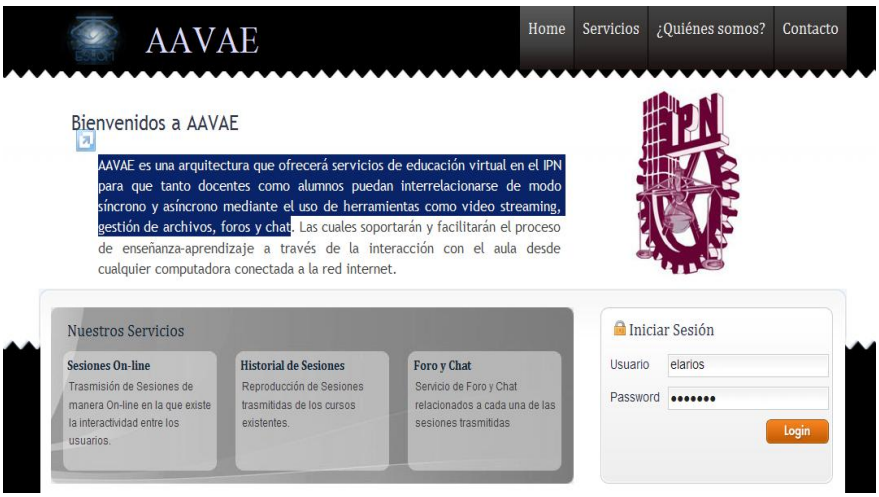


**Fig. 3.** AAVAE Educational Services System

D) Services Obtaining Module.

This module tests the AAVAE system connection with the different repositories where the information and/or services are offered by this system to users, in order to be sure that this process will be in a transparent way.

E) Interaction module.

Fig. 4 shows the user interface. This will be simple for a no expert user, who will use without any problem, all the available services.


**Fig. 4.** Interaction Screen with AAVAE system's user

The user will only select one of the services offered on the screen, in order to have access to them. Through this system, the user will have one additional support tool for his education.

## 5 Conclusions and future work

The main contribution of the proposed model is to provide comfort to the users of the educational environment system, on the basis of mobility allowed by acting, given them saving time and effort in the access to the information and/or services.

Besides, this research helps us to extend Domotic concept toward a Domotic Virtual concept, because it not only covers certain areas or buildings within the environment, it contemplates the whole educational environment according to the different available domains.

Mobile networks are becoming more common in educational institutions. Nowadays, it becomes a mean objective to achieve a computing ubiquitous which ensure a total interactivity at any time and from everywhere. In this way, this project

is focused on bring us closer to such objectives, attempting to develop an environment capable of providing the required services for a specific users, always in the most transparent way.

The system could be also a perfect basis to develop a ubiquitous computational environment anywhere that warrants it, establishing a protocol for the implementation of services by different mobile devices.

The application of this model is applied in many environments:

- *Health*. In this environment, it can be implemented in a hospital. For example, a patient can book a medical consultation by his cell phone, instead to make an appointment with the receptionist. Also, we can obtain information from a hospitalized patient. Furthermore, the doctor could review his daily agenda.
- *Cultural*. It can be implemented at museums where visitors will use their mobile devices to get information of locations, paintings, sculptures, exhibitions, etc.

**Acknowledgements**. The authors appreciate the support from CONACYT and Instituto Politécnico Nacional, particularly ESIME, ESCOM, UPICSA, CIC, SIP and COFAA for carrying out this work.

## 6 References

1. Nozick, J.: La maison intelligente. Editions du Moniteur, (1988)
2. Ramón, J., Millán, T., Huidobro, J.: Domótica: Edificios Inteligentes. Limusa, (2007)
3. Carreto, Ch., Menchaca, R.: Arquitectura de Colaboración mediante dispositivos Móviles Aplicada a la Administración del Conocimiento. TCM2004. ENC. Universidad de Colima, México (2004)
4. Muñoz, M.: Cómputo colaborativo consciente del contexto. Tesis de Maestría, CICESE, (2003)
5. Parsa, C., Garcia, J.: Improving TCP Performance over Wireless Networks at The Link Layer. ACM Mobile Networks and Applications Journal, 5(1), 57-71 (2000)
6. Murthy, S., Garcia, J.: A Routing Architecture for Mobile Integrated Services Networks. ACM Mobile Networks and Applications Journal. 3(4), 391-407 (1998)
7. Weiser: Ubiquitous computing. Intel Architecture Labs; (1994)
8. Weiser: Ubiquitous computing: origins, current research, and the future. Distinguished Lecture Symposium at University of British Columbia, Vancouver, British Columbia, Canada, (1993)

# Arquitectura Web para análisis de sentimientos en Facebook con enfoque semántico

Carlos Acevedo Miranda[1], Ricardo Clorio Rodriguez[1], Roberto Zagal Flores[1], and Consuelo V. García Mendoza[1]

[1]Escuela Superior de Cómputo, Instituto Politécnico Nacional, Ciudad de México, México
carls.9204@gmail.com,ricardo-clorio@hotmail.com,zagalmmx@gmail.com, varinia400@hotmail.com
http://www.escom.ipn.mx

**Resumen** Actualmente el potencial del análisis automático de sentimientos en redes sociales es relevante en el desarrollo de aplicaciones para múltiples propósitos. En este sentido, las publicaciones en Facebook escritas en español pueden contener información semántica relevante que permitirían clasificarlas en categorías de emociones, la complejidad del idioma hace que el análisis de esta información sea difícil y dependa de identificar palabras que tengan significado emocional. En este sentido, proponemos un enfoque que integra una aplicación web, una jerarquía semántica basada en *WordNet-Affect Hierachy* en español y un clasificador *Naive Bayes* que identifica las publicaciones en las emociones alegría, tristeza y enojo.. Los resultados experimentales muestran una precisión del 63 %.

**Keywords:** Sentiment Analysis, Social Network Analysis, Pattern Recognition

## 1. Introducción

Las personas pueden expresar en una publicación de forma indirecta algún tipo de emoción. Identificar estos sentimientos es una tarea sumamente complicada, debido a que se requieren diversos tipos de análisis de morfología, ortografía, sinónimos, entre otros. Este proceso cuando es manual resulta ser complicado y tedioso.

El análisis de sentimientos puede ser combinado con otras técnicas de análisis de redes sociales para identificar usuarios potenciales para recomendar campañas publicitarias, detectar conflictos de interés y aceptación de temas sociales en grupos de usuarios, entre otras aplicaciones.

De acuerdo al estado del arte en análisis de sentimientos, tratar de automatizar este análisis implica al menos los siguientes mecanismos en una arquitectura de software que de solución al problema:

- *Extraer texto:* Recuperar el texto de interés considerando la complejidad de la arquitectura de datos de las fuentes de información.

- *Normalizar texto:* Por medio de un tratamiento lingüístico recuperar únicamente palabras clave que se puedan asociar con emociones, tomando en cuenta polisemia, sinonimia, negaciones de verbos entre otros.
- *Clasificar texto:* Diseñar mecanismos de reconocimiento de patrones, a fin de alcanzar una mejor precisión al momento de clasificar las publicaciones en las categorías de sentimientos definidas.

En este trabajo, proponemos una de arquitectura de software que considera estos mecanismos para clasificar publicaciones de Facebook en tres emociones: *alegría*, *enojo* y *tristeza*. El sistema esta limitado a las siguientes restricciones de diseño: selección de publicaciones en español, usuarios mexicanos ubicados en la Ciudad de México y zona metropolitana, y se asume que las palabras de las publicaciones se han escrito con ortografía correcta.

Este documento se organizada de la siguiente manera: En la sección II se describen los trabajos relacionados, la sección III muestra la metodología, la sección IV explica los resultados obtenidos, y por último se discuten las conclusiones.

## 2. Trabajos relacionados

Diferentes algoritmos de clasificación han sido probados en análisis de sentimientos en [2], donde se extraen subtítulos de escenas de películas y se identifican aquellas que son emocionales usando clasificadores entrenados. Este enfoque utiliza etiquetas de emociones asociadas a un conjunto de palabras.

Actualmente para el análisis de sentimientos en texto existen corpus como *WordNet Affect* [3] y *Affective Norms for English Words* (ANEW) [4], que facilitan usar una estrategia semántica para detectar emociones en texto. Estas estrategias se ha usado en [7] y [8] donde se extrae titulares de noticias asociándolos en seis tipos de emociones con una precisión del 38 %.

Estos enfoques han sido combinados con algoritmos de clasificación, en [1] donde se clasificaron mas de 7000 publicaciones de twitter en opiniones positivas, negativas y neutras con una precisión del 61 %.

Nuestro trabajo propone un enfoque que combina un clasificador sémantico que consume una jerarquía de palabras enriquecida y un clasificador *Nayve Bayes*. Los resultados obtenidos respaldan el enfoque propuesto.

## 3. Metodología

Nuestra Arquitectura Web consiste en los siguientes componentes de software: extracción de publicaciones usando el núcleo de la interface de programación de Facebook [9] (*Facebook Graph API* ), pre-procesamiento de palabras, clasificador base semántico, clasificador *Nayve Bayes*, funciones de administración web y despliegue de resultados.

### 3.1. Componente de extracción de publicaciones

El kit de desarrollo de software de Facebook [10] (*Faceebook SDK*), fue empleado para poder extraer diversos atributos de los usuarios En la tabla 1 se muestran los atributos más importantes:

**Tabla 1.** Datos de usuario extraídos

| Campo | Descripción | Se almacena |
|---|---|---|
| ID Facebook | Id de usuario. | Si |
| Género | El género del usuario. | Si |
| Nombre de usuario | Nombre de usuario en Facebook. | Si |
| Correo | Email de registro en Facebook. | Si |
| Publicaciones | Publicaciones realizadas en el perfil. | Si |

Las publicaciones son extraídas y almacenadas cuando el usuario decide iniciar el proceso de análisis de sentimientos. El componente extrae las 100 publicaciones más recientes del muro de Facebook del usuario, en la Fig. 1 se muestra parte de la aplicación web usada para la extracción de información.

Posteriormente el texto de las publicaciones es normalizado procesando signos de puntuación (emoticones), filtrando palabras indeseadas (*stopwords*) y obteniendo la forma canónica de las palabras (lematización).

**Secuencias y signos de puntuación:** Existen secuencias de signos conocidas como emoticones que describen un contexto emocional: *:)*, *:(*, *:P*, *xD*, ¬¬, entre otros. Por esta razón, los emoticones no son eliminados del texto de la publicación. Los emoticones son empleados particularmente por usuarios jóvenes de Facebook El resto de los signos son eliminados, a excepción de **.**, **;** y **,**, porque separan ideas en un texto. En este caso la clasificación final de una publicación que contiene más de una idea, será el resultado promedio de la clasificación individual de cada una de las ideas.

**Filtrado de *stopwords*:** Existen palabras que son irrelevantes en el análisis de sentimientos en texto, como preposiciones, artículos, entre otras. Estas palabras son eliminadas de las publicaciones porque pueden generar resultados imprecisos durante la clasificación. La Fig. 2 muestra la visión general del comportamiento de este componente.

*Detección de la palabra pero:* Generalmente, cuando utilizamos la palabra *pero* en una oración, estamos explícitamente negando la idea antepuesta a esa palabra, restando relevancia y enfocándonos en la idea posterior. Lo anterior no es una regla infalible, pero se cumple en la mayoría de los casos por lo que se decidió emplearla.


**Fig. 1.** Interfaz para la extracción de datos

### 3.2. Componente para preprocesamiento de texto

Esta regla resulta ser de gran utilidad en los casos en los que en una misma publicación existen dos o más ideas en las que puede haber, de igual manera, dos o más sentimientos involucrados. Por ejemplo en la publicación: ahora sí me mojé horrible pero me encantó tanto jajaja", la primera idea refleja un sentimiento negativo que se ve anulado por la segunda idea que se encuentra posterior a la palabra "pero". Partiendo de esto, las ideas que precedan a la palabra "pero" son eliminadas, dejando sólo la idea o ideas que se encuentren posterior a esa palabra.

*Negaciones:* Debido a la naturaleza con la que nos expresamos, existen palabras que pueden cambiar radicalmente el sentimiento que deseamos transmitir, por ejemplo, en la expresión "No estoy feliz", la palabra "no" niega completamente la idea subsiguiente. Estas negaciones son tomadas en cuenta, de manera que si en el texto de la publicación se encuentra el adverbio "no", "nunca" o "ningún", a éste se le concatena un "_" seguido de la siguiente palabra. Y en caso de que no exista otra palabra más en la publicación, la palabra de la negación es eliminada. Para el ejemplo anterior: "No estoy feliz", el resultado de la publicación procesada es "no_feliz" debido a que "estoy" es *stopword*.

**Lematización:** Para eliminar las variantes morfológicas de las palabras que componen las publicaciones, se utilizó un lematizador con base en [11], las pala-

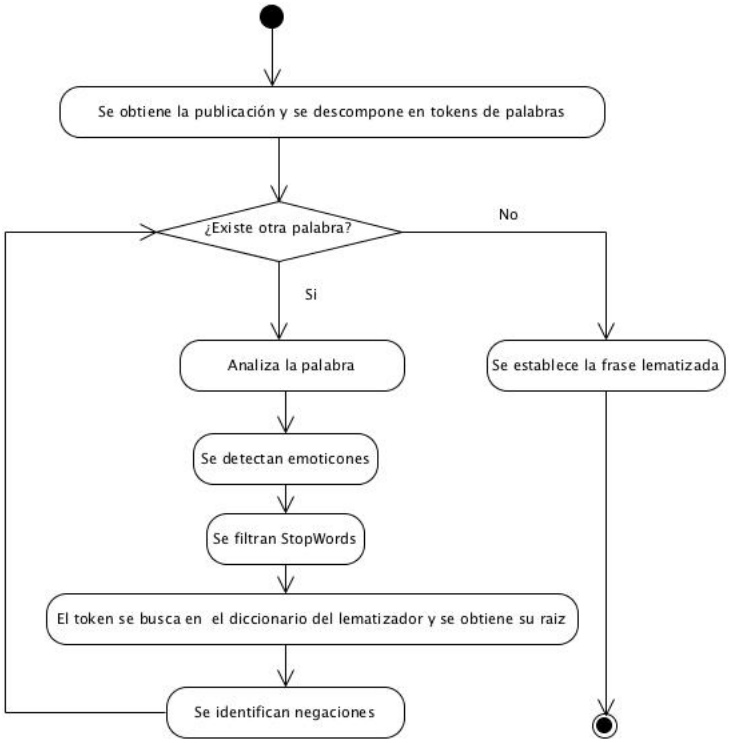


**Fig. 2.** Fases de ejecución del componente de preprocesamiento de texto

bras que no cuenten con su forma canónica son eliminadas de la publicación y no serán tomadas en cuenta en el clasificador.

### 3.3. Componente para clasificación de publicaciones

En este componente se combinan dos procesos: el primero emplea un recurso que contiene conceptos de sentimientos ponderados basada en *WordNet Affect* (que se usa como un clasificador base), estos conceptos están organizados y enriquecidos semánticamente como una Ontología. El segundo proceso ejecuta un clasificador *Naïve Bayes*. Si la publicación no puede asociarse a algún sentimientos, será clasificada como Ambigua.

**Clasificador semántico base:** El clasificador usa una taxonomía semántica tipo Ontología construida a partir de *WordNet-Affect* [3]. Esta jerarquía contiene diversos conceptos con carga emocional jerarquizados en diferentes niveles, cada niveles es un grado de intensidad sentimental.

En la tabla 2 se muestra parte de la jerarquía ontológica, la cuál se obtuvo como resultado de una adaptación al español del recurso *WordNet Affect* que

involucró el tratamiento de 771 conceptos al español. Estos conceptos están contenidos en una estructura jerárquica, que establece una ponderación asociada que es mayor a medida que el concepto es más cercano a la raíz de un concepto padre que represente una emoción. La estructura jerárquica fue enriquecida agregando a cada concepto sinónimos (que tienen significado emocional) denominados *sinónimos directos*, también a los conceptos se agregaron expresiones equivalentes conocidas como *emoticones* porque estos describen estados emocionales. Al no existir corpus oficiales que describan *emoticones*, se tomaron en cuenta aquellos que son más frecuentes en las publicaciones. Los *emoticones* seleccionados son expresiones directamente relacionadas con sentimientos, por lo tanto tienen la ponderación más alta.

Este recurso se emplea como un clasificador base, donde cada palabra de una publicación será buscada en la jerarquía. Si la palabra es encontrada, entonces esta recibe un valor que contribuirá numéricamente para decidir si la publicación pertenece a cierta emoción. Por ejemplo, si una publicación contiene la palabra *feliz*, la cual se encuentra en la jerarquía ontológica con un valor de ponderación 2, entonces esto contribuirá a asociar *feliz* con el sentimiento alegría, matemáticamente se expresa de la siguiente forma:

$$\text{Alegría+} = \frac{1}{\text{Ponderación de palabra}} = \frac{1}{2} \tag{1}$$

La jerarquía consiste en tres conceptos raíz: *alegría*, *enojo* y *tristeza*, a partir de estos existen ramificaciones de conceptos que jerarquicamente describen a estas emociones. Lo que permite que las palabras que están más cercanas a la raíz tengan un peso mayor que aquellas que no lo están, como se muestra en la Fig. 3 y 4.

El clasificador semántico base en caso de no poder clasificar una publicación en alguno de los tres sentimientos, invoca al clasificador *Naïve Bayes*

**Clasificador *Naïve Bayes*:** Recibe como entrada las palabras normalizadas de una publicación, y mediante un clasificador *Naïve Bayes* se calcula la probabilidad condicional respecto a cada una de los sentimientos, emplea la siguiente fórmula:

$$p(\text{Emoción} \mid \text{Publicación}) = \frac{p(\text{Emoción})p(palabra_i \mid \text{Emoción})}{\sum_{i=0}^{3} p(\text{Emoción}_i)p(\text{Publicación} \mid \text{Emoción}_i)} \tag{2}$$

El denominador de la fórmula (2), también conocido como evidencia, se comporta de manera constante en los cálculos por lo que es omitido, reduciendo la fórmula a:

$$p(\text{Emoción} \mid \text{Publicación}) = p(\text{Emoción})p(palabra_i \mid \text{Emoción}) \tag{3}$$

*Naïve Bayes* es un algoritmo de aprendizaje supervisado y fue seleccionado debido a los resultados que ha obtenido en problemas de clasificación de texto según [6].

**Tabla 2.** Muestra de conceptos y estructura base de la jerarquía desarrollada.

| Inglés | Tipo | Traducción | Sinónimos directos | Categoría | Ponderación | Emoción |
|---|---|---|---|---|---|---|
| joy | sustantivo | alegría | júbilo, placer, regocijo, deleite | Alegría | 1 | Alegría |
| joyfulness | sustantivo | júbilo | alegría, festividad | Alegría | 1 | Alegría |
| joyful | adjetivo | alegre | alegre, feliz, agradable | Alegría | 1 | Alegría |
| anger | sustantivo | enojo | ira, enfado, indignación | Enojo | 1 | Enojo |
| annoyance | sustantivo | molestia | enojo, fastidio, irritación, disgusto | Molestia | 2 | Enojo |
| chafe | sustantivo | fastidio | roce | Molestia | 2 | Enojo |
| sadden | verbo | entristecer | apenar, angustiar, afligir, consternar, desconsolar, acongojar, amargar, deprimir | Tristeza | 1 | Tristeza |

Este clasificador se entrenó de forma manual considerando 100 muestras de publicaciones clasificadas, un conjunto de prueba de 802 publicaciones: 227 de Alegría, 202 de Tristeza, 210 de Enojo y 163 clasificadas como Ambiguas. Los resultados que a continuación se describen, argumentan la base experimental de este enfoque

## 4. Resultados

Se realizaron cinco pruebas con una muestra de 802 publicaciones, se combinó diferentes estrategias hasta llegar al enfoque definitivo . Los resultados son los siguientes:

*Prueba 1: Usando clasificador base sin procesamiento de emoticones* Sin usar los emoticones la presición fue del 17 %. Este resultado fue tan bajo debido a que los usuarios de Facebook utilizan palabras coloquiales y emoticones para expresar sus sentimientos. En la muestra usada, se descubrió que 80 de cada 100 publicaciones contienen al menos 1 emoticon. En contraste, al considerar los emoticones la precisión se elevó hasta un 79 %.

*Prueba 2: Usando solo el clasificador Naive Bayes:* La precisión del clasificador con el entrenamiento mencionado en el apartado anterior fue de un 38 %.

*Prueba 3: Usando clasificador Naive Bayes con filtrado de publicaciones:* Para ésta prueba se consideraron todas las muestras al momento de clasificar una nueva publicación, sino únicamente aquellas publicaciones en las que apareciera la palabra en cuestión. Lo anterior ocurre porque se desconoce la cantidad de

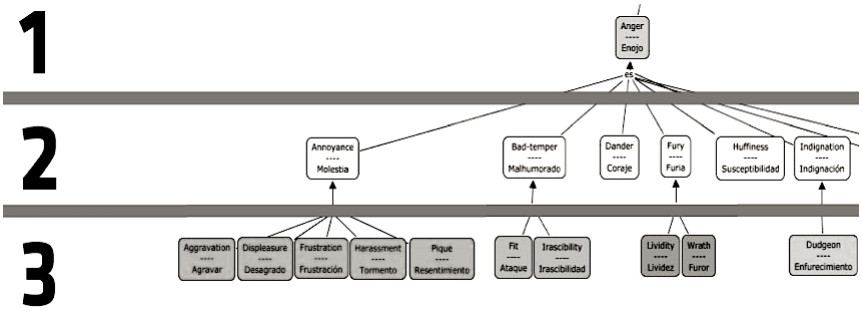


**Fig. 3.** Primeros tres niveles de ponderación de la jerarquía

palabras que están dentro de las publicaciones asociados aun un sentimiento con respecto a otros. La precisión para esta prueba fue del 44 %.

Teniendo en cuenta estos tres resultados la opción es elegir el clasificador semántico basado en la ponderación de la jerarquía. Este clasificador es muy preciso si la publicación a analizar contiene palabras de la jerarquía o algún emoticon.

Debido a esto decidimos realizar otras pruebas pero esta vez combinando los clasificadores anteriores. Dado que el clasificador basado en la ponderación de conceptos es el más preciso se decidió combinarlo con algún clasificador de la prueba 2 o 3 pero sólo en los casos en que las publicaciones no cuenten con palabras de la jerarquía o emoticones, es decir, cuando el clasificador asigne una publicación como ambigua. De esta manera en la jerarquía de conceptos se combina un recurso confiable como *WordNet Affect*, con un recurso basado en publicaciones que contienen un lenguaje coloquial como lo son las publicaciones de entrenamiento para Naïve Bayes. Las pruebas 4 y 5 son el resultado de esta combinación.

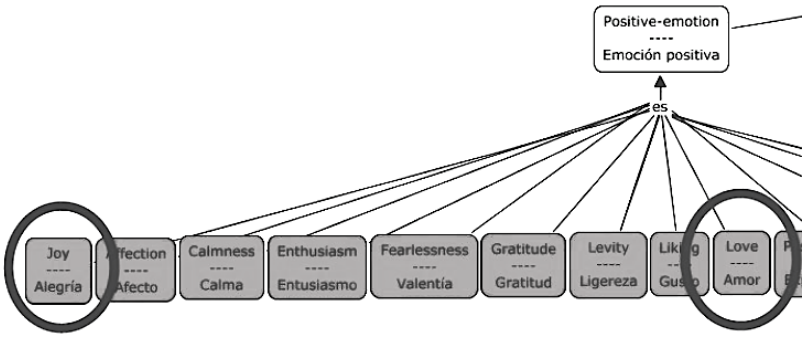


**Fig. 4.** Conceptos generales que definen alegría y amor

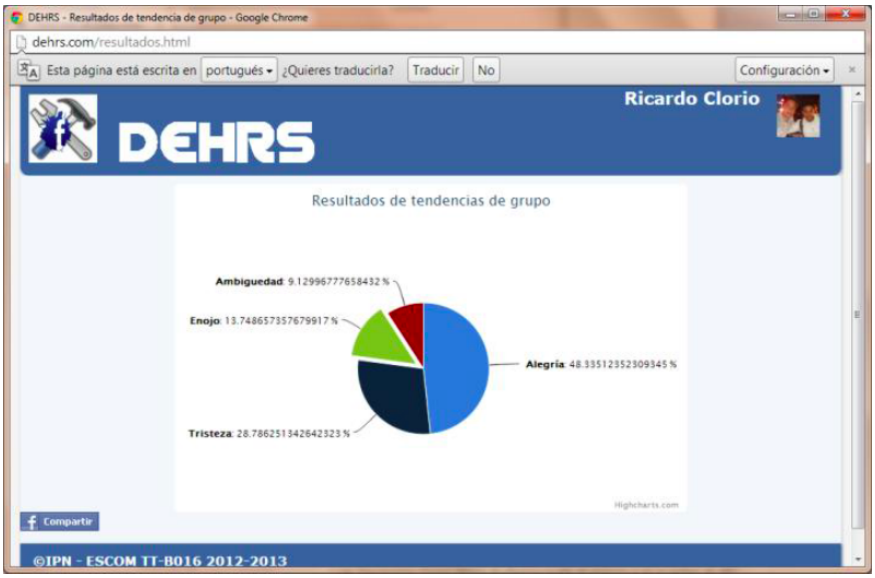


**Fig. 5.** Despliegue personal de resultados

*Prueba 4. Clasificador basado en jerarquía de conceptos y Naive Bayes con filtrado de publicaciones:* La precisión de esta combinación fue del 61 %. Es evidente que sea una precisión menor a la precisión del clasificador basado en la ponderación de conceptos, debido a que se da pie a clasificar publicaciones que antes sólo eran marcadas como ambiguas, por lo cual da pie a que el resultado de la clasificación sea errónea.

*Prueba 5. Clasificador basado en ponderación WNA y Naive Bayes:* La combinación de estos clasificadores es la utilizada en la herramienta, su precisión es del 63 %. Una de las ventajas de utilizar un algoritmo de aprendizaje supervisado, como *Naïve Bayes*, es que su precisión va en aumento a medida que más muestras clasifica ya que toma en cuenta todo lo que ha clasificado previamente a la hora de clasificar una nueva muestra.

Finalmente en la Fig. 5 los resultados son mostrados únicamente para las publicaciones personales del usuario que autorizó el análisis, o también se pueden mostrar las tendencias en sentimientos para un grupo de usuarios definidos mediante una consulta realizada por un super usuario del sistema.

## 5. Conclusiones

En este trabajo se presentó una opción útil para análisis de sentimientos en Facebook, combinando un clasificador semántico y un clasificador *Naïve Bayes* entrenado con publicaciones seleccionadas y que alcanza un desempeño del 63 %.

Sin embargo se detectaron casos donde la clasificación fue ambigua dado que existían palabras relacionadas a más de un concepto contemplado. Por ejemplo, el caso mas común fueron las publicaciones cercanas al concepto "amor".

En el ejemplo anterior, las publicaciones contienen palabras relacionadas a "amor" que también implícitamente estaban asociadas con "alegría", ver Fig. 4. En adición, la jerarquía de conceptos presentada no esta capacitada para detectar dicho concepto, y requiere de un enriquecimiento para contemplar más conceptos asociados a sentimientos.

También es muy importante considerar las características del lenguaje que usa el sector o grupo social que se usará para realizar las pruebas. El uso de emoticones, es común en poblaciones de edad joven y fue un factor decisivo en el diseño de la arquitectura del presente trabajo.

Finalmente es posible mejorar la precisión de clasificación , a través de mecanismos dinámicos que incrementen el número de conceptos asociados a la jerarquía semántica, en combinación de un incremento de los patrones que se usan el entrenamiento del clasificador *Naïve Bayes*. La aplicación web queda disponible en `http://148.204.57.31/dehrs`.

## Agradecimientos

Agradecemos el asesoramiento de Miguel Pardo Sixtos, Jesús Morales Alameda y David Ortega Pacheco de la Escuela Superior de Cómputo, así como el soporte económico de la Secretaría de Investigación y Posgrado del Instituto Politécnico Nacional por medio del proyecto multidisciplinario SIP-20130339.

## Referencias

1. G. Sidorov, S. Miranda, F. Viveros, A. Gelbukh, N. Castro, F. Velásquez, I. Díaz, S. Suárez, A. Treviño y J. Gordon, "Empirical Study of Machine Learning Based Approach for Opinion Mining in Tweets" Publicación, Centro de Investigación en Computación, Instituto Politécnico Nacional, México D.F. Septiembre 2012
2. C. Kalyan, Min Y. Kim. "Detecting emotional scenes using Semantic Analysis on Subtitles". Junio 2009. Disponible en: `http://nlp.stanford.edu/courses/cs224n/2009/fp/6.pdf`
3. C. Strapparava, A. Valitutti. "Wordnet-affect: an affective extension of wordnet". 2004. Disponible en: `http://hnk.ffzg.hr/bibl/lrec2004/pdf/369.pdf`
4. Margaret M. Bradley, P. Lang. "Affective Norms for English Words (ANEW): Instruction Manual and Affective Ratings". 1999. Disponible en: `http://www.uvm.edu/~pdodds/files/papers/others/1999/bradley1999a.pdf`
5. A. Mislove, S. Lehmann, Y. Ahn, J. Onnela, J. Niels. "Pulse of the Nation: U.S. Mood Throughout the Day inferred from Twitter" [online]. 2009. Disponible en: `http://www.ccs.neu.edu/home/amislove/twittermood/`
6. J. Pekins, "Text Calssification," Python text processing with nltk 2.0 cookbook, L. Subramanian, Ed. Aditya Belpathak, Noviembre de 2010, pp. 167 – 200

7. C. Strapparava, R. Mihalcea, Annotating and Identifying Emotions in Text , book chapter in Ïntelligent Information Access"', G. Armano, M. de Gemmis, G. Semeraro, and E. Vargiu, Springer, "Studies in Computational Intelligence", 2010.
8. C. Banea, R. Mihalcea, J. Wiebe, Sense-level Subjectivity in a Multilingual Setting, in Proceedings of the IJCNLP workshop on Sentiment Analysis where AI meets Psychology, Chiang Mai, Thailand (2011)
9. Facebook Developers, "Graph API", 2013 Disponible en: `https://developers.facebook.com/docs/reference/api/`
10. Facebook Developers, "Facebook para sitios web", 2013 Disponible en: `https://developers.facebook.com/docs/guides/web/`.
11. Molino Labs, "Lematizador", 2012 Disponible en: `http://www.molinolabs.com/acerca.html#lematizador`

# Diet Generator Using Genetic Algorithms

Catalán-Salgado Edgar-Armando, Zagal-Flores Roberto, Torres-Fernandez Yuliana,, and Paz-Nieves Alexis

ESCOM-IPN, Av. Juan de Dios Batiz s/n, GAM, Mexico DF

ecatalans@ipn.mx
zagalmmx@gmail.com
yuliana247@hotmail.com
alexis_suzumiya@hotmail.com

**Abstract.** Overweight and obesity are defined as abnormal or excessive fat accumulation that may be harmful to health and even can even result in death. This problem can be reduced for a person if this follows a proper diet, in which the consumption of kilocalorie, carbohydrates, lipids and proteins per day are restricted. Given a database of foods to find the 5 meals in each day of a week becomes a complex task. In this article a way to generate diets using genetic algorithms is presented, which one considers the restrictions mentioned and also allows establish preferences for certain food groups.

## 1 Introduction

Overweight and obesity are a chronic disease that can be treatable, that disease surge due to a imbalance energetic between consumed kilocalorie and expended kilocalorie[1].

This overweight generates a diversity of health problems, included but not limited to diabetes, respiratory problems, musculoskeletal problems,cardiovascular diseases, hypertension,thyroid, hypothyroidism, hyperthyroidism, hyperglycemia, cancer and psychological problems.

In Mexico, 72% of women and 66% of men suffers overweight or obesity, thus approximately 16.96 million people. In 2000, using a conservatory stage, the morbid rate for obesity related problems in population over 35 years was 195.71 for each 100000 with a total of 55749 deceases. For the same 2000, using a extended stage, the morbid rate for obesity related problems in population over 35 years was 433.6 for each 100000 with a total of 123511 deceases.

Overweight can be generated in different ways: consumption of more calories than necessary, alimentation deficit, lack of exercise, genetic inheritance, cultural factors, hormonal problems, diseases and medicine secondary effects.

A diet is a way to reduces this problem in a persons, depend on different factors and must be set by a specialist.

One diet is established limiting the quantity of kilocalorie consumed in a day, for example, 1300 kcal, 1500 kcal, etc.

The World Health Organization establish that is best to distribute the kilocalorie consumed in five time aliments per day as is specified in table 1.

**Table 1.** Percentage of dairy KCal consumption and their corresponding KCal in different diets.

| Name | Percentage | 1300 KCal | 1500 KCal | 1800 KCal | 2000 KCal |
|---|---|---|---|---|---|
| Breakfast | 20% | 260 KCal | 300 KCal | 360 KCal | 400 KCal |
| Lunch | 10% | 130 KCal | 150 KCal | 180 KCal | 220 KCal |
| Meal | 40% | 520 KCal | 600 KCal | 720 KCal | 800 KCal |
| Night tea | 10% | 130 KCal | 150 KCal | 180 KCal | 220 KCal |
| Dinner | 20% | 260 KCal | 300 KCal | 360 KCal | 400 KCal |

Furthermore a balanced diet feature is macronutrient intake balance, this macronutrient are carbohydrate, lipids and proteins and their suggested distribution is shown in table 2

**Table 2.** Corresponding KCal per nutrient in different diets

| Name | Percentage | 1300 KCal | 1500 KCal | 1800 KCal | 2000 KCal |
|---|---|---|---|---|---|
| Carbohydrate | 60 % | 780 KCal | 900 KCal | 1080 KCal | 1200 KCal |
| Lipids | 25 % | 325 KCal | 375 KCal | 450 KCal | 500 KCal |
| Proteins | 15 % | 195 KCal | 225 KCal | 270 KCal | 300 KCal |

Once we know the nutritional plan contribution of each nutrient, is necessary to know how much grams must be consumed in order to get a balanced diet, with this purpose the following equivalences are considered:

1. One Carbohydrate gram deliver 4 kcal
2. One Lipid gram deliver 9 kcal
3. One Protein gram deliver 4 kcal

Realizing the conversions our table, the distribution in grams terms is shown in table 3:

The problem resides in that given a database of N aliments how to find the appropriate combination to accomplish this distribution for a special needs of one individual. Furthermore how to find an appropriate combination for each aliment time of each day. Also a specific diet with specific aliment should bore the user fast.

The basis of this problem is to find a set of appropriate combination of aliments, the aliment database should contain one hundred or one million of

**Table 3.** Corresponding grams per nutrient in each diet type

| Name | Percentage | 1300 KCal | 1500 KCal | 1800 KCal | 2000 KCal |
|---|---|---|---|---|---|
| Carbohydrate | 60 % | 195 g | 225 g | 270 g | 300 g |
| Lipids | 25 % | 36.11 g | 42.66 g | 50 g | 55.55 g |
| Proteins | 15 % | 48.75g | 56.25 g | 67.5 g | 75 g |

aliments, but is necessary to consider most of them when the diet is generated to add versatility.

In this paper we show a way to generate the diet using genetic algorithms, not for the complexity nor the existence of high search space, simple for the ability of find different possible solution in any part of the search space.

Anyway the diet generated must be approved by one specialist, this algorithm does not replace them, is only a tool to help them.

## 2 Materials and Methods

A genetic algorithm emulates the biological evolutionary process in intelligent search, operates through a cycle of the following stages[2, 3].

1. Creation of a population of strings, representing possible solutions.
2. Evaluation of each string
3. Selection of best strings
4. Genetic manipulation to create a new population of strings

We consider as an aliment as any food stored in the aliment database, for which one we have the measure of kilocalorie, carbohydrate, protein and lipid for each 100gr.

An aliment time is one of the five possible defined by the World Health Organization, thus is: Breakfast, lunch, meal, night tea and dinner

Given a aliment database, the challenge is to find a the set of aliments in each aliment time, we solve this using a genetic algorithm as specified below.

### 2.1 Chromosome Representation

Being $a$ an aliment time, a chromosome $\mathbf{C}$ of $n$ aliments is represented in the following way:

$$\mathbf{C} = [a_1, ..., a_n]$$

### 2.2 Fitness Evaluation

Chromosome evaluation is made calculating the total of kilocalorie and comparing with the expected value according the diet. In fact, this cant be complete exact, is almost impossible to achieve by a collection of aliments an exactly sum

of 1300 kcal for example. So we allow to establish a percent $p$, expressed in the range [0,1],of accepted variation over the reference values for diet: reference kilocalorie value denoted by $r_1$, carbohydrate reference value denoted by $r_2$ , protein reference value denoted by $r_3$, and lipid reference value denoted by $r_4$

First calculate for $\mathbf{C}$ the total Kilocalorie $k$ using (1), total carbohydrate $h$ using (2), total protein $p$ (3), total lipid $d$(4)

$$k = \sum_{i=1}^{n} k(a_i) \quad (1) \qquad h = \sum_{i=1}^{n} h(a_i) \quad (2) \qquad t = \sum_{i=1}^{n} t(a_i) \quad (3) \qquad d = \sum_{i=1}^{n} d(a_i) \quad (4)$$

Also a proximity bonus is added to the evaluation, so if its closer to the reference value a bonus is added.
First we evaluate the total Kilocalories obtained using (1) in (5) in order to get the evaluation with respect to kilocalories.

$$f_1 = \begin{cases} 2 & \text{if } r_1 * (1 - p/2) <= k <= r_1 * (1 + p/2) \\ 0 & \text{if } r_1 * (1 - p) <= k < r_1 * (1 - p/2) \\ & \text{or } r_1 * (1 + p/2) < k <= r_1 * (1 + p) \\ -2 & \text{if } k < r_1 * (1 - p) \text{ or } k > r_1 * (1 + p) \end{cases} \quad (5)$$

Later we evaluate the total carbohydrate obtained using (2) in (6) in order to get the evaluation with respect to carbohydrates.

$$f_2 = \begin{cases} 2 & \text{if } r_2 * (1 - p/2) <= h <= r_2 * (1 + p/2) \\ 0 & \text{if } r_2 * (1 - p) <= h < r_2 * (1 - p/2) \\ & \text{or } r_2 * (1 + p/2) < h <= r_2 * (1 + p) \\ -2 & \text{if } h < r_2 * (1 - p) \text{ or } h > r_2 * (1 + p) \end{cases} \quad (6)$$

Similarly we evaluate the total protein obtained using (3) in (7) in order to get the evaluation with respect to proteins.

$$f_3 = \begin{cases} 2 & \text{if } r_3 * (1 - p/2) <= t <= r_3 * (1 + p/2) \\ 0 & \text{if } r_3 * (1 - p) <= t < r_3 * (1 - p/2) \\ & \text{or } r_3 * (1 + p/2) < t <= r_3 * (1 + p) \\ -2 & \text{if } t < r_3 * (1 - p) \text{ or } t > r_3 * (1 + p) \end{cases} \quad (7)$$

Finally we evaluate the total Lipids obtained using (4) in (8) in order to get the evaluation with respect to lipids.

$$f_4 = \begin{cases} 2 & \text{if } r_4 * (1 - p/2) <= d <= r_4 * (1 + p/2) \\ 0 & \text{if } r_4 * (1 - p) <= d < r_4 * (1 - p/2) \\ & \text{or } r_4 * (1 + p/2) < d <= r_4 * (1 + p) \\ -2 & \text{if } d < r_4 * (1 - p) \text{ or } d > r_4 * (1 + p) \end{cases} \quad (8)$$

To get the final fitness value we add four previous values using (9)

$$f = f_1 + f_2 + f_3 + f_4 \quad (9)$$

### 2.3 Selection

According with the evaluation we order the population from best fitness to lower fitness, we select half of the population that corresponds to the best evaluated chromosomes reproduces it using the crossover function.

### 2.4 Crossover

being $C^1$ and $C^2$ two chromosomes of the same dimension as follows

$$\mathbf{C}^1 = [a_1, ..., a_n]$$
$$\mathbf{C}^2 = [b_1, ..., b_n]$$

A single point crossover between this two chromosomes is used in order to generate another two chromosomes, being $p$ the cross point position we have

$$\mathbf{C} = [a_1, ..., a_p, ..., b_{p+1}, b_n]$$

$$\mathbf{C} = [b_1, ..., b_p, ..., a_{p+1}, a_n]$$

### 2.5 Mutation

Mutation only select one descendent and one position randomly and change its value.

## 3 Results and Discussion

We prove our algorithm with different parameters to see the convergence time, the graphics result is shown.

**Test 1**

Create a breakfast, with the following parameters:
Population size:15
Generations: 100
Number of aliments: 2
Crossover position: 1
Mutation frequency: each 5 generations

We shown the fitness evolution in fig.1 In this case the fitness value arrives to local maxima around generation 15 and stay there until 55 generation arrives, thus probably due to a mutation.

**Test 2.**

we create a meal with the following parameters:
Population size:15
Generations: 100
Number of aliments: 3
Crossover position: 1

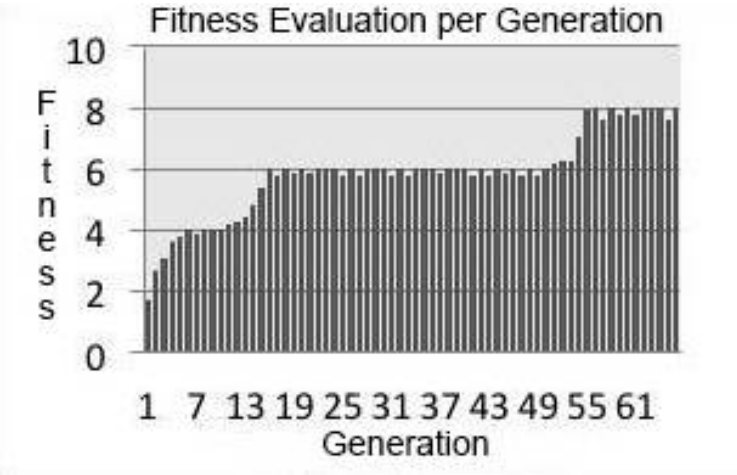


**Fig. 1.** Fitness value evolution for a breakfast of two aliments

Mutation frequency: each 5 generations

We shown the fitness evolution in fig.2. In this case the fitness value quickly arrives to local maxima value of six, but in generation twenty one arises to eight, thus probably due to a mutation.

## 4 Conclusions

In this paper a way to create a diet using genetic algorithms is used. As we shown in the section results we can generate each aliment time separately this give us the ability to satisfy the standard or to create our own percent to satisfy special needs.

The fact of generate seaparately each aliment time give a versatility to the diet generator, we can create days with two heavy aliments in meal time and another with four soft aliments.

We take advantage in the fact that the genetic algorithm dont ever converge to the same result, in this way we can generate different aliment configuration for the same parameters easily

This works can be improved developing the following:

1. Add to the aliment database the ability to generate diets for diabetic people
2. Expand the database to include prepared aliments and their corresponding ingredients
3. Expand the algorithm to consider the physic activities that the individual realizes in a day

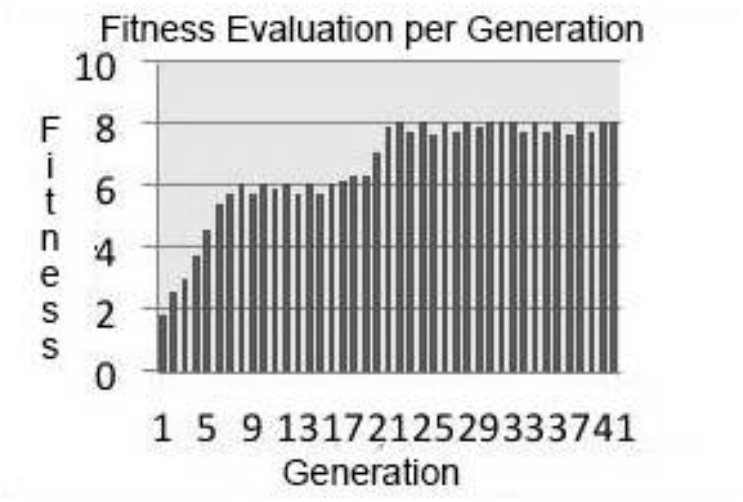


**Fig. 2.** Fitness value evolution for a meal of three aliments

4. Expand the algorithm to consider prohibited aliments in order to generate diets for allergic people.
5. A way to select or exclude an alimentary group would be desirable, or even a system of preferences would improve this system.

## Acknowledgments

The authors are grateful to the secretary of research and postgraduate of National Polytechnic Institute for the economic support given to the multidisciplinary project SIP-20130307

## References

1. http://www.who.int/mediacentre/factsheets/fs311/es/. Tech. rep., WHO, 2014.
2. Konar, A. *Artificial Intelligence and Soft Computing: Behavorial and cognitive Modeling of the human Brain.* CRC Press, 1999.
3. Mitchell, T. M. *Machine Learning.* McGraw-Hill, 1997.

# Performance Analysis of a Wireless Sensor Network for Seism Detection in an Overlay Cognitive Radio System

Hassel Aurora Alcalá Garrido[2], Mario Eduardo Rivero-Angeles[1], Izlian Yolanda Orea-Flores[2], Ramsés Rodríguez[3]

[1] Communication Networks Laboratory, CIC-IPN.

Av. Juan de Dios Bátiz, Col. Nueva Industrial Vallejo, Gustavo A. Madero, Mexico City, 07738.

[2] Telematics Department, UPIITA-IPN.

2580 Instituto Politécnico Nacional Avenue, Barrio La Laguna Ticomán, Gustavo A. Madero, Mexico City, 07340.

[3] SEPI ESIA-IPN

Zacatenco. Luis Enrique Erro Avenue, Zacatenco, Gustavo A. Madero. Mexico City, 07738

**Abstract.** This paper studies the performance of a wireless sensor network (WSN) with cognitive radio (CR) capabilities to gather information about structural health monitoring (SHM) of buildings in case of seismic activity. The system performance is evaluated in terms of energy consumption and average packet delay using a discrete event simulator. In order to efficiently use the resources of the network and considering that the WSN will be installed in office or home buildings, we propose the use of the empty (white) spaces in a conventional cellular system. Thus, the WSN will act as secondary network, which do not affect the quality of service of the primary network, since it will work in an overlay structure. The main performance parameter of the primary network is the blocking probability since a Blocked Call Cleared (BCC) system is considered. By using the data collected in the WSN and transmitted through the unused channels of the cellular system, it is possible evaluate the damage caused by the seismic activity in a certain building. The major benefit of using a WSN with CR capabilities compared to the traditional approach, i.e., only one sensor per building floor or even per building is that with the WSN it is possible to collect much more information related to both the seism and the effects on the monitored building without the additional traffic in the already crowded unlicensed spectrum.

**Keywords:** Wireless Sensor Networks (WSN), Cognitive Radio (CR), Blocked Calls Cleared (BCC) system, Seism detection, Structural Health Monitoring (SHM)

## 1 Introduction

Wireless sensor networks (WSN) are composed of a large number of small sensor nodes with limited computing power, which are limited by their size and lifetime; usually they have a single omnidirectional antenna [1] to communicate with each

other through wireless transmissions. The organization of their internal software and hardware must be configured properly in order to work effectively and be able to adapt dynamically to new environments, requirements and applications. Sensor networks must be able to adapt to different environmental changes in the monitored area, e.g. sensors may decrease their work cycles in order to reduce their power consumption when there is no significant change in general sensor readings [2].

Radio spectrum resources play a fundamental role in the wireless communication systems. The rapid growing demand for wireless communication services and some inefficient spectrum allocation methods result in the scarcity of the spectrum resources, which greatly hinders the development of future wireless communication systems. For instance, the fixed spectrum allocation approach ensures that wireless applications and devices do not cause any harmful interference with each other. However, it results in the inefficient use of the current radio spectrum. This results in scenarios where some bands are heavily occupied by busy radio services while other bands are seldom used at all. There are already great difficulties to find unassigned spectrum for the new broadband wireless communication services. One of the most promising solutions to overcome this problem is the cognitive radio (CR) technology. A CR device has the ability to identify an unoccupied spectrum band for temporarily usage, and vacate the spectrum when it is necessary. Therefore, CR is viewed as a technology to overcome the current inefficient usage of radio spectrum resources [3].

By dynamically changing its operating parameters, cognitive radio senses the spectrum, determines the vacant bands, and makes use of these available bands in a proper manner, improving the overall spectrum utilization. With these capabilities, cognitive radio can operate in licensed as well as unlicensed bands. In licensed bands wireless users with a specific license to communicate over the allocated band (the primary users, PUs), have the priority to access the channel. Cognitive radio users, also called secondary users (SUs), can access the channel as long as they do not cause interference to the PUs.

When a PU starts its communication, the cognitive radio user must detect the potentially vacant bands (spectrum sensing) and decide onto which channel to move (spectrum decision), finally adapt its transceiver so that the active communication is continued over the new channel (spectrum handoff). This sequence of operation outlines a typical cognitive cycle, which can also be applied over an unlicensed band by all cognitive radio users [4]. CR capabilities may also be exploited by WSNs, which are traditionally assumed to employ fixed spectrum allocation, and characterized by the communication and processing resource constraints of sensor nodes [5].

The BCC system is based on a TDMA (Time Division Multiple Access) system while the secondary network (the WSN) is a cluster based network that also uses a TDMA based protocol in the steady state (SS), considering that such protocol satisfies the functional requirements of the system by transmitting information in a collision-free manner. Note that the use of a random access protocol could cause loss of packages for proper monitoring and timely analysis of seism related data. The system performance is studied using discrete event simulations performed in C++.

This paper is organized as follows: First, Section 2, develops the design of an event-driven WSN applied to the early detection of damage in buildings in seismic areas with CR capabilities. The solution is aimed at improving the bandwidth

utilization considering the cellular system as a primary network. Also, some relevant numerical results are presented. We present future work and some conclusions of our work in Section 3.

## 2 System Operation

In this section we present the design of the CR system where the cellular system is used as a primary and the secondary network is the WSN for seism detection and monitoring. The system is now described in detail.

### 2.1. Secondary Network: WSN.

The main variables that affect the performance of a WSN are: number of nodes in the network, number of Cluster Heads (CH), transmission probability, coverage area, duration of steady state and time slot size.

The system operation begins by distributing the nodes in a random manner in the desired coverage area. Then, they are classified as either CH or Cluster Member (CM). This is done by nodes transmitting a control packet to the entire network using the slotted NP-CSMA (Non-persistent Carrier Sense Multiple Access) protocol. The first $N$ nodes that successfully transmit their packet become CH. The rest of the nodes also transmit their control packet in order to be associated as CMs to their closest CH. At that time, all nodes are aware of their role in the network, either as CH or CM, and CMs know at which CH they are associated to. Hence, each CH creates a routine time and assigns a time slot in a TDMA structure to each CM to transmit its information. In figure 1, we can see the basic system operation. It can be seen that there are two distinct phases: cluster formation and steady state. Note that in the cluster formation, transmissions are high energy demanding since all nodes have to transmit to the entire network while the steady state is a collision-free period where nodes report their reading to their respective CH and then the CH transmits the gathered data to the sink node.

To analyze the performance of the steady state phase, we consider an average of $M$ CMs per cluster, each transmitting packets of $P$ bits. If the total transmission rate is $R$ bits/sec, then the transmission time of the packet $T$ is $P/R$, this is taken as the duration of the slot. Hence, the frame duration is $MT$ [6].

It is important to notice that the CH consume much more energy than the CM simply because in the steady state CHs remain active at all times receiving data from the CMs and transmitting this data to the sink node. Again, the transmission to the sink is usually highly energetic since the sink node can be placed at a large distance from the network. Therefore, it is important to rotate the function of the CH to all nodes in the system. Building on this, it is considered that the steady state only lasts 20 seconds. After this time, clusters are broken in order to select new nodes as CHs.

To calculate the energy consumed in the WSN, the following values are proposed:

$E_{Tx}^{CF} = 1\ unit\ of\ energy$ used to transmit during the CF phase. (1)

$E_{Tx}^{SS} = 0.5\ unit\ of\ energy$ to transmit from the CM to the CH at the steady state. (2)

$E_{Tx}^{CH-BS} = 1.5\ unit\ of\ energy$ consumed to transmit from the CH to the Base Station. (3)

$E_{Rx} = 0.1\ unit\ of\ energy$ consumed for packet reception. (4)

The rationale behind this is to consider general energy consumption and not to consider specific sensor nodes. Indeed, the actual energy consumption can be easily extended to any commercial node since the energy consumption is normalized at the value of $E_{Tx}^{CF}$. The presented model attempts to capture the following behavior: a) when a packet is transmitted in the CF stage, nodes perform high-cost transmissions since all nodes in the network must follow the transmission of other nodes that are determining which cluster they will be assigned; b) while transmitting during the steady state phase, nodes already know to which CH they belong to. Since in average, CM are close to the corresponding CH, these transmissions are less energetic; c) CH consume more energy to transmit the gathered information to the sink node since typically, the sink node is found outside the network area; d) packet reception consumes much less energy than packet transmissions.

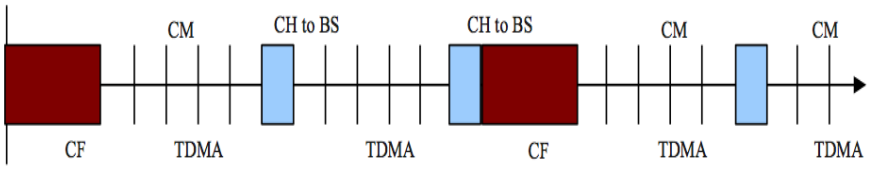


**Fig. 1.** Basic operation of the secondary network (WSN)

It is assumed that the length of the message of the structural health monitoring is 1 Kbit; taking into account the standard values for commercial devices, the value of 11 Mbps is taken as the baud rate of the wireless node. From this, it is easy to see that the size of the slot required to transmit the packet in the secondary network is 0.1 milliseconds.

## 2.2 Primary Network: Cellular System

In the case of the primary network, a simple BCC system is considered. Hence, nodes that arrive to the system and find no available resources are blocked. The variables considered are: arrival rate, average service time, number of servers, frame duration, and slot duration.

We consider an infinite population model, i.e. the traffic intensity remains unchanged regardless of the number of users being served in the system. In particular, we assume that the system can have a maximum of *N* clients with an active call and if a new customer arrives when all servers are busy, the customers are blocked, i.e., it is denied their access to the system and they leave without being served [7]. Users arrive to the system according to a Poisson process, but only those who find available channels may be served.

In particular, we consider a TDMA based system such as GSM, GPRS or EDGE, which is composed of *N* slots per frame to serve users. When a user arrives, it is

assigned a slot and it will use it until the active call ends.

In Fig. 2, we can see an example of the allocation of the slots. At the beginning, the first and second frames, all time slots are busy. Thus, if a user requests to be served by the system, it will be rejected. In the third frame, slot 2 is free and can be used by a user who asks to be served by the system. In the last frame, a new user has occupied slot 2 again and slot 4 is now free.

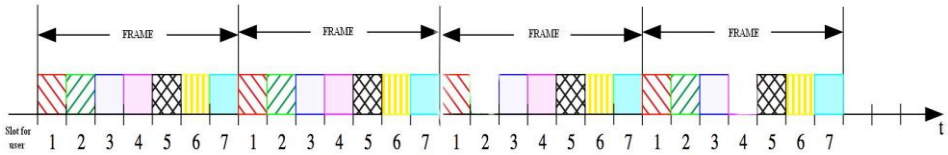


**Fig. 2.** TDMA in BCC System

In a GSM system, the frame is divided into eight time slots; the duration of a frame is 125 milliseconds and the size of the slot is approximately 15.625 milliseconds. Each user making a call is assigned a specific time slot for transmission, which enables multiple users to use the same channel simultaneously without interfering with each other.

Blocking probability is analyzed when the network operates with the TDMA scheme and it is compared to the Erlang B blocking formula for an offered traffic load in the range of 0.1 to 1.

### 2.3 Numerical Results

In this section, the system is evaluated in terms of the average cluster formation time for the secondary network and blocking probability for the primary network. To this end, the following system parameters are considered: The number of nodes in the network ranges from 10 to 100 and are distributed in an area of 400 square meters (20m x 20m which corresponds to a typical building floor area in Mexico City). The number of CHs varies in the range of 10% to 50% of the nodes in the system. For example, if we have 100 nodes in the network, in the simulation we analyzed the case where there are 10, 20, 30, 40, and 50 CH.

Fig. 3 shows the average cluster formation time for different number of nodes in the network. It can be seen that with a transmission probability of 0.001 there is a large number of collisions with few nodes in the network, but as the number of nodes increases, also the collision probability slightly increases. For the case of the transmission probability of 0.1 for a small number of nodes there are few collisions, as the number of nodes in the network increases, the cluster formation time also increases due to the large number of collisions. Analyzing the value of 0.01, we note that the number of collisions is small when we have few nodes and when we increase the number of nodes there is not an abrupt increase in the graph, also the collision probability slightly increases. Therefore, 0.01 can be an appropriate value for the considered environment.

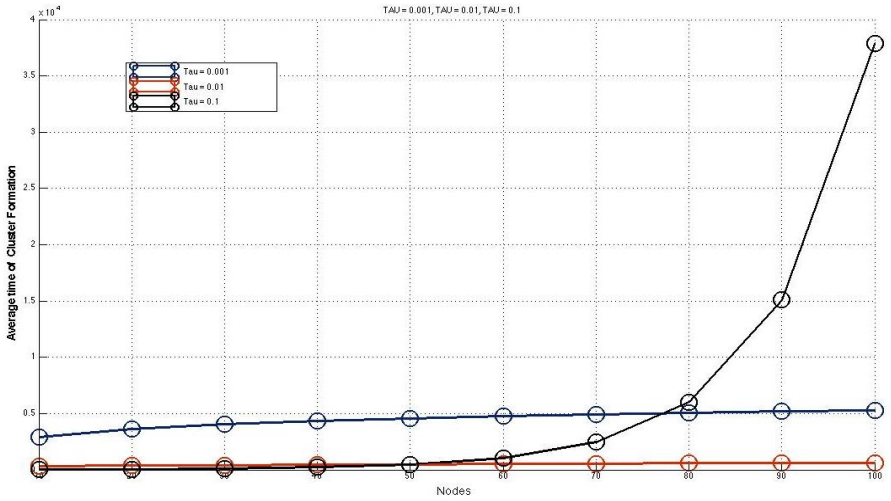


**Fig. 3.** Average cluster formation time with transmission probability 0.001, 0.01 and 0.1.

In Fig. 4, the blocking probability of the primary network for the simple BCC system is presented. If we have a few servers, the blocking probability is high. As the number of servers increases, the blocking probability decreases.

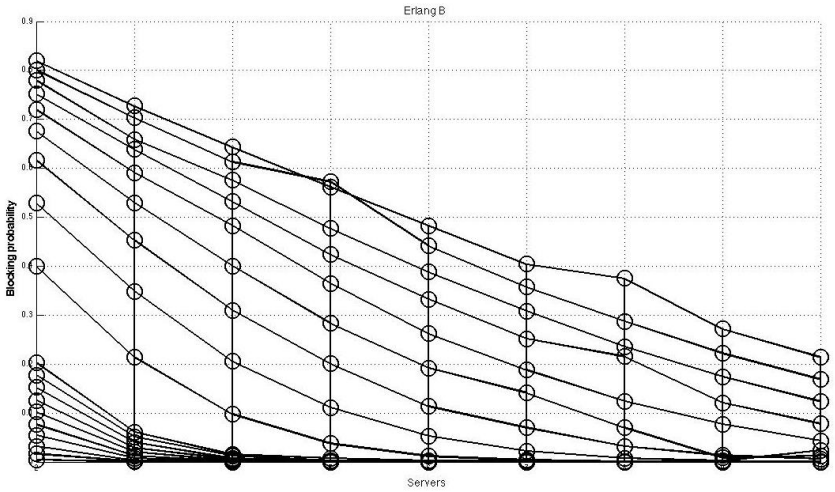


**Fig. 4.** Blocking probability of primary TDMA network without regarding to the number of servers.

In Fig. 5, we can notice the blocking probability relative to the offered traffic. When there is a small traffic load on the network, the blocking probability is small; while a very large offered traffic entails a high blocking probability.

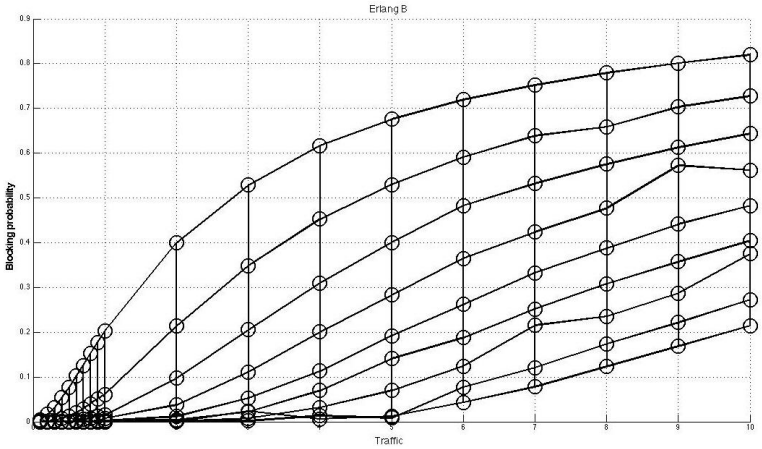


**Fig. 5.** Blocking probability of primary TDMA network without regarding to the offered traffic.

Finally, in Fig.6, we can see a comparison of the blocking probability in the primary network for the simple BCC system and with the TDMA structure for 8 time slots with the traffic load in the range of 0.1 to 1. In general, it can be seen that there is a good match between those results with a slight difference for high offered loads.

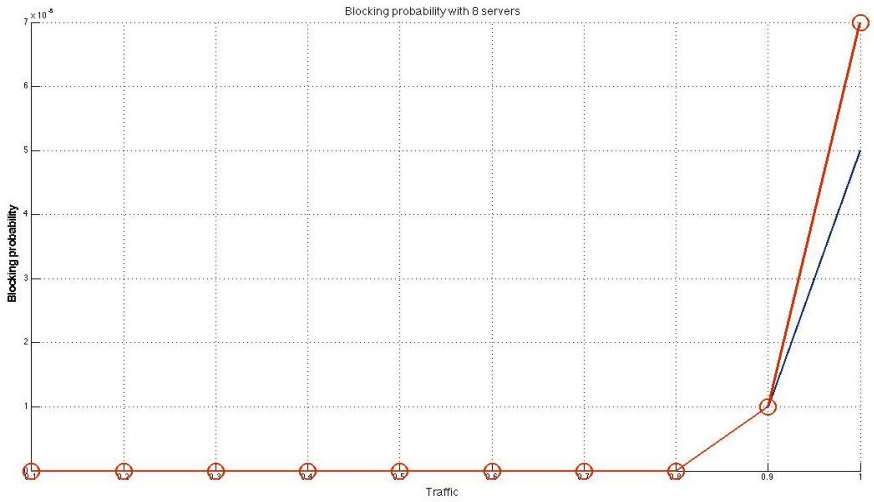


**Fig. 6.** Comparison of the blocking probability in the primary network with and without the TDMA structure.

## 3 Conclusions and future work

A WSN is proposed to be monitoring seismic activity and for transmission of relevant data in case of telluric movements in buildings by making use of the white spaces from a cellular system under a cognitive radio network.

We note that a cellular system as a primary network is suitable for the transmission of data to the secondary network since the blocking probability can be lower than 5% while maintaining empty spaces in the TDMA frame.

Furthermore, in our future work, we plan to model the behavior of the primary and secondary network mathematically and verify analytical results with simulation results.

## References

1. Hu, X., Wang, B., & Ji, H. (2013). "*A Wireless Sensor Network-Based Structural Health Monitoring System for Highway Bridges"*. Computer-Aided Civil and Infrastructure Engineering , Pp. 193-209.
2. Pradnya, G. & Anjali, M. (2008). "*A survey of architecture and node deployment in Wireless Sensor Network"*. IEEE. Pp. 426-430.
3. Xue, J., Feng, Z. & Chen, K. (2013). *"Beijing Spectrum Survey for Cognitive Radio Applications"* . Beijing Univesity of Posts and Telecommunications. Beijing: IEEE.
4. Akan, B., Karli, O. & Ergul, O. (2009). "*Cognitive Radio Sensor Network"*. IEEE Network.
5. Reddy, V., Krisha R. & Reddy, M. (2011). "*Sensor Networks for Cognitive Radio: Theory and System Design"*. IEEE.
6. Rom, R. & Sidi, M. (1989). "*Multiple Access Protocols. Performance and analysis"*. Haifa, Israel: Springer-Verlag. Pp. 1-7.
7. Kleinrock, Leonard. (1975). "*Queueing systems*". John Wiley & Sons, Inc. Pp. 103

# Bitcoin y Privacidad 101

Armando Becerra

Consultor en Seguridad de la información, privacidad y protección de datos, México

armando.becerra@ifai.org.mx

**Abstract.** En este artículo se presenta una visión general de las implicaciones a la privacidad del uso de las llamadas *cripto-monedas*, y su principal representante hasta el momento, el Bitcoin. El artículo pretende destacar algunas consideraciones sobre estas tecnologías: la expectativa razonable de privacidad, la seguridad de la información y el posible abuso por parte de los usuarios.

## 1 Introducción

El Internet ha transformado la forma en que la macro y microeconomía se desarrollan, hoy en día cerca de dos billones de personas están conectadas a Internet [1] y se estiman intercambios a través de *e-commerce* por ocho trillones de dólares se considera incluso que la madurez en Internet está directamente relacionada al Producto Interno Bruto.

En este entorno es razonable esperar la digitalización de elementos primordiales de la economía como son los sistemas de pago y las divisas, sin embargo muy pocos vislumbraban que el concepto de las *cripto-monedas*, y su principal representante, el *Bitcoin (BTC)*, tuvieran un impacto tan profundo: se le considera la primera moneda digital descentralizada de la historia, su economía es mayor que la de algunos países pequeños y la capitalización de su mercado se estima en más de un billón de dólares.

## 2 Uso de tecnologías P2P

Ante las amenazas de informáticas, el espionaje gubernamental o simplemente por una noción de *"preservar la privacidad en línea"*, la población ha demostrado inclinación y hasta confianza hacia el uso de las tecnologías de comunicación *peer-to-peer o punto a punto (P2P)*, en un mundo sin *derecho al olvido* [2], muchas personas están optando por estas soluciones para mantener sus actividades en línea fuera de vigilancia, pues actúan como un canal de comunicación instantáneo y a su vez son independiente a terceros que las controlen o monitoreen [3].

La historia de las redes *P2P* puede remontarnos a sitios que han enfrentado serios problemas de derechos de autor (e.g. Pirate Bay [4]), y disidencia civil contra sistemas totalitarios (e.g. TOR [5]): en Arabia Saudita e Irán por ejemplo, la policía religiosa ha encontrado muchas dificultades para evitar que los jóvenes utilicen

mensajería Bluetooth a través de los celulares para llamar y mandar mensajes a completos extraños, ya sea para coquetear o para la coordinación de protestas.

A este punto es difícil entender exactamente quién creo el *Bitcoin*, ya que se hizo bajo el seudónimo de *Satoshi Nakamoto* [6], que podría ser un individuo o un grupo de desarrolladores. En cualquier caso, fue una respuesta a la creciente desconfianza del público hacia la moneda tradicional y a los bancos centrales.

Aprovechando los recursos computacionales existentes, el *BTC* se sostiene en la infraestructura proporcionada por los usuarios y en la comunicación directa entre las partes, bajo la premisa de realizar transacciones anónimas al igual que con las comunicaciones *P2P*.

## 3 Privacidad en las transacciones

El modelo de banco central tradicional alcanza un nivel de privacidad aceptable en relación de que el acceso a la información está limitado a partes interesadas de confianza. Sin embargo para ciertos usuarios existe la preocupación por reducir el número de entidades que intervienen en estas transacciones:

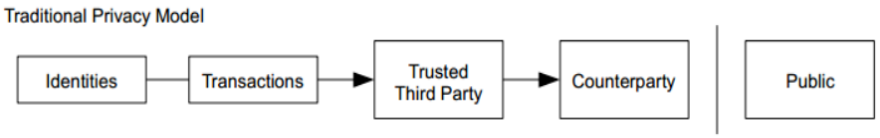


**Fig. 1.** Modelo tradicional de privacidad en transacciones

A través del cifrado *inherente* en el esquema de funcionamiento de las *cripto-monedas,* se pueden utilizar claves públicas y privadas para la realización de las transacciones, así el público en general puede ver que alguien está enviando una cantidad de *BTC* a otra persona, pero sin información que vincule esta acción a una persona en particular, algo muy similar a la información publicada en las bolsas de valores, donde se conoce el tiempo y el tamaño de las operaciones individuales, sin mencionar las partes que intervienen:


**Fig. 2.** Modelo de transacciones cifradas

## 4 Privacidad relativa

Sin bien la concepción del *Bitcoin* contempla un nivel de anonimato similar al de otros esquemas P2P, se podría considerar que a su vez es la red de pagos más transparente jamás creada [7]: todas las transacciones de Bitcoin se almacenan pública y permanentemente en la red, lo que significa que cualquiera puede ver los fondos y transacciones de una dirección Bitcoin.

Si bien el uso de BTC representa beneficios a la privacidad como el hecho de poder crear un número ilimitado de entidades de *Bitcoin* (o carteras, donde se almacena la moneda), cada transacción única es registrada, así por ejemplo alguien podría mandar un BTC a la dirección *"1NiJGiZ2eBvQfKiD7eeG2rtBa6MdHYRXLr"* y saber que esta transacción se hizo pues los "libros" e estas transacciones son públicos, y nada evitaría que alguien realizara una base de datos con el comportamiento de una cartera en particular. Por otro lado, muy pocos bienes lícitos podrían adquirirse por Internet sin que intervenga una forma de identificación [8], como la dirección de envío de la compra. Finalmente, en lugar de prohibir los *BTC*, si estos se vuelven un método de pago de uso corriente entonces seguramente estarán sujetos, quizá no a una regulación específica, pero sí a identificación del comprador. Para fines prácticos y lícitos una moneda no puede garantizar la privacidad de los usuarios.

## 5 Abuso en la privacidad

TOR es una red de túneles virtuales que permite a los usuarios navegar con privacidad en Internet, a los desarrolladores, crear aplicaciones para el intercambio de información sobre redes públicas sin tener que comprometer su identidad, ayuda a reducir o evitar el seguimiento que hacen los sitios web de los hábitos de navegación de las personas y a publicar sitios web y otros servicios sin la necesidad de revelar su localización.

Los objetivos de TOR como proyecto de software libre son admirables, sin embargo la posibilidad de navegar y crear servicios anónimos ha permitido el desarrollo de actividades a toda luz cuestionables, por ejemplo: pornografía infantil, venta de drogas, tráfico de información sensible o clasificada, lavado de dinero, armas, entrenamiento especializado en temas delictivos, entre otros. El mercado negro tradicional ha encontrado un lugar fértil para expandirse utilizando estas plataformas [9].

Pese a que no hay cifras exactas sobre el crecimiento o popularización de plataformas como TOR para el intercambio de bienes ilícitos, definitivamente hay *un antes y un después* con la utilización *cripto-monedas* como el *BTC* debido a que las transacciones son directas de un usuario a otro, sin ninguna institución mediadora de manera directa.

## 6 Conclusiones

*BTC* es una tecnología que ha sorprendido en la sociedad de la información pues está generando grandes cambios en la concepción del dinero y la economía. Existe un desafía inmenso para explotar el potencial minimizando los riesgos existentes: el anonimato relativo, las transacciones internacionales o la consideración de las carteras de *cripto-divisas* como un dato que podrían revelar información de los individuos. El BTC sirve también como referencia respecto a la necesidad del trabajo *inter y trans* disciplinar, pues las tecnologías disruptivas requieren tanto del análisis tecnológico, como del político, legal, económico y por supuesto, el social. Todas las problemáticas identificadas en este artículo, entre otras existentes y por venir, representan un campo fértil para la investigación relacionada al balance *entre la privacidad y la publicidad* de los usuarios al utilizar tecnologías en línea.

## Referencias

1. "Internet matters: The Net's sweeping impact on growth, Jobs, and prosperity", 2011, http://www.mckinsey.com/insights/high_tech_telecoms_internet/internet_matters).
2. ROSEN, Jeffrey, "The Right to be Forgotten", Symposium Issue: The Privacy Paradox, 2012. (Consultable en http://www.stanfordlawreview.org/online/privacy-paradox/right-to-be-forgotten).
3. SCHMIDT Eric, COHEN Jared, "The New Digital Age: Reshaping the Future of People, Nations and Business", John Murray Publishers, 2013, p. 69.
4. El fundador de The Pirate Bay seguirá en prisión preventiva un mes más. (Consultable en http://www.abc.es/agencias/noticia.asp?noticia=1588712)
5. TOR, Overview, "Activist groups like the Electronic Frontier Foundation (EFF) recommend Tor as a mechanism for maintaining civil liberties online". (Consultable en https://www.torproject.org/about/overview.html.en).
6. NAKAMOTO, Satoshi, "Bitcoin: A Peer-to-Peer Electronic Cash System". (Consultable en: https://bitcoin.org/bitcoin.pdf).
7. Bitcoin.org, "Proteja su privacidad", (Consultable en: https://bitcoin.org/es/proteja-su-privacidad).
8. El lado oscuro del comercio en Internet, El Financiero, 2013 (Consultable en http://www.dineroenimagen.com/2013-08-22/24860).
9. Becerra, A., "Mitos y Realidades de la Internet Profunda", Revista .Seguridad UNAM #20, 2014. (Consultable en: http://revista.seguridad.unam.mx/numero-20/mitos-y-realidades-de-la-internet-profunda)

# Sistemas mHealth para la adquisición de señales EEG

Cesar Fabian Reyes Manzano[1], Blanca Alicia Rico Jiménez[2] y Laura Ivoone Garay Jiménez[3]

[1]Instituto Politécnico Nacional, UPIITA, SEPI, D.F., México.
cesarrm5@hotmail.com
[2]Instituto Politécnico Nacional, UPIITA, informática, D.F., México.
bricoj@ipn.mx
[3]Instituto Politécnico Nacional, UPIITA, SEPI, D.F., México.
lgaray@ipn.mx

**Resumen.** El incremento en el uso de dispositivos móviles ha generado un crecimiento de puntos de acceso, públicos y privados, esto es aprovechado por los sistemas mHealth, los cuales utilizan la infraestructura de los servicios móviles para brindar servicios de salud, realizando aplicaciones como el monitoreo de señales biológicas. Una de estas aplicaciones puede ser la medición de la señal de electroencefalografía (EEG), la cual consiste en adquirir la señal eléctrica de la corteza cerebral de forma no invasiva.
Este artículo propone un sistema capaz de obtener múltiples registros por medio de módulos con 19 sensores de señal EEG y un envío de datos usando el protocolo Wi-Fi hacia un servidor por medio de socket TCP.
El sistema desarrollado permite la realización de hasta 12 estudios en forma paralela y de manera remota, como puede ser el hogar del paciente, una clínica rural, etc., con una eficiencia del 99.21% de datos trasmitidos correctamente.

**Palabras clave:** electroencefalográfica, mHealth, TCP.

## 1 Introducción

La electroencefalografía consiste en medir la señal eléctrica de la corteza cerebral por medio de electrodos colocados sobre el cuero cabelludo [1]. Este es un método no invasivo que permite conocer el estado del cerebro con alta resolución temporal. El conocer el estado del cerebro es de gran ayuda para el diagnóstico de enfermedades neurológicas, sin embargo, la demanda de servicio en el sector salud y la infraestructura generada por el sector público es insuficiente para los usuarios demandantes, por lo cual, es deseable contar con sistemas que coadyuven a la atención de los pacientes optimizando la infraestructura disponible [2]. Una alternativa de solución propuesta es el uso de sistemas mHeath, los cuales utilizan la infraestructura de las redes de sistemas móviles para transmitir el flujo de información entre el paciente y el médico, sin importar la distancia a la que se encuentren [3].

En la actualidad, se han desarrollado sistemas de adquisición móvil con la finalidad de obtener señales electroencefalográficas. El tipo de aplicación del equipo condicio-

na la resolución, frecuencia de muestreo y el tipo de tratamiento de la señal tanto a nivel analógico como digital. En las interfaces Hombre Máquina se buscan parámetros generales que permitan identificar estados de actividad neurológica para controlar procesos o desencadenar acciones. Es por esto que se da prioridad a la transmisión en tiempo real sobre la fidelidad de la información, pero sin comprometer la calidad. Uno de estos sistemas es el EPOC ® (Emotiv, USA), que se usa en sistemas de interface Cerebro-Computadora (BCI) y cuenta con 14 canales [4]; la colocación de los electrodos se distribuye en la zona motora, debido a que se utiliza para el control de dispositivos a partir de señales asociadas al movimiento.

En cambio, en el uso para estudios clínicos es de suma importancia mantener la mayor fidelidad posible tanto temporal como espacialmente debido a que se busca analizar, clasificar y asociar morfologías de la señal EEG a patologías clínicas, así como la interpretación de esta señal con métodos automáticos utilizando técnicas de procesamiento [5,6,7,8]. Para estas aplicaciones se pueden encontrar en el mercado el sistema "EEG: DSI 10/20" de la compañía QUASAR™ , que cuenta con 21 electrodos [9]; y el "B-Alert X24" de la compañía "Advances Brain Monitoring" [10] con 20 electrodos. Ambos proponen la colocación de los electrodos en base al sistema 10-20, el cual es un estándar médico que ayuda a una correcta interpretación de la lectura de la señal. Todos los sistemas considerados cuentan con comunicación inalámbrica, a una computadora personal o a un dispositivo móvil, utilizando Bluetooth lo que permite la movilidad exclusivamente dentro del área de registro. Los sistemas cuentan con un software de uso específico proporcionado por el fabricante para el envío o almacenamiento de las señales adquiridas.

Los sistemas mHealth utilizan la infraestructura de los dispositivos móviles para brindar servicios de salud con la finalidad de generar una cobertura en cualquier lugar y cualquier momento [11]. Estos sistemas pueden ser usados en el monitoreo a pacientes con enfermedades crónico degenerativas, como es el caso de la Diabetes Mellitus. Un ejemplo es una aplicación para iPhone ® (APPLE, USA) que ayuda a monitorear la cantidad de glucosa del paciente por medio de una conexión a un dispositivo medidor de glucosa. La aplicación informa al paciente cuando y cuanta insulina debe aplicarse [12]. Otra función relevante de los sistemas mHealth es el monitoreo a distancia de pacientes, conocida como telemetría. Estos sistemas han tenido un amplio desarrollo en el área de cardiología, entre los avances se encuentra la adquisición de la señal electrocardiográfica (ECG) por un dispositivo que la envía a PDA (asistente personal digital) por medio de Bluetooth, y la PDA a su vez la envía a un servidor por medio de una conexión a internet. La aplicación busca auxiliar en el diagnóstico de arritmias cardiacas en niños, que no pudieron ser detectadas en exámenes de corta duración [13].

Estos sistemas han evolucionado con la introducción de nuevos dispositivos móviles, como es el proyecto MTM-1, que realiza la misma función de proyecto anterior usando teléfonos inteligentes con sistema operativo Android [14]. Es importante mencionar que los nuevos dispositivos móviles cuentan con una mayor capacidad de procesamiento lo que permite realizar aplicaciones para la búsqueda y análisis previo de características de la señal ECG, reduciendo la cantidad de datos enviados y teniendo una mayor interacción con el usuario [15].

Los avances mostrados anteriormente dan las bases para plantear nuevos objetivos en los que se encuentra el medir señales más complejas que la señal ECG, como es la

señal de electroencefalografía que cuenta con un número mayor de canales y una amplitud menor. Por otro lado, el crecimiento de sistemas de conexión a la red creada para los sistemas telefónicos, dan pauta a la posibilidad de crear dispositivos embebidos que utilicen una conexión a internet sin la necesidad de un teléfono móvil intermedio [16].

Considerando los avances en las prestaciones tanto de procesamiento, como de cobertura y memoria de los dispositivos móviles, este trabajo propone el diseño y construcción de un sistema de adquisición de señal EEG siguiendo la filosofía mHealth, es decir, realizar el registro de señal EEG por medio de sistemas móviles que envíen los datos a través de puntos de acceso Wi-Fi.

En la siguiente sección se describe el funcionamiento general del sistema, y a detalle cada uno de sus elementos. En la sección 3 se describen los dispositivos que adquieren la señal EEG para enviarla al servidor que son denominados electroencefalógrafos. En la sección 4 se describe el manejo de conexiones hacia el servidor y el almacenamiento de los datos recibidos. En la sección 5 se muestran los resultados obtenidos y la evaluación de estos. En las últimas secciones se presentan la discusión y las conclusiones.

## 2 Descripción del sistema

El módulo de adquisición de la señal EEG (electroencefalógrafo) permite el envío de la señal adquirida a través de internet por medio del protocolo Wi-Fi, con el fin de que se pueda realizar el estudio de electroencefalografía desde cualquier lugar, que cuente con un punto de acceso Wi-Fi. La señal es recibida en un servidor por la aplicación desarrollada, la cual se nombró "Alimón". Ésta se encarga de establecer y manejar las conexiones, así como del almacenamiento de los datos recibidos. En la figura 1, el diagrama del sistema muestra tres módulos de adquisición de señal EEG que envían los datos al servidor a través de diferentes puntos de acceso. Cada uno de los elementos se describe a continuación:

- **Electroencefalógrafo:** Es un sistema de registro de señales electroencefalográficas que contiene un microcontrolador LM4F232H5QC (Texas®, USA), el cual se encarga de tomar la lectura de los 19 sensores de electroencefalografía, digitalizarlos y enviarlos por Wi-Fi a un punto de acceso, para su transmisión a través de la red.
- **Punto de acceso:** Este es un enrutador que tiene la función de direccionar y controlar el flujo de los paquetes enviados a través de una red WLAN, así como asignar direcciones IP a los elementos de la red y acondicionar los datos para envío a través de internet. El enrutador usado es el modelo DIR-615 (D-Link, USA) en el que se configuraron los datos de la red (nombre de la red, seguridad WPA2, etc.) y un permiso para la utilización del puerto por el que se envían los datos (TCP-4444), esto se realiza en la página de configuración del enrutador (http://192.168.0.1).
- **Servidor:** Es una computadora personal marca Lenovo, modelo Ideapad Y400 con procesador i7 y 6 Gb en RAM, con sistema operativo Fedora 19 y configurada con una IP fija. En esta computadora se ejecuta el programa "Alimón", que se encarga

del manejo de las conexiones de cada uno de los sistemas de registro.

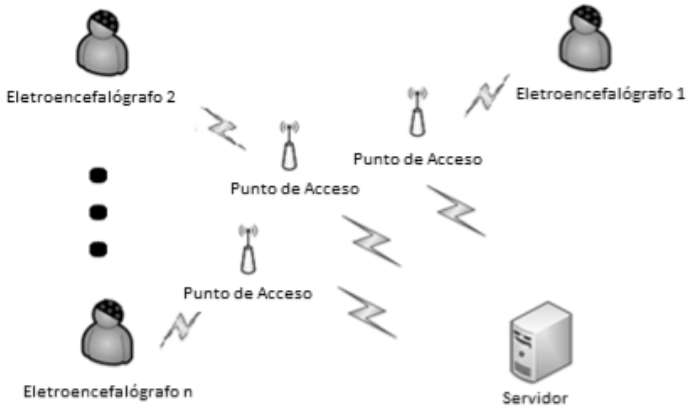


**Fig. 1.** Diagrama del sistema mHealth para la adquisición de la señal EEG

## 3 Adquisición de datos

El electroencefalógrafo realiza la adquisición de las señales electroencefalográficas. En la figura 2 se muestra el diagrama general del sistema. Las señales son obtenidas por medio de 19 sensores los cuales tienen 2 salidas analógicas: una correspondiente a la señal electroencefalográfica, la cual es tomada por electrodos de contacto superficial, amplificada con una ganancia de 1000 y filtrada con una banda de 0.05 a 130 Hz; y otra salida correspondiente a la impedancia de la interface electrodo-piel. Una descripción detallada de este dispositivo se encuentra en [17].

Las señales adquiridas por los sensores son digitalizadas por un microcontrolador usando una frecuencia de muestreo de 500 Hz y una resolución de 12 bits, para posteriormente empaquetarlas y enviarlas por medio de un módulo Wi-Fi.

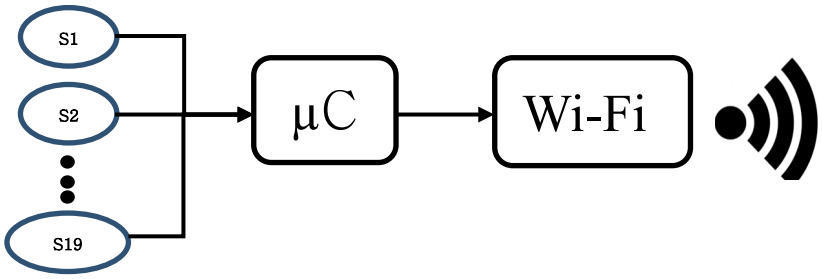


**Fig. 2.** Diagrama de electroencefalógrafo.

En la figura 3 se muestra el diagrama de flujo del proceso de digitalización y envío de las señales en el microcontrolador y se describe a continuación:

- Se configura el electroencefalograma en la red WLAN correspondiente al punto de acceso.
- Se crea un socket tipo TCP en modo cliente hacia el servidor.
- Se envían los datos correspondientes al electroencefalógrafo (nombre del equipo, frecuencia de muestreo, resolución de la muestra y longitud del paquete).
- Se inicia el registro de las señales electroencefalográficas con una frecuencia de muestreo de 500 Hz.
- Al almacenar 8 muestras de señal electroencefalográfica por canal, se realiza un muestreo de la señal de impedancia.
- Genera un paquete de datos con las muestras realizadas (8 de las señales electroencefalográficas y una de impedancia.)
- Envía el paquete por el socket TCP.
- Regresa y espera nuevamente el almacenamiento de 8 muestras.

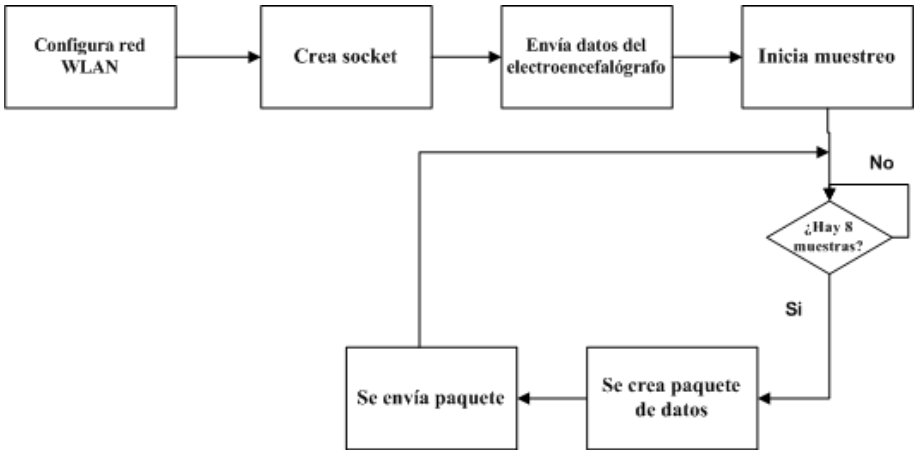


**Fig. 3.** Proceso de adquisición y envío de las señales electroencefalográficas y de impedancia.

Este sistema se repite para cada uno de los usuarios monitoreados, distinguiéndose únicamente por el nombre que se asigna a cada equipo para su reconocimiento por el programa "Alimón".

## 4 Manejo de conexiones y almacenamiento de la señal

Para controlar las conexiones de los dispositivos que registran desde diferentes puntos de internet, se desarrolló un programa en lenguaje Java versión 1.7.0_45 denominado "Alimón". Éste se ejecuta en el servidor y sigue el proceso mostrado en el diagrama de actividades de las figuras 4 y 5, el cual se describe a continuación:

- Crea socket TCP en modo servidor.
- Espera la conexión de un cliente.

- Al recibir una petición de conexión, el programa realiza la conexión y se genera un hilo de procesamiento en donde se crean los archivos necesarios para el almacenamiento de las señales.
- El hilo principal regresa a esperar una petición de conexión.
- El hilo creado, inicia un ciclo de recepción, desempaquetado y almacenamiento de la señal.
- El programa muestra los datos recibidos en 2 pantallas. Una correspondiente a las señales electroencefalográficas y otra para las señales de impedancia.
- El hilo cierra la conexión y finaliza cuando el electroencefalógrafo deja de enviar paquetes por más de 180 segundos.

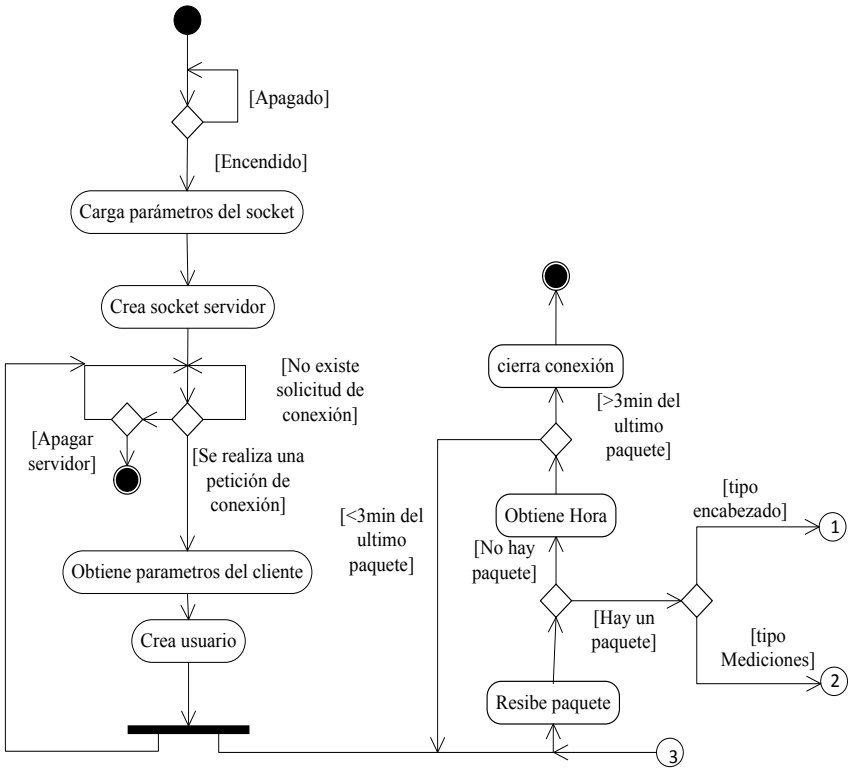


**Fig. 4.** Diagrama de actividades del programa "Alimón" para el manejo de conexiones y almacenamiento de la señal.

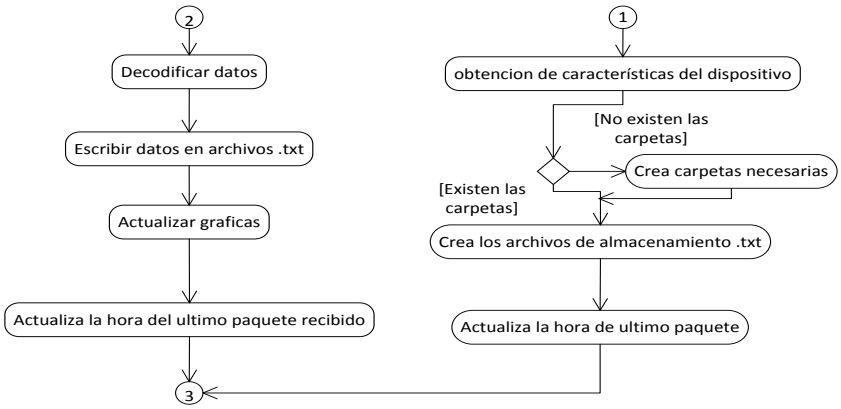


**Fig. 5.** Diagrama de actividades del programa "Alimón" para el manejo de conexiones y almacenamiento de la señal (continuación).

## 5 Resultados y evaluación

Se obtuvo un sistema de adquisición de señal electroencefalográfica capaz de transmitir la señal adquirida a través del protocolo Wi-Fi y enviar por medio de internet a un servidor donde se almacena y visualiza la señal. El programa para el manejo de conexiones y almacenamiento de datos es mostrado en la figura 6, donde se observa gráficamente el estado de la conexión de los dispositivos y las señales obtenidas para cada uno de ellos. La información de las señales obtenidas se guardó en formato texto con la finalidad de que se pueda analizar posteriormente mediante cualquier paquetería comercial o de uso libre.


**Fig. 6**. Imagen de programa para el manejo de conexiones y almacenamiento de datos.

Para realizar la evaluación del sistema se utilizó un contador como señal de prueba y se realizó la transmisión por 20 minutos. Finalmente se obtuvo la relación de paquetes recibidos con respecto a los paquetes no recibidos, para obtener los paquetes enviados correctamente en cada transmisión. La prueba se repitió 30 veces y se realizó una prueba de normalidad del conjunto de mediciones utilizando la prueba omnibus de D'Agostino-Pearson (p=0.5). Los resultados se presentan en la Tabla 1.

**Tabla 1.** Tabla de porcentajes de datos recibidos correctamente.

| Número de repeticiones | 30 |
|---|---|
| Tiempo de transmisión | 20 min |
| Promedio | 99.22% |
| Desviación Estándar | 0.5996% |

Realizando el análisis de normalidad, se concluyó que los porcentajes obtenidos de los paquetes recibidos correctamente corresponden a una distribución gaussiana o normal.

Posteriormente se realizó la prueba de capacidad de conexión máxima del sistema, en la que se simuló la conexión de módulos de adquisición de electroencefalografía enviando datos en forma paralela. El programa "Alimón" tiene capacidad de hasta 12 módulos en paralelo, para no comprometer la visibilidad de la información en la pantalla de despliegue, aunque la cantidad máxima está determinada por las capacidades de la computadora o dispositivo utilizado como servidor. Esta prueba se repitió 10 veces confirmando la viabilidad de la capacidad máxima propuesta con los elementos utilizados.

## 6 Discusión

En este trabajo se obtuvo un sistema mHealth capaz de conectar hasta 12 módulos de registro de señales EEG en forma simultánea a través del protocolo de comunicación Wi-Fi 802.11 b/g con una eficiencia del 99.22 % en la transmisión de la información, lo que implica que llegó ordenada y sin pérdidas. Usar este protocolo permitió realizar una comunicación inalámbrica por medio de redes WLAN de alta calidad, por lo que el ó los pacientes pueden estar en una o varias salas dentro o fuera de la zona donde se ubica el servidor que almacena y analiza la información, siempre y cuando estén dentro del área de cobertura de la red. Esta característica marca la diferencia de este equipo con respecto a los encontrados comercialmente para electroencefalografía, como los mencionados en la sección 1. Este tipo de sistemas mHealth, se han propuesto a nivel experimental para otras señales tales como temperatura [11] y electrocardiografía [18] con el objetivo de probar técnicas de transmisión entre sistemas de registro conectados a computadoras personales y el servidor.

Debido a que el protocolo Wi-Fi es uno de los más usados en forma comercial, el sistema tiene la posibilidad de crear redes con la mayoría de dispositivos existentes en el mercado y presenta varias ventajas en comparación con el protocolo Bluetooth como son: mayor eficiencia, mayor rango de alcance, mayor velocidad de trasmisión, entre otras (ver Tabla 2). Aunado a esto, el pertenecer a la familia de protocolos

TCP/IP permite enviar datos a través de internet aún fuera del hospital, mediante el uso de sockets. Esto genera la ventaja de poder enviar las señales adquiridas directamente desde el dispositivo a un servidor en internet, sin la necesidad de una PC intermedia.

**Tabla 2.** Comparación entre protocolos Bluethooth y Wi-Fi (Lee, Su, & Shen, 2007)

| Estándar | Bluethooth | Wi-Fi |
|---|---|---|
| IEEE Spec. | 802.15.1 | 802.11 a/b/g |
| Banda de Frecuencia | 2.4GHz | 2.4GHz, 5GHz |
| Velocidad de transferencia | 1Mb/s | 54 Mb/s |
| Rango nominal | 10m | 100m |
| Potencia de transmisión nominal | 0 - 10 dBm | 15 - 20 dBm |
| Número de canales de RF | 79 | 14 (2.4 GHz) |
| Ancho de banda | 1 MHz | 22 MHz |
| Tipo de modulación | GFSK | BPSK, QPSK |
| Cifrado | EQ cifrado de flujo | RC4 stream cipher (WEP), AES block cipher |
| Autenticación | secreto compartido | WPA2 |
| Protección de datos | 16-bit CR | 32-bit CRC |
| Coeficiente de eficiencia | 94.41 | 97.18 |

## 7 Conclisión

Este sistema contribuye en el desarrollo de sistemas mHealth que hacen posible el monitoreo de señales biológicas desde diferentes lugares. La propuesta contempló la generación de un sistema móvil de registro de señal electroencefalográfica con la capacidad de enviar en forma inalámbrica la información a un dispositivo que puede localizarse dentro o fuera de la zona física de registro lo que es una característica indispensable en la generación de sistemas mHealth. Es importante recalcar que algunas patologías, tales como la epilepsia, no son predecibles y que el EEG es el estudio clínico estándar en la identificación de crisis convulsivas, por lo que el registro de esta señal en forma continua sería lo más deseable para la búsqueda de los patrones precursores. Sin embargo, el costo en morbilidad por la atención continua de los pacientes lo hace inviable en el sector público con la infraestructura que se cuenta actualmente. Es por ello que la propuesta plantea la posibilidad de manejar la recepción simultánea de información permitiendo optimizar el uso de la infraestructura disponible en el hospital y en el centro de investigación sobre este tipo de señales.

Por otro lado, la utilización de la transmisión por Wi-Fi garantiza la calidad de la recepción de la señal transmitida que es un requisito técnico indispensable para fines de diagnóstico clínico.

Otro punto importante es que este sistema propone la creación de archivos de almacenamiento con un formato que maneja la paquetería comercial o de uso libre disponibles con el objetivo de aportar bases de datos para el análisis de esta señal bajo diferentes condiciones. Asimismo, la propuesta plantea la posibilidad de manejar la recepción simultánea de información permitiendo optimizar el uso de la infraestructura disponible en el hospital.

## Referencias


1. S. Sanei y J. Chambers, EEG signal prossesing, Chichester, England.: John Wiley & Sons Inc., 2007, pp. 10-19.
2. INEGI, «"Estadísticas del Sector Salud y Seguridad Social",» 2004. [En línea]. Available: http://www.inegi.gob.mx/prod_serv/contenidos/espanol/bvinegi/productos/continuas/sociales/salud/2003/cuaderno20a.pdf. [Último acceso: 30 07 2014].
3. Ping Yu;Wu, M.X. ; Hui Yu ; Xiao, G.Q., «The Challenges for the Adoption of M-Health,» Service Operations and Logistics, and Informatics, 2006. SOLI '06. IEEE International Conference on, pp. 181 - 186, 2006.
4. Emotiv, «Quick Start Guide & Maintenance,» 2014. [En línea]. Available: http://emotiv.com/eeg/setup.php. [Último acceso: 08 07 2014].
5. V. Venkatesh, S. Rulla, G. S., P. S., M. Munk y V. Venkatesh, «EEG signals are informative for individual cue-response combinations in a visuomotor task.».
6. N. Kannathal, J. Chee, K. Er, K. Lim y O. H. Tat, Chaotic Analysis of Epileptic EEG Signals. In The 15th International Conference on Biomedical Engineering, Springer International Publishing, January, 2014, pp. 652-654.
7. M. Ozbalik, V. Gonzalez-Montoya, S. Gowda y L. Morton, «Limitations of Quantative EEG Analysis in the Adult ICU.,» Neurology,, vol. 82, nº 10, 2014.
8. C. F. Reyes, T. J. Contreras, B. Tovar, L. I. Garay y M. A. Silva, «Detection of absence epileptic seizures using support vector machine.,» de In Electrical Engineering, Computing Science and Automatic Control (CCE), 2013 10th International Conference on, México, 2013.
9. QUASAR USA, «QUASAR USA,» 2014. [En línea]. Available: http://www.quasarusa.com/products_dsi.htm. [Último acceso: 14 06 2014].
10. I. Advanced Brain Monitoring, «Advanced Brain Monitoring, Inc.,» 2012. [En línea]. Available: http://www.b-alert.com/. [Último acceso: 23 04 2012].
11. R. S. .. Istepanian, A. Sungoor, A. Faisal y N. Philip, «INTERNET OF M-HEALTH THINGS "m-IOT",» de Conf Proc IEEE Eng Med Biol Soc., London, 2011.
12. P. A., T. J., G. K y M. M., «Designing Mobile Applications to support type 1 diabetes education,» de 11th World Conference on Mobile and Contextual Learning, Helsinki, 2012.
13. E. Kyriacou, C. Pattichis, M. Pattichis, A. Jossif, L. Paraskeva, A. Konstantinides y D. Vogiatzis, «An m-Health Monitoring System for Children,with Suspected Arrhythmias,» de Conference of the IEEE EMBS, Lyon, 2007.
14. Z. Kirtava, T. Gegenava y M. Gegenava, «mHealth for Cardiac Patients Telemonitoring and Integrated Care,» de IEEE HEALTHCOM 2013 - The 1st International Workshop on Service Science for e-Health, Portugal, 2013.

15. A. M. Patel, P. K. Gakare y A. N. Cheeran, «Real Time ECG Feature Extraction and Arrhythmia Detection on a Mobile Platform,» International Journal of Computer Applications , vol. 44, nº 23, pp. 40-45, 2012.
16. R. Istepanian, N. Philip, X. H. Wang y S. Laxminarayan, «Non-telephone Healthcare: The Role of 4G and Emerging Mobile Systems for Future m-Health Systems,» Communications in Medical and Care Compunetics, vol. 2, pp. 9-16, 2011.
17. C. f. Reyes, Sistema móvil para adquisición y transmisión de la señal EEG asistido con realidad aumentada para auxiliar el diagnóstico clínico, Mexico, D.F: SEPI-UPIITA-IPN, 2014.
18. E. Kyriacou, C. Pattichis, M. Pattichis, A. Jossif, L. Paraskeva, A. Konstantinides y D. Vogiatzis, «An m-Health Monitoring System for Children,» de Conference of the IEEE EMBS, Lyon, 2007.
19. J.-S. Lee, Y.-W. Su y C.-C. Shen, «A Comparative Study of Wireless Protocols: Bluetooth, UWB, ZigBee, and Wi-Fi,» de The 33rd Annual Conference of the IEEE Industrial Electronics Society (IECON), Taipei, Taiwan, 2007.

# Aplicación móvil para ayudar al aprendizaje de niños autistas

Jenny Vega-Hernández[1], Carlos Hernández-Nava[2], Blanca Rico-Jiménez[3]

Unidad Profesional Interdisciplinaria en Ingeniería y Tecnologías Avanzadas, IPN

jennylvh_14@hotmail.com, {hernandeznc, bricoj}@ipn.mx

**Abstract.** The Autism Spectrum Disorder (ASD) is characterized by a deficit of intellectual development, that affects the socialization, communication, and emotional reciprocity, producing repetitive and unusual behaviors. With the technological advances, now is possible to develop software, that includes images and sounds, elements that are more attractive, allowing a dynamic learning to people with this disorder, all this, from electronic tablets. In order to collaborate and provide a technological tool based on a mobile device, this paper presents an Android App, which generates a visual and aural environment in the daily activities of people with ASD, the visual environment covers the use of augmented reality to describe visually the use of common items, as well as a section that defines the emotional state based on the choice of an image and an agenda formed by images with the daily activities, and the aural environment covers the use of sounds that are played for each common item or to listen the activities of the agenda. These sounds can be recorded by the user.

**Palabras clave:** Realidad Aumentada, Marcador, Autismo, Android.

## 1 Introducción

En México se maneja una cifra de 45,000 niños autistas entre toda la población. Datos de la Clínica Mexicana de Autismo, a cargo del doctor Carlos Marcín Salazar, quien menciona que el autismo se incrementa 17% cada año y que se ignora el número de adultos que existen en el país con este padecimiento [1].

Para apoyar a este gran número de personas existen varios métodos, sin embargo se pretende ayudar a estimular las actividades de niños que padecen de este síndrome apoyándose de la tecnología. Para ello, se ha decidido desarrollar una aplicación que apoye a esta comunidad de niños haciéndoles más atractiva y comprensible la forma de aprendizaje, y esta misma apoya de cierta forma a los padres y asesores ya que evitarán cargar con excesivo material.

Este trabajo, propone atraer la atención del paciente para el método de secuencia, consiste en que el niño observe imágenes y pueda lograr la imitación de lo que

observa, esto se realiza mostrando actividades cotidianas con imágenes dinámicas sobre un apartado de realidad aumentada (RA). La forma en que usualmente se realiza este método, es mostrando diversas imágenes con los distintos pasos que deben seguirse, a través de brindarles una aplicación móvil basada en Android, que genere un entorno visual y auditivo dentro del ambiente en que se desenvuelve.

## 2 Planteamiento del problema

El trastorno del espectro autista (TEA) presenta distintos síntomas, entre los que se encuentra un crecimiento irregular, escases en habilidades para comunicarse, dificultad para poder establecer relaciones sociales, un marcado rechazo al contacto físico con otras personas y apego a realizar actividades rutinarias.

Los padres de familia o terapeutas suelen tener libros con bastantes fotografías, recortes e ilustraciones de pictogramas para poder comunicarse con los niños. Para ellos es de gran ayuda tener el nombre de los objetos y la imagen ilustrativamente.

Aquellos padres que por primera vez se les diagnostica que tienen un hijo con el síndrome de autismo, necesitan ir poco a poco recolectando este tipo de material, lo cual en ocasiones requiere de mucho tiempo y suele ser costoso.

Para los niños es poco llamativo el hecho de ver las imágenes o pictogramas ya que pueden estar borrosas y ser de muy mala calidad. Ellos tienen la dificultad de comunicarse porque no siempre cuentan con el material necesario en el momento que se requiere, lo cual ocasiona confusiones y suele generar agresiones por parte del menor. Los pequeños que sufren de este trastorno imitan las imágenes que observan, pero como se mencionó anteriormente a veces las imágenes no llaman mucho su atención.

## 3 Solución propuesta

En la sección anterior se ha descrito la problemática que tienen las personas que trabajan con niños con autismo y los problemas que enfrentan los menores para poder aprender y comunicarse de una mejor manera.

De acuerdo con lo mencionado se plantea la creación de una aplicación móvil en una tableta electrónica, definida por el diseño de 4 módulos los cuales estarán propuestos de acuerdo a las necesidades principales de los niños.

Los primeros tres módulos, se establecen con imágenes (pictogramas) y sonidos con los que los usuarios podrán interactuar de forma sencilla, el cuarto módulo pretende afrontar el problema de la imitación, desarrollando un apartado de RA que sea muy sencillo y útil donde muestre una serie de imágenes que el menor debe imitar, lo anterior se realiza por medio de la detección de marcadores colocados en distintos artículos de uso diario.

# 4 Marco teórico

Para introducir el marco de referencia en que se sitúa el proyecto, es necesario remarcar la importancia que tiene una aplicación móvil, que es un conjunto de programas que se ejecutan en un dispositivo móvil, en el caso de este proyecto en una tableta electrónica [2] con el sistema operativo Android [3]. La aplicación que se presenta en este proyecto incluye un módulo de realidad aumentada (RA), lo cual posibilita la generación de información que combina la realidad física con la realidad virtual mediante un proceso informático.

La RA es una tecnología que permite la interacción del usuario con el mundo virtual y real que lo rodea, consiste en la combinación de imágenes reales junto a imágenes, texto o gráficos generados por una computadora. Para lograr esta tecnología, se podría dividir el desarrollo de RA en 2 partes perfectamente diferenciadas. Por un lado la generación de marcador, por otro el contenido de lo que se mostrará cuando se apunte directamente al marcador.

La biblioteca usada para introducir realidad aumentada es QCAR de QUALCOMM, trabaja para Android, y utiliza técnicas de visión artificial para alinear de forma exacta los gráficos con los objetos subyacentes. Unity3D es la plataforma para crear los contenidos 3D interactivos y Vuforia [4] es el sistema de desarrollo de RA.

# 5 Desarrollo de la aplicación

El sistema está formado de cuatro módulos: 1) oraciones, 2) agenda, 3) estado de ánimo y 4) realidad aumentada. El funcionamiento de los módulos oraciones, agenda y estado de ánimo trabajan apoyados en imágenes o pictogramas [5] y sonidos, es por eso que se agrupan en un solo recuadro, el cuarto módulo presenta imágenes en realidad aumentada. La arquitectura completa se muestra en la Fig. 1.

## 5.1 Módulo 1: Oraciones

Los materiales visuales ya sean dibujos, pictogramas, fotografías o símbolos son elementos de gran ayuda para los niños y las niñas con autismo tanto para el aprendizaje y desarrollo de la comunicación, como para aumentar su comprensión y regular su comportamiento es necesario que la interfaz de este módulo contenga una serie de imágenes y sonidos que ayuda al usuario a identificar objetos, números, acciones, etc., y con ello poder formar oraciones. El módulo permite al usuario agregar, eliminar o modificar las imágenes y sonidos, con la finalidad de personalizarlo de acuerdo a las necesidades de cada uno de los usuarios. Las categorías que se consideran como útiles son principalmente 10 las cuales se enlistan en la tabla 1.

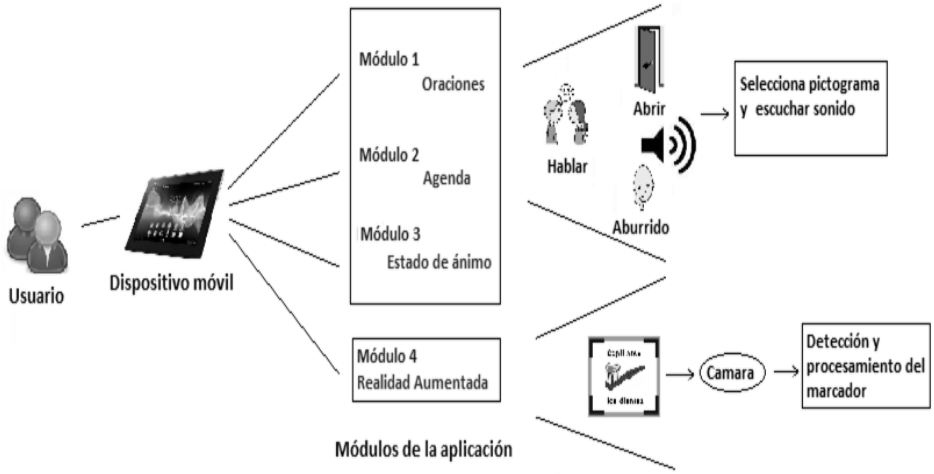


**Fig. 1.** Arquitectura de la aplicación

Para realizar la creación de las oraciones es necesario elegir el tipo de usuario, si el tipo de actor es un niño se tendrá la opción de elegir una categoría y seleccionar imágenes para crear una oración y poder reproducirla. Si el tipo de actor es administrador, podrá editar los datos como el nombre agregar la imagen y sonido. En la fig. 2. Se observa del lado izquierdo las categorías listadas en la tabla 1. Del lado derecho los dibujos que pertenecen a cada categoría, las imágenes se arrastran a la parte superior y con el botón se puede reproducir la oración completa asociada a las imágenes seleccionadas, se observa el ejemplo donde la frase será "mamá papá".

**Tabla 1.** Categorías del módulo Oraciones

| Categorías | |
|---|---|
| Intereses | Alimentos |
| Artículos | Adjetivos |
| Frases | Aprendizaje |
| Entornos | Salud |
| Personas | Acciones |

### 5.2 Módulo 2: Agenda

El módulo de agenda personaliza a través de fotografías las actividades que los niños deben realizar en un día. Permite elegir el día que desea editar, y seleccionar las imágenes correspondientes a las actividades planeadas en el día de la semana al que corresponda. Para crear la agenda de forma personalizada es necesario que el actor con el rol del administrador elija el día y las acciones que el niño deberá de realizar. En la fig. 3. Se muestra un ejemplo, el día lunes con cuatro actividades.


**Fig. 2**. Módulo de oraciones


**Fig. 3.** Módulo de agenda

### 5.3 Módulo 3: Estado de ánimo

Contiene imágenes que representan los diferentes estados de ánimo, se muestran los más communes: enojado, aburrido, triste, enfermo, cansado y feliz.

El niño elige la imagen que corresponde con su estado de ánimo, posteriormente se despliega una lista de imágenes editadas por el administrador, que muestran diferentes actividades. El niño selecciona lo que quiere realizar y lo que no desea hacer ese día, con el fin de evitar disgustos o groserías por parte del niño. Las actividades mostradas pueden ser personalizadas de acuerdo a cada niño.

Este módulo permite al administrador del sistema editar los datos tanto nombre como imagen y sonido. El niño elige el estado en que se encuentra en ese momento, una vez que se haya llevado a cabo esa elección se le muestra una nueva interfaz con las actividades que a al usuario en particular le gusta realizar, ver la fig. 4.


**Fig. 4.** Estados de ánimo

### 5.4 Módulo 4: Realidad aumentada

Este módulo permite mostrar imágenes en realidad aumentada, en donde los usuarios podrán fijar la cámara del móvil al marcador que se encuentra sobre el objeto [6], una vez que se reconozca el marcador muestra con una serie de imágenes el uso del artículo captado o actividad a realizar. Las imágenes que incluye son de uso cotidiano (ejemplo: cepillo de dientes, vaso, cuchara, ropa, etc.).

En la Fig. 5. se ilustra la forma en que se colocan las fotografías de los pasos que el menor debe seguir por ejemplo para lavarse los dientes, la idea es que se le muestre al niño de una forma dinámica los pasos a seguir, con esto se evita tener imágenes pegadas por todos los sitios del lugar.

Este módulo envía al usuario a la cámara de realidad aumentada, el usuario debe ponerla frente a uno de los marcadores para poder visualizar las secuencias.

## 6 Resultados

**Módulo de oraciones**: es posible editar el nombre de la imagen, seleccionarla de la galería del dispositivo o tomar una fotografía, seleccionar un sonido desde el dispositivo o grabar la voz del usuario, ver la fig. 6.

**Módulo de agenda:** el administrador tiene la posibilidad de seleccionar las imágenes correspondientes a cada día de la semana, elegir el sonido de las actividades que se realizaran durante el día. Además permite a través de un clic

corto para reproducir el sonido, si se desea cancelar la acción será necesario dar un clic largo para colocar un tache sobre la imagen y con eso indicar que esa acción se cancela. Si el tipo de actor es administrador, podrá editar los datos tanto nombre como imagen y sonido.

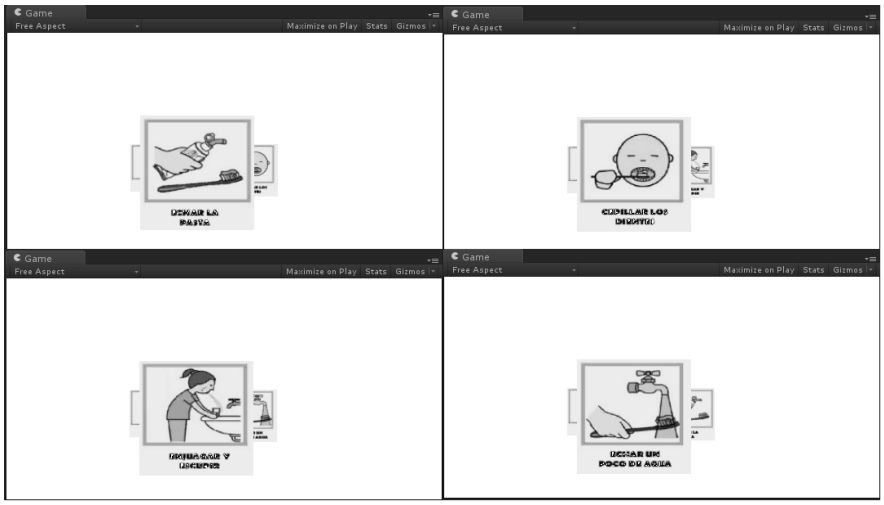

**Fig. 5.** Detección de marcador secuencia de imágenes

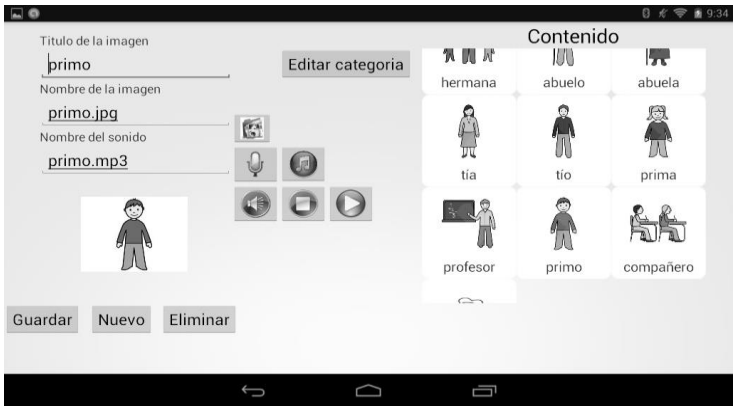


**Fig. 6.** Resultados para el módulo de oraciones

**Módulo estado de ánimo:** permite al niño elegir el estado de ánimo en que se encuentra y seleccionar la imagen que corresponda a la acción que le gustaría realizar en ese momento. Si el tipo de actor es administrador, podrá editar los datos tanto nombre como imagen y sonido.

**Módulo realidad aumentada:** la cámara se debe enfocar a un marcador para poder observar las imágenes. La aplicación permite observarlas de forma secuencial y por medio de un cubo el cual rota para observar cada imagen, ver la fig. 7.


**Fig. 7**. Resultados del módulo de realidad aumentada de forma secuencial

De igual modo cada marcador tiene una segunda forma de visualizar el contenido por medio de un cubo el cual muestra las imágenes en cada una de sus caras que van cambiando, ver Fig. 8.

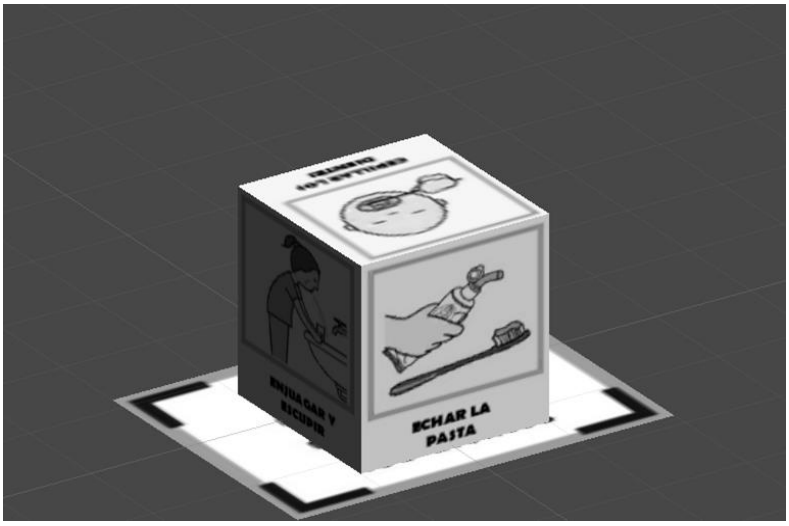


**Fig. 8** Resultado de realidad aumentado a través de la rotación de un cubo

## 7 Conclusiones

Se ha presentado una aplicación móvil que integra diferentes módulos en una tableta electrónica, ésta fue probada por diversos niños y jóvenes con autismo en la institución DOMUS [7] para validar si realmente atrae la atención al aprender con el método de secuencias y fomentar un dinamismo en el proceso de aprendizaje. Obteniendo comentarios positivos de la aplicación móvil y satisfacción total tanto de las personas que les enseñan a los niños, como la de los mismos niños que imitan lo que observan y escuchan en la tableta electrónica. Por lo que se concluye que las nuevas tecnologías de desarrollo de aplicaciones móviles pueden ayudar e impactar para mejorar los procesos de aprendizaje de personas con autismo.

Como trabajo a futuro se puede integrar una variedad más amplia de secuencias de realidad aumentada, trasladar la aplicación a otros sistemas operativos y que se puedan editar más las interfaces para lograr una mejor adaptación a cada usuario.

## Agradecimientos

Agradeciendo al Instituto Politécnico Nacional, a la Institución DOMUS por las facilidades y el apoyo brindado para validar este proyecto; así como a los asesores de este trabajo por sus consejos, su apoyo y el ánimo que siempre me brindaron.

## Referencias

1. Ajenjo, M (2012), Para comprender el autismo, [17-09-2013], http://eleconomista.com.mx/columnas/columna-especial.
2. TabletArea, [citado 12-09-2013], http://www.tabletarea.com/caracteristicas.html
3. Qué es Android: Características y Aplicaciones, [14-10-2013], http://www.configurarequipos.com/doc1107.html.
4. Qualcomm, Realidad Aumentada [14-03-2014], http://latam.qualcomm.com/products/augmented-reality.
5. ARASAAC, [14-01-2014], URL: http://www.catedu.es/arasaac/
6. Aumentaty, [13-03-2014], http://www.aumentaty.com/es/content/markerless-ar
7. Asociación del Instituto de Autismo Centro Educativo DOMUS, A.C. http://www.institutodomus.org

# Portable embedded system for the measurement of a vertical high jump

Adrián Castañeda[1], Axel Elías[2], and David Elías[3]

[1] UPIITA - IPN, Electronics Department
D.F., MX, 5729-6000 ext. 56882
acastanedag@ipn.mx
http://www.upiita.ipn.mx
[2] Instituto de Investigaciones Dr. José María Luis Mora
D.F., MX, 5598-3777
aelias@iijlmora.mx
http://www.www.mora.edu.mx
[3] Centro de Investigación y de Estudios Avanzados del IPN
D.F., MX, 5747-3800
delias@cinvestav.mx
http://http://www.cinvestav.mx/

**Abstract.** In this article we launch a low cost design of an embedded portable system to measure the height of a vertical jump through contact platforms. The "SALTOMETRO" , name given to the embedded system, can measure up to 32s of flight time with a resolution of 500$\mu$s, can calculate the vertical jump height and show it in a liquid crystal display (LCD) in less than 2s. "SALTOMETRO" consists of a microcontroller that operates in a 1MHz frequency, a LCD, a Li-Ion battery, a conditioning signal stage for passive or active circuits whit normally open (NO) or normally closed (NC) switches or signals and can use any type of contact platform, either commercial or made in laboratory does not require of a computer for its operation and the lithium ion battery (Li-Ion)of 1200 mA/h can last up to one week without recharge with an approximate use of 3 hours per day. The cost of construction is below $35 dollars.

**Keywords:** embedded system, vertical jump, contact platform

## 1 Introduction

To evaluate the anaerobic power there are several of tests. These have been classified into direct and indirect, as well as of field and of laboratory [1].Measuring the height of a vertical jump is an indirect methodology applied in the laboratory, while in field, there are a great amount of studies that evaluate the effects of different training programs [2]; there are also studies that compare the leaps of athletes of different sports [3], or studies that appraise different level of performance in one kind of sport [4, 5], and some that relate the physical condition

with health [6, 7].

The three basic methodologies to measure the height of the vertical jump [8, 9] are:

**Numerical integration:** Considered as the direct or reference method, it obtains the height of the leap, by the use of strength platforms.

**Mark differentiation:** It makes use of non-standardized mechanisms to realize marks with parts of the body, making it difficult to compare the results between different tests that use this methodology because they depend of the part of the body that is marked [10].

**Time of flight:** It requires the use of mechanical contact platforms [11]or opto-electronic ones [2].

The time of flight and the mark differentiation are the most utilized laboratory and field methods because these require simpler, cheaper and easy to acquire material [10, 12]. The main advantage of time of flight over the mark differentiation is that it gives a more objective measure of the height of the leap [10], in addition, it is a more valid and reliable procedure [12] and its use is part of the many scientific methodology studies [2, 7, 13–25]; although, various works have evidenced that this method systematically registers more height of leap than the one acquired by numerical integration because of the extension in the landing that the angles of the ankle, knee and hip present [26–28].

In the market, we can find opto-electronic systems parallel to the ground to measure the time of flight such as Photocell Contact Mat, the Jump Bosco Infrared System [29] and the SportJump System Pro [8]. Contact platform systems such asthe Ergo Jump Bosco/System [30], the Tapewitch Signal Mat, Model CVP 1723 (Mijares and colaborators., 1995); DIGITIME 1000 [31] and the CHRONOJUMP Boscosystem. All the systems, except for DIGITIME 1000, Tapewitch Signal Mat and Ergo Jump Bosco System require a computer to measure and capture the time and have not been validated, with the exception of Photocell Contact Mat and CHRONOJUMP Boscosystem [9].

The study of anaerobic power by the test that measures the height of the leap has proven to be the most used methodology by the scientific community, but there is a small variety of equipment to measure it. Their difficult accessibility, cost, validation and portability, has made the data difficult to compare with their homologous around the world, shortening the possible impact that these could have as a collective knowledge; this is why, the objective of this work is to design an embedded portable system for the measurement of the height of the vertical jump using the methodology of flight time through a contact platform that does not require a computer for its functioning; that it would be easy to make with a low cost; that can use the contact and optics platforms from different commercial or own systems; that it would also be validated and certified by calibrated equipment, achieving a better level of certainty and confidence in

the measures realized; and finally, that the time that contact platforms underestimate will become a constant that can be eliminated out of the equation so researchers in all over the world can compare the obtained results.

## 2 Meterials and Methods

### 2.1 Mathematical aspects

In a high jump, the behavior of the gravity center of a person works as a projectile thrown with determined angle, or in the best case scenario as a vertical shaft. The elevation of the gravity center of the test subject corresponds to the height of the jump, which depends on the vertical speed of the takeoff $V_0$; in other words, $H_{max} = V_0^2/2g$. See Fig. 1.

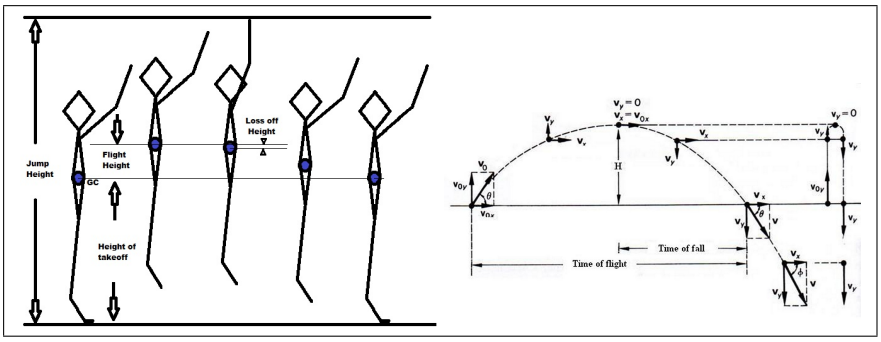


**Fig. 1.** High jump and its description as a parabolic throw

To simplify the calculation, the computational cost and to achieve that the device does not have accelerometers or force platforms, we can see that when the center of mass arrives to the maximum height, its velocity is equal to cero so in that moment it behaves likes a free falling object [33]. Then the vertical movement $H = g * t_{fall}^2/2$; where $g = 981cm/s^2$ and tfall is the time from the maximum height until it touches the ground (time of fall). If we measure the time of flight that is the double of the time of fall, then the calculation of the maximum height reduces to:

$$H_{max} = 122.6 * t_{flight}^2(cm) \tag{1}$$

### 2.2 Development of the system's hardware

The first stage of the SALTOMETRO is the conditioning of signals of active, passive, normally open (NO) or normally close (NC) sensors. Most of the sensors

in the market have plug stereo connectors or RCA, but in this case a jack stereo connection was used because of its size, making this a design parameter. After the entry there is a DPDT switch (Sw1), which is connected to an opto-coupler TLP521-1 (IC1) through a diode (D1). The objective of IC1 is adapting the signal that comes from the sensor, independently if it's active, passive, NO or NC and it does not provide protection or isolation of voltage to the microcontroller ATTINY2313 (IC2) because the sources of voltage are the same ones.

The Sw1 switch selects if the type of sensor is NO or NC (please note the form of activating the opto-coupler) while the diode D1 works to avoid that the active sensors inject the current to light up the led and send false alarms. In the transistor's collector output of IC1 there is a resistance of $15k\Omega$ next to a C1 capacitor to land of $10\mu F$ to form a down pass filter of $150ms$ time charge to avoid noise from the hardware into the measurement of jumps below $2.76cm$. Once the signal is filtered, it is sent to the microcontroller (IC2) in a pin for monitoring external interruptions (PD2) and the processing of the measurement is sent to a LCD device to show an alphanumerical result. Finally, a pulse button (Sw2) is placed to start a new measurement when the operator requires it. Observe the Fig. 2

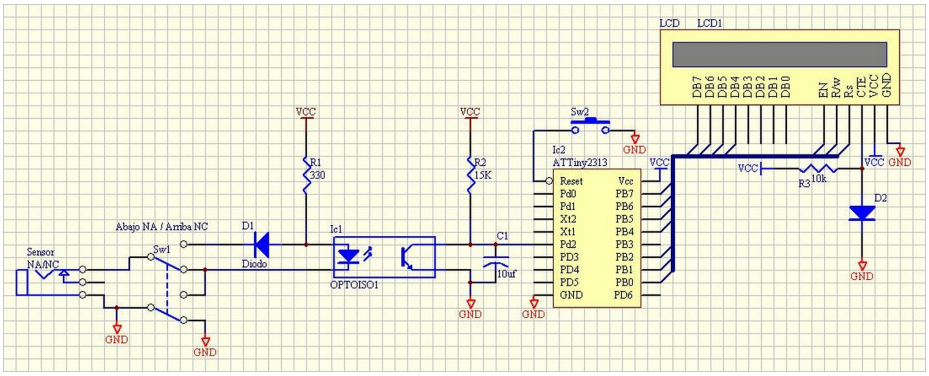


**Fig. 2.** Schematics of the SALTOMETRO

### 2.3 Development of the system's software

The SALTOMETRO software is coded in C language and is divided in the following subprograms: Main, Monitor and timer. The "Main subprogram" is in charge of configuring the microcontroller with the side of the interruption pin in flank of ascent and the timer countdown each $500\mu s$, as well as, initiating the variables of control, height and time. Once the machine is configured, the

microcontroller will wait for the timer and interruption events. The Monitor routine is in charge of verifying the interruption pin to know if the person is located on the platform or in flight; stopping the TIMER routine; calculating the height of the jump and showing the result in the LCD. Finally, the Timer function is in charge of counting the machine cycles, generating interruptions each $500\mu s$. Observe the Fig. 3 of the flowchart.

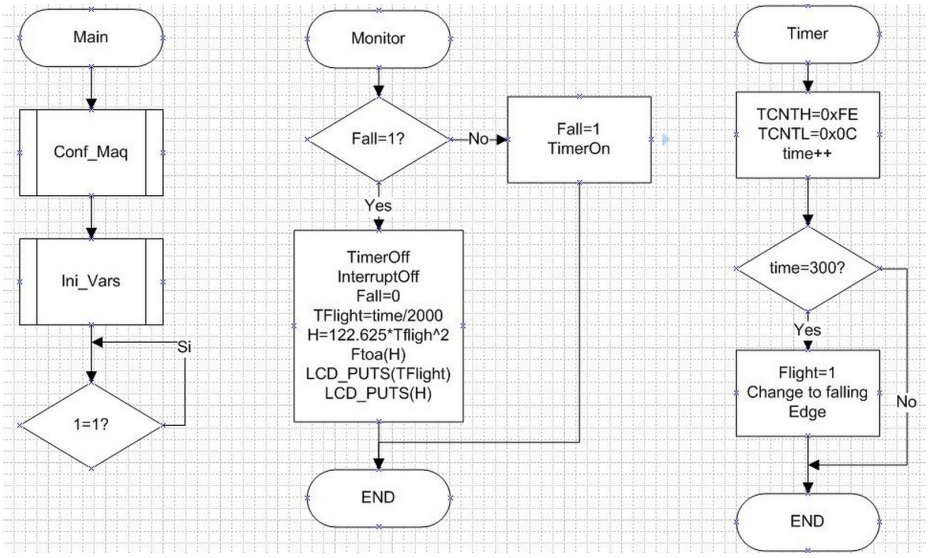


**Fig. 3.** Flowshart of SALTOMETRO

The logic of the program is based on the following execution sequence:

1. Ask the test subject to stand over the platform
2. Turn on the SALTOMETRO or press Reset (Sw2)
3. Configure microcontroller
4. Initiate Variables
5. Ask the test subject to execute the jump
6. Monitoring the platform for the takeoff event
7. Initiate timer
8. After $150ms$, change monitoring of platform in the descent
9. In the moment test subject and platform make contact
   (a) Stop the timer
   (b) Stop interruptions
   (c) Calculate the height of jump
   (d) Show result
10. Record the result
11. Repeat step 1 for another measurement.

### 2.4 Instruments

**Contact platform** A contact platform with metallic strips was used and assembled with gymnasium wooden floor so it could soften the fall after the jump. The contact detection area is $0.90m^2$ and the method of detection is by aperture and/or closure of the metallic strips while the contact of feet occurs. The methodology used for the construction of the contact platform is that recommended by CHRONOJUMP Boscosystem [32].

**Osciloscope** We used a digital Tektronix color oscilloscope, model TS20146, of 4 channels, 100MHz, 1GS/s bandwidth, memory of 2.5kpts, mathematical functions (including FFT), advanced triggers, transference of data and 1GS USB storage.

**Digital signal generator** In this case, a Tektronix digital signal generator, model AFG3101, was used. The generator can create standard and arbitrary programmed functions; it has one channel with a rank from1MHz to 100 MHz, 1 Gs/s, 14-Bit resolution, AM/ FM/ PM/ FSK/ PWM modulations, GPIB, USB, LAN and color screen.

### 2.5 Experimental design

The experiment consists of 2 phases:

1. The objective of the first phrase is to determine the linearity, exactitude and precision of the device in an interval from $200ms$ to $1500ms$ that corresponds to the jumps of heights from $4.9cm$ to $278.85cm$. To achieve this, the AFG3101 digital signal generator is programmed with a squared signal of 5v amplitude and a variable width of pulse in the proposed rank; the sequence is repeated 10 times and the calculations of height and times are registered by the SALTOMETRO; meanwhile, with the TS2014B oscilloscope, which is connected in a parallel with the device and the signal generator, we register each event and verify the width of pulse and the type of wave delivered by AFG3101.
2. The second phase has the objective of observing the signal of response of the contact of platform when connected to the SALTOMETRO, if it has rebounds, added delays by the coupling stage, and in consequence, the device's errors while measuring the time of flight and calculating the height of the jump. For this, the contact platform is connected to the SALTOMETRO in parallel with the TS2014B oscilloscope, the execution sequence is made and every event is registered.

## 3 Results

Ten events were registered in each interval for the filling of table 1, as explained next. In the first column, we can find the time of flight in ms generated artificially by the AFG3101 signal generator. The second column shows the average in ms of the 10 events in each registered interval and shown by the SALTOMETRO.

In the third column, the standard deviation of the previous column is shown. The fourth column shows the calculations of the real height due to the times of flight generated in column 1. In the fifth column, the average of time calculated by the SALTOMETRO with only one decimal digit is shown. Finally, in column 6, the magnitude of error due to the difference between the real height and the average of calculated heights is shown by the SALTOMETRO.

**Table 1.** Results of experimental design, phase 1

| **TV(ms)** | **Mean TV(ms)** | $\sigma(ms)$ | **H Real(cm)** | **H Calc(cm)** | **ERROR(cm)** |
|---|---|---|---|---|---|
| 200 | 199.9 | 0.459468292 | 4.904 | 4.9 | 0.0040 |
| 300 | 300.1 | 0.459468292 | 11.034 | 11.0 | 0.0340 |
| 400 | 400 | 0.471404521 | 19.616 | 19.6 | 0.0160 |
| 500 | 500 | 0.40824829 | 30.65 | 30.7 | 0.0500 |
| 600 | 600 | 0.333333333 | 44.136 | 44.1 | 0.0360 |
| 700 | 700.1 | 0.516397779 | 60.074 | 60.1 | 0.0260 |
| 800 | 800 | 0.471404521 | 78.464 | 78.5 | 0.0360 |
| 900 | 900.05 | 0.368932394 | 99.306 | 99.3 | 0.0060 |
| 1000 | 1000 | 0.527046277 | 122.6 | 122.6 | 0.0000 |
| 1100 | 1100.05 | 0.437797518 | 148.346 | 148.4 | 0.0540 |
| 1200 | 1200.15 | 0.474341649 | 176.544 | 176.5 | 0.0440 |
| 1300 | 1299.95 | 0.368932394 | 207.194 | 207.2 | 0.0060 |
| 1400 | 1400.05 | 0.368932394 | 240.296 | 240.3 | 0.0040 |
| 1500 | 1499.95 | 0.368932394 | 275.85 | 275.8 | 0.0500 |
| - | - | - | - | - | - |
| - | **Average $\sigma$** | **0.43104572** | - | **Average error** | **0.0261** |

To know in detail the characteristics of precision, exactitude and linearity of the device, the measurements of central tendency and deviation or separation of the data related to their arithmetic average are shown. In table 1 we can observe that the average of standard deviation of time of flight in all the rank of measurements is 0.431 ms and that the error average in the calculation of the height is barely 0.0261 cm. Fig. 4 shows the correlation of the registered data with the generated ones and the tendency line in all the rank of time.

Figure 5 shows the SALTOMETRO device and its two contact platforms made with floor for gym.

## 4 Discusion

In this research we present the design of a portable embedded system for the measurement of the high jump with the flight time methodology through contact platforms with a stage of signal conditioning that allows the use of contact platforms and optics from different commercial systems and can be built by people with few electronic abilities and with an approximate cost of $35 US dollars. The system shows linearity in the rank between $200ms$ and $1500ms$ and shows equivalency to an interval of heights from $4.9cm$ to $275.85cm$. The obtained results show that the device is exact, precise and linear with an average standard deviation of $0.431ms$ for the time of flight and an average error in the

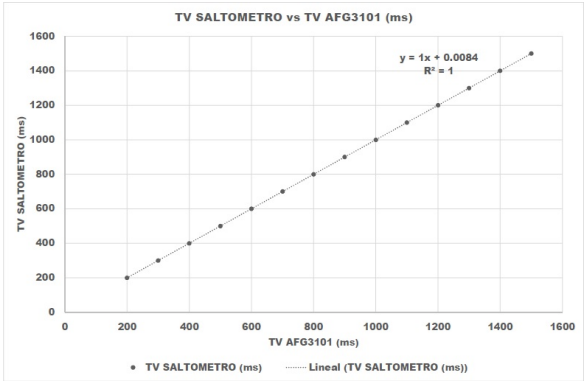


**Fig. 4.** Response of SALTOMETRO in all the rank of time

**Fig. 5.** SALTOMETRO and contact platforms

calculation of height of $261\mu m$ due to the round out to one decimal number. The SALTOMETRO is not the best device that is offered in the marked because it does not offer connection of any type to a computer; nevertheless, some of its best stand out qualities are: the size and its portability ($11x7x2.5cm$ and $60g$); its battery lifetime, low cost, and its automatic calculation and visualization of the flight height in LCD. In addition, with the performed researches made with certified equipment, linearity, exactitude, precision and recurrence of the device can be guaranteed; people that use this device will be able to compare their results with certainty because the errors or discrepancies will be due only to the method and not the equipment.

## Acknowledgments

The authors thank the support from CONACYT, UPIITA-IPN, CINVESTAV and CONADE for carrying out this work.

## References

1. RODRGUEZ, F.A., ARAGONS, M.T.: Valoracin funcional de la capacidad de rendimiento fsico. , Ed. Interamericana McGraw-Hill, Madrid, (1992).
2. IMPELLIZZERI, F.M., RAMPININI, E., CASTAGNA, C., MARTINO, F., FIORINI, S. and WISLOFF, U.: Effect of plyometric training on sand versus grass on muscle sorenessand jumping and sprinting ability in soccer players. British Journal of Sports Medicine 42, 42-46 (2008).
3. SLEIVERT, G., BACKUS, R. and WENGER, H.: Neuromuscular differences between volleyball players, middle distance runners and untrained controls. International Journal of Sports Medicine 16 (6), 390-398 (1995).
4. COMETTI, G., MAFFIULETTI, N.A., POUSSON, M., CHATARD, J.C. and MAFFULLI, N.: Isokinetic Strength and Anaerobic Power of Elite, Subelite and Amateur FrenchSoccer Players. International Journal of Sports Medicine 22 (1), 45-51 (2001).
5. VAQUERA, A., RODRGUEZ, J.A., VILLA, J.G., GARCA, J. and VILA, C.: Cualidades fisiolgicas y biomecnicas del jugador joven de Liga EBA. Motricidad: EuropeanJournal of Human Movement 9, 43-63 (2002).
6. TABERNERO, B., VILLA, J.G., MRQUEZ, S. and GARCA, J.: Cambios en el nivel de condicin fsica relacionada con la salud en mujeres participantes en un programa municipal de baile aerbico. Apuntes: Educacin Fsica y Deportes 61, 74-79 (2000).
7. RUIZ, J.R., ORTEGA, F.B., GUTIERREZ, A., MEUSEL, D., SJSTRM, M. and CASTILLO, M.J.: Health-related fitness assessment in childhood and adolescence: a Europeanapproach based on the AVENA, EYHS and HELENA studies. Journal of Public Health 14 (5), 269-277 (2006).
8. GARCA, J., PELETEIRO, J., RODRGUEZ, J.A., MORANTE, J.C. and VILLA J.G.: Validacin biomecnica de un mtodo para estimar la altura de salto a partir del tiempo de vuelo. Archivos de Medicina del Deporte 20 (93), 28-34 (2003).
9. GARCA, J. and PELETEIRO, J.,: Tests de salto vertical (II): Aspectos biomecnicos. RendimientoDeportivo.com, N7, (2004), `http://www.rendimientodeportivo.com/N007/Arti032F.htm`, [Consulted 01/06/2014]

10. KLAVORA, P.: Vertical-jump Tests: A Critical Review. Strength and Conditioning Journal 22 (5), 70-75 (2000).
11. GARCA, J., PELETEIRO, J., RODGRGUEZ, J.A., MORANTE, J.C., HERRERO, J.A. and VILLA, J.G., The validation of a new method that measurescontact and flight times during vertical jump. International Journal of Sports Medicine 26 (4), 294-302 (2005).
12. ARAGN, L.F.: Evaluation of Four Vertical Jump Tests: Methodology,Reliability, Validity, and Accuracy. Measurement in Physical Education and ExerciseScience 4 (4), 215-228 (2000).
13. DAL MONTE, A., FAINA, M. and MIRRI, G.: Fatigue and sport, Functional Neurology 17 (1), 7-10 (2002).
14. MAFFIULETTI, N.A., DUGNANI, S., FOLZ, M., DI PIERNO, E. and MAURO, F.: Effectof combined electrostimulation and plyometric training on vertical jump height. Medicineand Science in Sports and Exercise 34 (10), 1638-1644 (2002).
15. GIRARD, O., VASEUX, D. and MILLET, G.P: Comparison of efficiency of three trainingprograms in tennis players. Science y Sports 20, 45-47 (2005).
16. GIRARD, O., LATTIER, G., MICALLEF, J.P. and MILLET, G.P.: Changes in exercise characteristics, maximal voluntary contraction, and explosive strength during prolongedtennis playing. British Journal of Sports Medicine 40 (6), 521-526 (2006).
17. LAFORTUNA, C.L., MAFFIULETTI, N.A., AGOSTI, F. and SARTORIO, A.: Gendervariations of body composition, muscle strength and power output in morbid obesity. InternationalJournal of Obesity 29 (7), 833-841 (2005).
18. LEHANCE, C., CROISIER, J.L. and BURY, T.: Optojump system efficiency in the assessment of lower limbs explosive strength. Science y Sports 20, 131-135 (2005).
19. TESSITORE, A., MEEUSEN, R, CORTIS, C. and CAPRANICA, L.: Effects of differentrecovery interventions on anaerobic performances following preseason soccer training. Journal of Strength and Conditioning Research 21 (3), 745-750(2007).
20. MARGINSON, V., ROWLANDS, A.V., GLEESON, N.P. and ESTON, R.G.: Comparisonof the symptoms of exercise-induced muscle damage after an initial and repeated boutof plyometric exercise in men and boys. Journal of Applied Physiology 99 (3), 1174-1181 (2005).
21. ARTERO, E.G., ESPAA, V., ORTEGA, F.B., JIMNEZ, D., CARREO, F., RUIZ, J.R., GUTIRREZ, A. and CASTILLO, M.J.: Useof whole-body vibration as a mode of warming up before counter movement jump. Journal of Sports Science and Medicine 6 (4), 574-575 (2007).
22. RAMPININI, E., BISHOP, D., MARCORA, S.M., FERRARI, D., SASSI, R. and IMPELLIZZERI, F.M.: Validity of simple field tests as indicators of matchrelatedphysical performance in top-level professional soccer players. International Journalof Sports Medicine 28 (3), 228-235 (2007).
23. BERTUCCI, W., HOURDE, C., MANOLOVA, A. and VETTORETTI, F.: Mechanicalperformance factors of the bmx acceleration phase in trained riders. Science y Sports 22, 179-181 (2008).
24. BUCHHEIT, M.: Field tests to monitor athletic performance throughout a teamsportseason, Science y Sports 23, 29-31 (2008).
25. SARTORIO, A., AGOSTI, F., DE COL, A., MAZZILLI, G., MARAZZI, N., BUSTI, C. GALLI, R. and LAFORTUNA, CL: Muscle strength and power, maximum oxygen consumption, and body composition in middle-aged short-stature adults with childhoodonsetgrowth hormone deficiency. Archives of Medical Research 39 (1), 78-83 (2008).

26. HATZE, H.: Validity and reliability of methods for testing vertical jumping performance. Journal of Applied Biomechanics 14 (2), 127-140 (1998).
27. KIBELE, A.: Possibilities and limitations in the biomechanical analysis of countermovementjumps: a methodological study. Journal of Applied Biomechanics 14 (1), 105-117 (1998).
28. BACA, A.: A comparison of methods for analyzing drop jump performance. Medicine and Science in Sports and Exercise 31 (3), 437-442 (1999).
29. VIITASALO, J.T, LUHTANEN, P., MONONE, H.V., NORVAPALO, K., PAAVOLAINEN, L., SALONEN, M.: Photocell contact mat: a new instrument to measure contactand flight times in running. Journal of Applied Biomechanics 13 (2), 254-266 (1997).
30. BOSCO, C., LUHTANEN, P., KOMI, P.V.: A simple method for measurement of mechanical power in Jumping. Eur. J. Appl. Physiol 50 (2), 273-282 (1983).
31. Luthanen, P.: Evaluacin fsica de los jugadores de ftbol. Apuntes 21 (82), 99-102 (1984).
32. Bernat, B.: Instrucciones para la construccin de una plataforma de contactos para la medicin de la capacidad de salto/s, (2011),
33. TIPPENS. P.: Fisica Conceptos y Aplicaciones. McGraw-Hill, Mxico (2001).
34. Chronojump Boscosystem, `http://chronojump.org/construction_contact_platform_es.html`, [Consulted 14/06/2014].

# Design of an electronic breastplate for automatic detection of 4 types of techniques of TaeKwonDo

Adrián Castañeda[1], Enrique García[1], Ernesto Limón[1], and Victor Vázquez[1]

UPIITA - IPN, Electronics Department
D.F., MX, 5729-6000 ext. 56882
acastanedag@ipn.mx, egarciat@ipn.mx, balam_9099@hotmail.com,
roberto.tellez.00@gmail.com
http://www.upiita.ipn.mx

**Abstract.** This paper presents the design of an electronic breastplate for automatic detection of 4 types of techniques taekwondo in the thoracic section of the body (Bandal Chagui, Yop Chagui, Tuit Chagui y MontongChirugui); in order to discriminate if an impact should be considered as valid and transmit it wirelessly to a computer with a program to display the marker For the development of this work biomechanical analysis of the 4 different techniques in 10 different athletes were performed with 5 XSENS inertial sensors IMU of 9 degrees of freedom by using only the 3 axes acceleration data and finding the Pearson correlation index for each; subsequently the detection algorithm was implemented in an embedded system whit an ATM328 microcontroller in an Arduino UNO tarjet, ADXL345 accelerometer, XB24AWIT Zigbee radio and a computer program in Visual C# for counting points. The device has 3.53 x 8.53 x 7.76 cm in dimensions and weighs 180 grams. Operates on a 9 volt battery that lasts 50 minutes in active mode. The communication range is up to 50m and has a maximum time following the impact response of 250 ms.

**Keywords:** TaeKwonDo, embedded system, IMU, computer interface

## 1 Introduction

The Taekwondo is a Korean martial art that has been developed like a sport. Its popularity is due to the method to acquire greater fitness, being a self-defense method and to become an Olympic sport. Taekwondo has a variety of techniques where their movements in a competition are made with legs and additionally with hands. Due to its scoring system where victory is obtained by knocking out the opponent or getting the mayor quantity of points, practitioners of Tae Kwon Do prefer to use techniques that allow them to easily rate and gives them a greater advantage to win the competition.

The science that studies the different sports is the sport biomechanics. Sobarzo P. defines as: Sports biomechanics is responsible for conducting studies to sports practices to search for better performance, development of technical,

training and designing accessories for different disciplines. The overall objective of the sports biomechanics research is to develop a detailed understanding of the specific motor sports and performance variables to improve performance and reduce the incidence of injury. This results in the investigation of the specific techniques of sport, design a better sports equipment, apparel, and identify practices that predispose to injury [1].

Taekwondo practitioners typically have a large arsenal of kicks. Some biomechanical studies have focused on the techniques of upper body and others on the lower limb [2]. Peter et al [3] compared the straight punch forward from two different initial positions; the clear hand taekwondo straight punch in reverse position from the forward position was studied in relation to its standard execution model and to their success and power [4]. Hwang analyzed whip front kick to investigate patterns of muscle forces pairs of hip, knee, and ankle and the amplitudes of the segmental movements relative to the pairs of effective muscle forces applied [5]. Wohlin was interested in the kinetics and angular kinematics of the body during the kick and studied American athletes of taekwondo during the execution of the hook kick with rotation [6]. The spinning back kick was studied by Serina and Lieu focusing on the speed developed during the kick [7].

Luigi T. said that Most biomechanical investigations have tried taekwondo kicks, which can be broadly classified into three groups: linear and circular rotating. Linear kicks are the simplest in terms of mechanical efficiency analysis [2] and Falco P. concludes that Despite the high relevance of leg techniques in Taekwondo, there are, to date, few biomechanical studies to help us understand the effectiveness thereof. From a biomechanical perspective, the ability to be analyzed in relation to the strength and time, but also in relation to space [8].

Existing electronic breastplates are extremely expensive and therefore are only used in official competitions; however, have caused controversy, as discussed for the taekwondones and coaches, the benefits are not as many, because you never know when it will give a good point. As the athlete Uriel Avigdor Adriano (bronze medalist at the Pan American Games) said: Like it or not, we have to use It. It is a legal method because no longer much involved judges, rather than decisions, but sometimes accuracy is questionable, because impact whit force in the breastplate and it no mark the point and sometimes mark with a grazed [9].

The proposed device is to generate a monitoring system that is able to tell if a hit is valid, without having to use a second sensor in the Foot Guards, using sensors only in breastplate and looking for patterns in the different types of attacks, to know if this hit as it should be. The proposed design aims to reduce the cost of equipment, making it available to a larger group of people, allowing competitors to get used to using the equipment, getting adequate training to provide the athlete knowledge if the blows are impacting the right way.

## 2 Meterials and Methods

We consulted with Professor Jos Luis Onofre (coach of the national team Taekwondo 2008) and Prof. Carlos Gerardo Hernndez Segura (coach Taekwondo CE-

CyT # 2 Miguel Bernard Perales, interpolitécnico champion) on the techniques used to have a good development, both agreed that the most important thing is the basics, so hitting techniques thoracic are selected: Bandal Chagui, Yop Chagui, and Montong Chirugui and Tuit Chagui.

As the device detects the impact on the person receiving it is considered using accelerometers to measure the transfer of impact since this would allow the system to be relatively independent of the type and shape of the breastplate, and avoid the need to alter the current structure of the conventional breastplates and the ability to characterize the impact through the waveform obtained techniques accelerometer received and thus preventing false positive results in the system.

### 2.1 Testing Protocol

For testing protocol took into account the following control variables: Folio, date and time of the measurement, and number block replay, Name, Age, Level, Height, Weight, Gender, Type of kick, Target Distance, practicing time.

For measurement of velocity and acceleration of the kicks, X-sens MTx sensors were placed in the iliac crest, knee joint and ankle; for the fist in the shoulder joint, elbow and carpal joint. To measure the transfer of impact on the breastplate one MTi-G sensor X-sens on the left strap is placed. The accelerometers are set taking into account anatomical position in the sagittal plane watching from the right side of the test subjects. See figure 1 and 2.

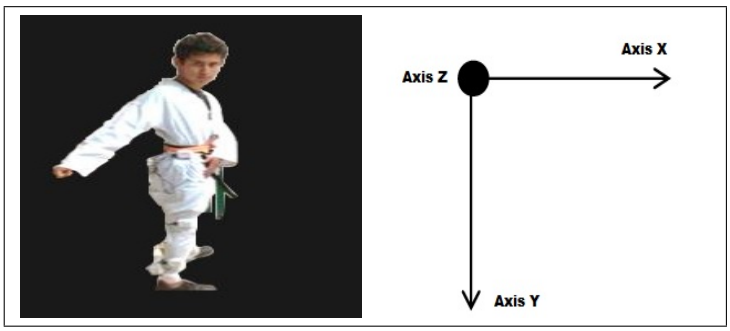


**Fig. 1.** Accels placed in test subject and orientation axis

It had the participation of 10 athletes, 1 yellow, 1 Advanced Green, 4 Blue, 2 Red and 2 Black 2nd Dan. To the person who made the impact was named attacker, while the one who is impacted due to technique was called receptor.

Once installed sensors on the attacker and receiver and the control variables captured the system is configured to acquire 50 samples per second for each axis of the accelerometer, the attacker subsequently stated the type of technique as the stroke, same as should be performed as quickly as possible. In each four

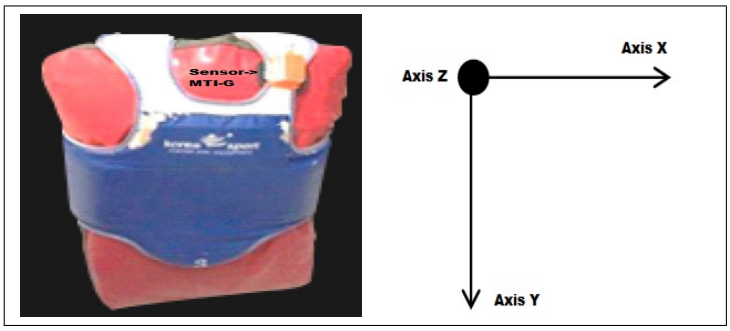


**Fig. 2.** Accels placed in breastplate and orientation axis

prior art attempts were made in order to test the subject to understand the procedure. As a teacher 2nd Dan finds itself it was well executed. After testing the 10 records every stroke is stored with a wait interval of 30 seconds between each, with a rest period of 5 minutes for the change of technique.

### 2.2 Biomechanical Analysis

In figure 3 the graph of acceleration in the receiver at the time of contact of a Tuit Chagui technique is shown, where you can see an abrupt change in $-64m/s^2$ in an interval of 2 ms.

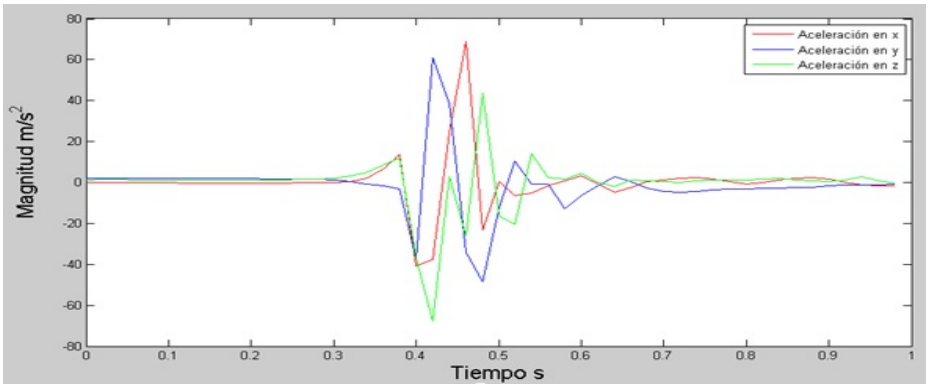


**Fig. 3.** Accelerometer signals in TuitChagui impact

In each of the 10 records per technic per athlete average in the receiver accelerations at impact was made, obtaining a detection threshold for the al-

gorithm. In Bandal Chagui $-60.225m/s^2$, Yop Chagui $-41m/s^2$, Tuit Chagui $-61-67m/s^2$ y MontongChirugui $-54.56m/s^2$.

For analysis of the signals proceeded to tie all the signals according to the first peak when the punch is received and a window of 120ms is taken (6 samples). See figure 4.

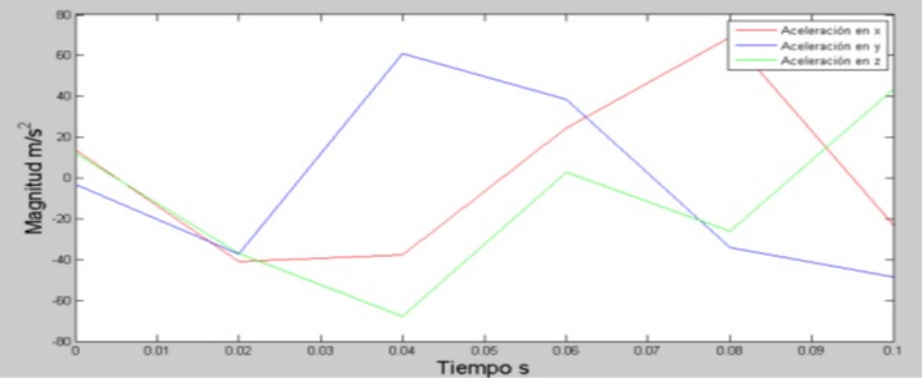


**Fig. 4.** Accelerometer signals in TuitChagui impact

Thereafter, proceeded to perform the correlation of each of the signals obtained to observe the degree of similarity or difference between each of them, which is calculated using the Pearson sample correlation coefficient

$$r = \frac{\Sigma_n \left(A_n - \bar{A}\right)\left(B_n - \bar{B}\right)}{\sqrt{\left[\Sigma_n \left(A_n - \bar{A}\right)^2\right]\left[\Sigma_n \left(B_n - \bar{B}\right)^2\right]}} \tag{1}$$

The following tables show the Pearson correlations for a person in the Tuit Chagui technique.

**Table 1.** Subject 1 X axis correlation. Tuit Chagui technique

| - | 1 | 2 | 3 | 4 | 5 | 6 |
|---|---|---|---|---|---|---|
| **1** | 1 | 0.844 | 0.8844 | 0.8889 | 0.6344 | 0.9525 |
| **2** | 0.844 | 1 | 0.9666 | 0.9627 | 0.9049 | 0.7896 |
| **3** | 0.8844 | 0.9666 | 1 | 0.9982 | 0.8355 | 0.874 |
| **4** | 0.8889 | 0.9627 | 0.9982 | 1 | 0.8101 | 0.8873 |
| **5** | 0.6344 | 0.9049 | 0.8355 | 0.8101 | 1 | 0.506 |
| **6** | 0.9525 | 0.7896 | 0.874 | 0.8873 | 0.506 | 1 |
| - | - | - | - | - | - | |

**Table 2.** Subject 1 Y axis correlation. Tuit Chagui technique

| - | 1 | 2 | 3 | 4 | 5 | 6 |
|---|---|---|---|---|---|---|
| **1** | 1 | 0.9571 | 0.826 | 0.815 | 0.8988 | 0.6156 |
| **2** | 0.9571 | 1 | 0.8799 | 0.8493 | 0.9336 | 0.7017 |
| **3** | 0.826 | 0.8799 | 1 | 0.99 | 0.9805 | 0.4092 |
| **4** | 0.815 | 0.8493 | 0.99 | 1 | 0.9578 | 0.3894 |
| **5** | 0.8988 | 0.9336 | 0.9805 | 0.9578 | 1 | 0.4382 |
| **6** | 0.6156 | 0.7017 | 0.4092 | 0.3894 | 0.4382 | 1 |
| - | - | - | - | - | - | |

**Table 3.** Subject 1 Z axis correlation. Tuit Chagui technique

| - | 1 | 2 | 3 | 4 | 5 | 6 |
|---|---|---|---|---|---|---|
| **1** | 1 | 0.509 | 0.7097 | 0.899 | -0.2028 | 0.8451 |
| **2** | 0.509 | 1 | 0.5439 | 0.5429 | 0.4586 | 0.1655 |
| **3** | 0.7097 | 0.5439 | 1 | 0.9332 | 0.4812 | 0.3291 |
| **4** | 0.899 | 0.5429 | 0.9332 | 1 | 0.1667 | 0.6255 |
| **5** | -0.2028 | 0.4586 | 0.4812 | 0.1667 | 1 | -0.6103 |
| **6** | 0.8451 | 0.1655 | 0.3291 | 0.6255 | -0.6103 | 1 |
| - | - | - | - | - | - | |

Whit this correlation tables the signals that have a higher correlation than 50% in all three axesaxes were averaged to obtain a pattern signal; likewise, Pearson correlation was made for each athlete for each technique to obtain a general pattern per technique for all the subjects. Below in figure 5 the signal pattern for all individuals in the art of Tuit Chagui is shown.

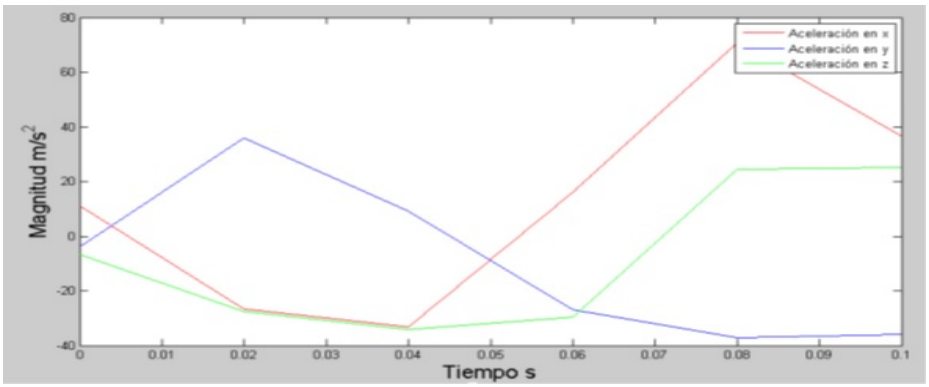


**Fig. 5.** Pattern signals in TuitChagui technique

### 2.3 Development of the system's hardware

Then the figure 6 is observed where the module is displayed with the ADXL345 accelerometer and XBee connected to the microcontroller in the Arduino card and XBee works as a receiver connected to the PC.

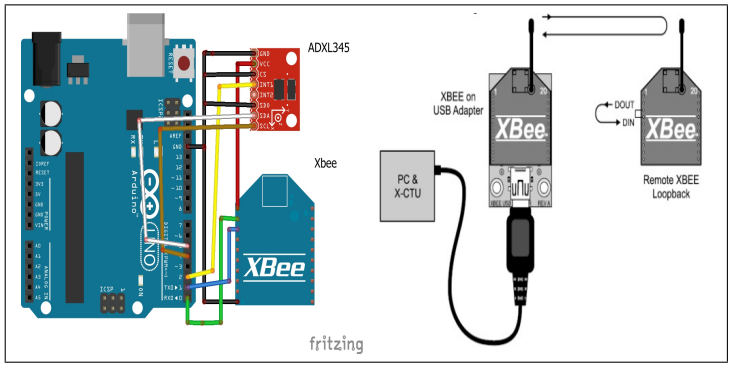


**Fig. 6.** Electronic circuit connections.

### 2.4 Development of the system's software

Through the Arduino platform code able to get the accelerometer data every 2 ms for 120 ms of ADXL345 sensor was programed as scheduled interruptions. Using these data proceed to perform the correlation signals with pattern (previously obtained in the biomechanical analysis) to determine if the impact point should be recognized as a point, and send a code via the zigbee module so that the data can be received and interpreted by the computer software platform developed under the Visual C # to thereby a corresponding increase or no increase in the competitor's score is performed. The main program waits for the ADXL345 accelerometer tells the threshold is exceeded to begin to be considered an impact. When an impact is detected can be considered starts evaluating through the following algorithm:

1. Impact Validation
2. Pearson correlation calculation
3. Technique comparison
4. Technique validation
5. Interface comunication

The computer program figure 7, receives a code breastplate ordering to the scoreboard to increase the score, taking the impact as valid.


**Fig. 7.** PC program

## 3 Results

Was developed and built a device which measures 3.53 cm x 8.53 cm x 7.76 cm and weights 180 g and can be placed on the left of a conventional Korea Sport breastplate. Operates on a 9 volt battery that lasts 505 minutes in active mode. The communication range is up to 50m and has a maximum time following the impact response of 250 ms. See figure 8.

**Fig. 8.** Accels placed in test subject and orientation axis.

Already located in the breastplate 10 samples of each technique for a practitioner of Tae Kwon Do was captured, which were compared with the prototype samples previously proposed, getting a higher level of average correlation of 90% in all techniques. With this confirm that the data obtained with the ADXL345 sensor, are consistent with those obtained by the MTi-G sensor.

Finally device test were made to detect how many false positives for each technique that the electronic breastplate would mark. To achieve this objetive the ten athletes launch fourteen strikes in the electronic breastplate while one 2 Dan black belt observe each technique, then in every strike we fill a table were if the technique were well executed and the PC software mark a god point we put one and if not we put zero. Subsequently an average of eache technique of the ten athletes was made, obtaining a 85% of assertiveness. Like we can see in the table 4. One is well detected and 0 is not detected or fail.

**Table 4.** Subject 1 X axis correlation. Tuit Chagui technique

| Impact | Bandal | Montong | Tuit | Yop |
|---|---|---|---|---|
| **1** | 1 | 1 | 1 | 1 |
| **2** | 1 | 1 | 1 | 1 |
| **3** | 0 | 0 | 1 | 1 |
| **4** | 1 | 1 | 0 | 1 |
| **5** | 1 | 1 | 1 | 1 |
| **6** | 1 | 0 | 1 | 1 |
| **7** | 1 | 1 | 1 | 0 |
| **8** | 0 | 1 | 1 | 1 |
| **9** | 1 | 1 | 1 | 1 |
| **10** | 1 | 1 | 1 | 1 |
| **11** | 1 | 1 | 0 | 1 |
| **12** | 1 | 1 | 1 | 1 |
| **13** | 1 | 1 | 1 | 1 |
| **14** | 1 | 1 | 1 | 1 |
| - | - | - | - | - |
| **Assertiveness** | 85% | 85% | 85% | 92% |

## Acknowledgments

The authors thank the support from UPIITA-IPN and IPN TAEKWONDO athletes for carrying out this work.

## References

1. Sobarzo, P.: Biomecánica Deportiva. El faro, 88, 8-10 (2008)
2. Luigi, T., Willy, P.: Un análisis biomecánico de la patada descendente modificada de taekwondo. Revista de Artes Marciales Asiáticas, 2, 28-39 (2007)
3. Pieter, F., Pieter, W., Heijmans, J.: Movement analysis of taekwondo techniques. Asian Journal of Physical Education, 10(3), 45-58(1987)
4. Stull, R., Barham, J.,: An analysis of movement patterns utilized by ifferent styles in the karate reverse punch in front stance. Biomechanics in Sports VI. Proceedings of the 6th International Symposium on Biomechanics in Sports, 233-243 (1990)
5. Hwang, I.: Analysis of the kicking leg in taekwondo. Biomechanics in sports III & IV, (1987)
6. Wohlin, S.: A biomechanical description of the taekwondo turning hookkick. Unpublished Masters Thesis, Montana State University, (1989)

7. Serina, E. , Lieu, D.: Thoracic injury potential of basic competition taekwondo kicks. Journal of Biomechanics, 24(10), 951- 960(1991)
8. Falco, M.: Tesis Doctoral. Estudio sobre Parámetros Mecánicos y distancia de golpeo de Bandal Chagui en Tae Kwon Do. Universidad de Valencia, (2009)
9. Xataca México:, Tae Kwon Do y el peto electrónico en los panamericanos. http://www.xataka.com.mx/eventos-de-tecnologia/taekwondo-y-el-peto-electronico-en-los-panamericanos, [Consulted 22/01/2014]

# Reviewing Committee

Anzueto Rios Alvaro
Ken Arroyo Ohori
Victor Barrera Figueroa
Christophe Claramunt
Adrian Castañeda Galván
Antonio Concha Sánchez
Carlos de la Cruz
Quetzatcoatl Duarte
Cyntia Enriquez
Imelda Escamilla
Oscar G. Filio Rodriguez
Thomaz E. Figueiredo Oliveira
Hiram Galeana Zapién
Laura Ivoone Garay Jiménez
Jose E. Gomez
Domingo Lara
Aldo Gustavo Orozco Lugo
Giovanni Guzman Lugo
Andres Lucas Bravo
Vladimir Luna
Ludovic Moncla
Hugo Jimenez
Jose M. Lopez Becerra
Itzama Lopez Yañez
Miguel Ángel León Chávez
Rolando Menchaca
Marcoantonio Moreno Ibarra
Saul Puga Manjarrez
Walter Renteria-Agualimpia
Mario H. Ramírez Díaz
Mario Eduardo Rivero Angeles
Francisco Rodríguez Henríquez
Miguel Olvera Aldana
Patricio Ordaz Oliver
Izlian Orea
David Pacheco
Rolando Quintero Tellez
Jorge Rojas
Grigori Sidorov
Miguel Jesus Torres Ruiz
Shoko Wakamiya
Roberto Zagal
Raul Zavala
Lourdes Martínez
Sabino Miranda
Raul Monroy
Antonio Neme
Obdulia Pichardo-Lagunas
Rafael Rojas-Hernández
Grigori Sidorov
Israel Tabarez
Valentín Trujillo Mora
Edgar Vallejo
Nestor Velasco Bermeo

# Additional reviewers

Blanca Rico Jiménez
Mario Aldape Perez

Impreso en los Talleres Gráficos
de la Dirección de Publicaciones
del Instituto Politécnico Nacional
Tresguerras 27, Centro Histórico, México, D.F.
agosto de 2014
Printing 500 / Edición 500 ejemplares